GEOSTATISTICAL ANALYSIS OF MAGNETOMETRY TECHNIQUES TO DELINEATE LOCATIONS OF BURIED FERROMETALLIC DRUMS IN HAZARDOUS WASTE SITES

By

EDWARD MOLASH II

Bachelor of Science

University of Delaware

Newark, Delaware

1981

Submitted to the Faculty of the
Graduate College of the
Oklahoma State University
in partial fulfillment of
the requirements for
the Degree of
MASTER OF SCIENCE
December, 1991

GEOSTATISTICAL ANALYSIS OF MAGNETOMETRY TECHNIQUES TO DELINEATE LOCATIONS OF BURIED FERROMETALLIC DRUMS IN HAZARDOUS WASTE SITES

Thesis Approved:

William F. McTernan
Thesis Adviser

Donald R. Sullivan

Raulee Henry

Thomas C. Collins
Dean of the Graduate College

PREFACE

The suitability and effectivess of two types of magnetometer surveys used for the location of buried steel drums in a hazardous waste site was investigated. The analysis utilized geostatistical techniques which facilitated the delineation of critical spatial wavelengths inherent in each survey. A weighted linear estimation technique, known as kriging, allowed for the determination of sets of interpolated values of the measured magnetometer readings. Limitations on the data analysis due to sampling configurations were addressed. Proposals for improving acquisition techniques for magnetic surveying in hazardous waste studies were explained.

I wish to express my gratitude to the individuals who assisted me in this project and during my coursework at Oklahoma State University. In particular, I wish to thank my major advisor, Dr. William F. McTernan, for his motivation, guidance, and relevant advice on the subject matter. I also wish to express gratitude towards the other members of my thesis committee, Dr. Marilee Henry and Dr. Donald Snethen for their patience, assistance and pertinent commentary during the course of this work.

TABLE OF CONTENTS

Chapter Page

Chapter Page

LIST OF TABLES

LIST OF FIGURES

CHAPTER I

INTRODUCTION

The use of geostatistics as a method to determine the suitability of sampling configurations and provide interpolated estimates of magnetometer surveys has been investigated.

The importance of defining the locations of point sources of toxic substances within hazardous waste sites is relevant in terms of both regulatory compliance and the technical analysis of contaminant transport phenomena in the subsurface. Statutorily, the removal of "tanks, drums, or other bulk holding units" of hazardous substances is mandated in the National Contingency Plan (NCP), section 300.65, Title 40, Code of Federal Regulations, as a prescribed procedure to abate the threat to the public health for hazardous waste sites assigned to the Comprehensive Environmental Response, Compensation, and Liability Act (CERCLA). The federal regulations recognized the importance of not allowing surface waters to leach through contaminated soils in the unsaturated zone to reduce potential risk to groundwater resources. This factor has significance because once infiltration to groundwater occurs, the engineering design for abatement becomes time intensive (on a scale of many years), technically difficult, larger in areal distribution, and exponentially more expensive (typically in the millions of dollars).

The technical analysis of hazardous waste sites requires the definition of the spatial distribution of certain critical parameters relating to contaminant plumes in order to determine decision models for abatement system design. These models, whether analytical or numerical, simulate flow

and transport phenomena of contaminant leachates in the unsaturated or saturated zones considering hydrodynamic, chemical, and biological properties. The currently utilized modeling configurations require that the amounts, locations, and distributions of the buried contaminant sinks be defined for establishing reliable transport models.

One of the more common sources of hazardous wastes are contained in buried steel drums or tanks. In hazardous waste disposal sites the existence, number, and / or areal distributions of buried drums are unknown factors. The location and removal of these buried steel drums is an appropriate first action in responding to hazardous waste disposal sites which threaten groundwater resources.

Magnetic surveys have been commonly used in recent years to estimate the locations of buried ferrometallic drums, underground storage tanks, buried pipes, and the boundaries of hazardous waste disposal sites. Magnetometry utilizes the earth's natural magnetic field as the inducing element for the detection of ferrometallic objects in the subsurface. Any object placed in an external magnetic field becomes magnetized by induction. The magnitude of this induced magnetic field is a complex function of many factors, but is dominated by the target's mass and a material property known as magnetic susceptibility. Most soils and earth materials have very low magnetic susceptibilities, contrasting with iron and steel, which develop unusually strong induced magnetic fields. Induced fields are vectorially added to the earth's ambient magnetic field, the resultant of which is anomalously high in the vicinity of the buried ferrometallic object.

Two types of magnetic observations are used in hazardous waste site assessments, the total magnetic field and vertical magnetic gradient surveys.

The total magnetic field survey measures the scalar magnitude of the earth's magnetic field, **h**, and includes components from the earth's ambient field along with components from all of the induced fields, at some level above the earth's surface. The vertical magnetic gradient (the first derivative of the earth's magnetic field in the vertical direction, d**h**/dz) is estimated by taking simultaneous readings of the total magnetic field at two different vertical levels above the earth's surface and recording the difference between the two readings. This difference is then divided by the vertical distance between the individual sensors to obtain an estimate of the vertical magnetic gradient. It has been claimed in the literature (Hood et al.,1979; Barongo, 1985; Forrest, 1991) that vertical gradient measurements have certain intrinsic advantages over total magnetic field data:

1) the vertical gradient is less sensitive to interference from nearby laterally bordering cultural objects, such as fences;

2) the data are free from diurnal variations;

3) the regional gradient is removed from the data;

4) individual objects in the near surface have greater lateral resolution, i.e. multiple buried objects in the same vicinity can be individually identified;

Typical targets in hazardous waste site studies are buried ferrometallic 55 gallon drums. Drums are relatively small objects compared to the typical dimensions of landfills. Consequently, the design of the spacing and geometry of the survey sampling grid is critical to the success of locating buried drums. For a specific survey, the probability of adequately defining the target locations when the survey spacing is significantly greater than the spatial wavelengths produced by the

isopotential surface of the resultant magnetic field is very low. When the survey spacing is sufficient to define the surface, a method for interpolating the values from the individually sampled locations is needed. Geostatistics provides the capabilities to accomplish this type of analysis and has been used for this study.

The data used in this effort came from the remedial investigation of the Western Processing Superfund site, located at 7215 S. 196th Street in Kent, Washington. The surveys were conducted by independent contractors working under contract for the U.S. Environmental Protection Agency during the Fall of 1986 (French, Williams, and Foster, 1987). This facility operated from 1961 to 1983 as an industrial waste processing and recycling facility, receiving animal byproducts, brewers yeast, and a wide variety of industrial waste products, including solvents, flue dust, battery chips, acids, and cyanide solutions. The preliminary assessment of the site, essentially through document review and aerial photo analysis, had determined that several filled waste water lagoons, reaction ponds, subsurface impoundments, and several burial sites for drums of potentially toxic wastes might exist. In 1982 the site was placed on the EPA's National Priorities List. The EPA issued an administrative order to cease all operations at the site and initiate remediation procedures. Initial activities under the emergency response included the removal of impounded liquids, stockpiled drums, and contaminated soils. All surface facilities were removed from the site by 1984. The early phase of remediation discovered 73 contaminants in soil samples, including 20 metals and 53 organics. Forty six priority pollutants were found in the groundwater at the site.

The site is near the center of the Duwamish Valley, once a marine

embayment, now filled with up to 500 feet of fluvial and lacustrine deposits. Depth to the water table for this unconfined aquifer typically occurs at less than ten feet, while topographically low areas may have completely saturated soils during wet periods. The soils at the site are predominantly glacial outwashes, consisting of silty sands and sandy silts with very high hydraulic conductivities. Groundwater in the area moves laterally at rates measured in the hundreds of feet per year. Coupled with the prolific rainfall typical of the area, rapid recharge rates for unconfined aquifers are expected.

The final phase of remedial operations for the Western Processing site was a subsurface investigation which included the extensive use of geophysical methods to guide systematic drilling and soil sampling. The specific objectives were to locate the buried drums, tanks, utilities, and process lines for subsequent removal. The geophysical methods used were inphase and quadriture electromagnetic induction, total field and vertical gradient magnetometry, and ground penetrating radar. The magnetometer surveys were collected simultaneously along a survey grid with a 10 foot line spacing using a EDA Omni IV proton precession magnetometer. The proton precession magnetometer utilizes the precession of spinning protons or nuclei of the hydrogen atom in a hydrocarbon fluid that measures the total magnetic intensity. The spinning protons in the fluid behave as small, spinning magnetic dipoles. These magnets are aligned or polarized temporarily by the application of a uniform magnetic field generated by a current in a coil of wire. The precessing protons then generate a small signal in the same coil used to polarize them. This signal has a frequency that is precisely proportional to the total magnetic field intensity and is

independent of the orientation of the magnetometer. The proportionality constant, which relates the frequency-to-field intensity, is the atomic constant, the gyromagnetic ratio of the proton. The precession frequency is measured by digital counters as the absolute value of the total magnetic field intensity with an accuracy of less than 1 gamma in the earth's field of approximately 50,000 gammas. Both the total field and gradient data were recorded by an internal microprocessor on the magnetometer. A companion base station magnetometer allows for automatic diurnal drift correction via internal software of the magnetometer. The vertical gradient data does not require diurnal drift corrections.

A methodology of spatial domain statistics, commonly known as geostatistics, provided techniques which allowed for the evaluation of the spatial structure of the total magnetic field intensity and vertical magnetic gradient variables. The geostatistical method had two applications which were useful relative to this study. First, the adequacy of the sampling grid in the spatial domain could be determined. Secondly, when the spatial semivariance / covariance of the sampled data could be adequately modeled, geostatistics provided a method for extending the sampled data set. The derivation of an optimum set of weights, defined by solving a set of simultaneous equations using the information from the semivariance / covariance structure, provided interpolated estimates for the magnetometer data that gave minimum estimation variances.

The effectiveness of the geostatistical interpolations of the two magnetics data sets were determined by two separate methodologies. One effectiveness criterion compared the geostatistical estimates within the magnetic anomalies to expected results derived from independent empirical

studies of the magnetic responses for steel drums. The other criterion contrasted the statistical characteristics of interpolations to that of the original measured samples. The generalized analytical methodology that was used included:

1) determination of the bivariate statistical parameters of the measured data sets for total magnetic field intensity and vertical magnetic gradient,

2) Calculations from the measured data sets of experimental semivariances, degrees of stationarity, and anisotropy components for the regional variables (total magnetic field intensity and vertical magnetic gradient),

3) structural analysis of the experimental semivariances was performed by the fitting of continuous mathematical functions to the experimental data, and cross-validation of the resultant models with the measured data using a hole-by-hole suppression technique,

4) using the previously derived model, interpolation estimates of the regionalized variables via kriging,

5) Validity of the kriged estimates in the following manner:

a) Generation of cross-validation statistics using a hole-by-hole suppression technique,

b) Comparison of univariate statistical properties of the kriged values to those of the original data for preservation of the original stochastic properties of the regional variable under consideration,

c) Examination of the error variances produced during kriging,

d) comparison of the magnetic anomalies derived from the

geostatically interpolated data to results derived from independent empirical studies of the magnetic responses for steel drums, and

6) Determination of the adequacy of the sampled support and the utility of kriging to extend the measured data set.

The results of the geostatistical analysis showed that the total field intensity and vertical gradient data displayed distinctly different spatial statistical properties. The total magnetic field intensity data exhibited dominant spatial frequencies which allowed the semivariances to be rigorously modeled using the 10 ft support network. The subsequent interpolated estimates for the total field intensity had very good statistical correlations with the original sampled data, with some minor distortions of the distributions of the results. These distortions were concluded to be the result of the mathematics of the estimation process. The resultant anomalies, using the measured data with the geostatistical estimates, produced spatial configurations (center of mass separation, anomaly widths) which agreed with other empirical studies on the magnetic responses of buried drums.

Converse to the total intensity data, the vertical magnetic gradient data displayed much higher spatial frequencies in its semivariogram. More than 69% of the semivariance existed at spatial wavelengths less than that of the sampling grid. Consequently, a rigorous mathematical definition of the semivariance could not be derived. A different type of analysis has been performed on the vertical magnetic gradient data, whereby an iterative technique was utilized to find an improved estimate for the vertical gradient semivariance function. It was found that the iterative procedure, somewhat similar to a Bayesian updating process, provided semivariance models which

improved the quality of the kriged estimates. The vertical gradient data displayed very large variances in the original measured samples and in the subsequent kriged estimates. For future applications, the utility of estimation by kriging for vertical magnetic gradient data would be contingent on whether: a) there is a definite need for interpolated values; b) additional vertical gradient field measurements are unavailable and not acquirable; c) the time required to rigorously perform the necessary analyses is available.

CHAPTER II

GEOSTATISTICAL ANALYSIS OF MAGNETOMETRY METHODS

Regional Variable Theory

Geostatistics is an abstract theory of statistical behaviour, developed by mining engineers who attempted to use statistical methods to estimate and interpolate the spatial distribution of ore grades in mineral deposits (Krige, 1966). Geostatistics utilizes the concept of the regional variable (Matheron, 1971), which has properties between that of a truly random variable (that can only be described in terms of stochastic properties) and one with completely deterministic properties. Regional variables are continuously distributed throughout a 1, 2, or 3 dimensional space with a geographic variation too complex to be represented by any workable mathematical function. The spatial point-to-point variation has a deterministic component in the sense that "neighboring" sample observations will have somewhat similar values, but it will also have stochastic properties that prevents that value from being precisely determined.

Support of the Measured Sampling System

The size, shape, orientation and spatial arrangement of the sampled observations in a 1, 2, or 3 dimensional system is referred to as the support of the regional variable. The apparent "short range" stochastic variations with one support system may actually be structured if examined at smaller scales. Conversely, the apparent structured component of the regional variable may behave stochastically when studied at larger scales. Therefore, the regional variable will exhibit different characteristics as its support is

modified. The support for the Western Processing Site geophysical survey is in the form of a regularly spaced survey grid with 10 foot centers. Alternating columns in the north-south direction have been "shifted" by 5 feet. The result is a triangular grid which has a large number of measured sample points which are separated by multiples of 10 feet and 11.18 feet. Figure 1 displays a portion of the survey grid. The entire grid used in this analysis was 240 feet to the east by 240 feet to the north, corresponding to 1.322 acres. This area was identified in the E.P.A.'s preliminary investigation as the area with the highest probability of containing cachements of buried drums. A total of 576 sampled points were acquired simultaneously for the total magnetic field and vertical magnetic gradient data.

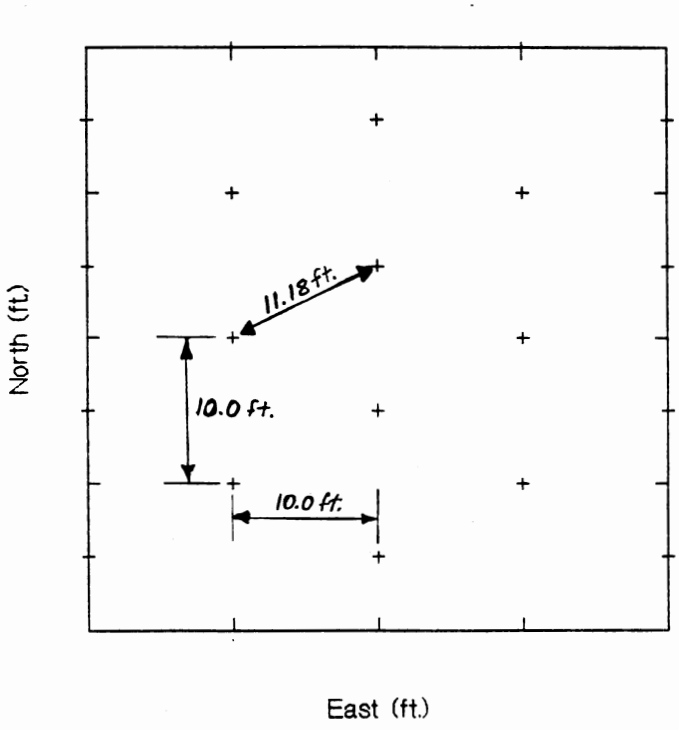

Figure 1 - Portion of the Geophysical Survey Grid and the Dominant Sample Spacings.

The data were acquired by an EDA OMNI IV Total Field Magnetometer/ Gradiometer by Northern Technical Services (NORTEK) of Redmond, Washington in the Fall of 1986. NORTEK was contracted by the EPA to perform the magnetometer surveys as part of the remedial investigation at that site. This instrument used for the surveys was a proton precession magnetometer. It utilizes the precession of spinning protons or nuclei of the hydrogen atom in a hydrocarbon fluid to measure the total magnetic field intensity. The precession magnetometer depends on the measurement of the free-precession frequency of protons (hydrogen nuclei) which have been polarized in a direction approximately normal to the direction of the earth's ambient magnetic field. When the polarizing field is suddenly removed, the protons precess like a spinning top, with the localized geomagnetic field supplying the precessing force (corresponding to that of gravity in the spinning top analogy). The proton precesses at an angular velocity, known as the Larmor precession frequency, which is proportional to the total magnetic field intensity (Telford et al., 1982). The proportionality constant which relates the precession frequency to the total magnetic field intensity is the gyromagnetic ratio of the proton, i.e. the atomic constant. The measurement of the precession frequency is accomplished by means of a coil surrounding the sample. The proton, being a moving charge, induces in the coil a voltage which varies at the precession frequency. The unit commonly used to represent magnetic field intensity is the 'gamma', which is equivalent to 1 nanotesla, 10^{-5} oersteds or 7.958×10^{-4} ampere-turn/meters (Telford et al., 1976). Typically, proton precession magnetometers are accurate to less than 1 gamma in a field of 50,000 gammas. A companion base station magnetometer allowed for an automatic diurnal (cyclical daily variations related to the

positions of the sun and moon) drift correction via internal software of the magnetometer.

Total field measurements were read simultaneously on two individual magnetometers separated vertically by 0.5 meters at each sampling point. The difference between the individual readings were divided by the separation distance, which produced estimates of the vertical magnetic gradient.

Fundamental Statistical Concepts

A regionalized random variable Z(x) can be considered to be a particular realization of a spatially distributed random function $\underline{Z}(x)$. Two experimentally derived data points $Z(x_i)$ and $Z(x_{i+h})$, separated by a distance h (in map view), can then be considered to be two different realizations of the same random variable Z(x). The statistical estimation of the spatial distribution of a regionalized variable is not rigorously possible if limited to a single realization in a given support. In order to make estimates of the regional variable Z(x) at points which are not discretely sampled, certain statistical assumptions regarding the homogeneity and spatial behaviour of Z(x) must be made. The first order moment of Z(x) is its expectation E, more commonly known as its mean (Knighton and Wagenet, 1987) , which is defined as:

$$E[Z(x)] = \mu \qquad (1)$$

The sample estimate for the expectation of Z(x) for n observations is calculated by:

$$\mu = \overline{x} = 1/n \sum_{i=1}^{n} Z(x_i) \qquad (2)$$

The second order moment of Z(x) is defined as its variance, a measure of the

dispersion of the regionalized variable:

$$\mathrm{Var}[Z(x)] = 1/(n-1)\ E[\{Z(x_i) - \mu\}^2] = \sigma^2 \quad (3)$$

Which is operationally estimated by:

$$s^2 = 1/(n-1)\sum_{i=1}^{n}[Z(x_i) - \bar{x}]^2 \quad (4)$$

The covariance between two regional variables X and Y is defined as the 1,1 central moment (Haan, 1977):

$$\mathrm{Cov}(X,Y) = E(XY) - E(X)\ E(Y) \quad (5)$$

The sample estimate of the population covariance is computed from:

$$s_{X,Y} = 1/(n-1)\sum_{i=1}^{n}(x_i - \bar{x})(y_i - \bar{y}) \quad (6)$$

With the first two moments and the covariance defined, the spatial covariance of the regional variable can be defined simply as a measure of how Z(x) varies at sets of points separated by a distance h:

$$\mathrm{Cov}[Z(x_i),Z(x_{i+h})] = C(h) = E[\{Z(x_i) - \mu(x_{i+h})\}\{Z(x_{i+h}) - \mu(x_{i+h})\}] \quad (7)$$

If Z(x) can be considered as a second order stationary process, i.e. the first two moments are the same throughout the observed terrain, then $u(x_i) = u(x_{i+h})$, and the spatial covariance can be simplified to:

$$C(h) = E[Z(x_i)\ Z(x_{i+h})] - \mu^2 \quad (8)$$

When h=0, the covariance assumes the value of the population variance,i.e.

$$C(0) = \mathrm{Var}[Z(x)] \quad (9)$$

This relationship can only be true if the regionalized variable is stationary through its first two moments. This assumption is known as the intrinsic hypothesis (Matheron, 1971). With second order stationarity the covariance and correlation can be considered as functions of only the length of the displacement vector **h**.

The standard error of a set of values is their standard deviation

divided by the square root of the number of samples. The standard error estimates the standard deviation of the sample mean as an estimator of the population (or "true") mean.

The skewness, or third moment about the mean, is a dimensionless number that characterizes the relative degree of asymmetry of a distribution about its mean. It is defined as:

$$\text{Skew}(x_1 \ldots x_n) = 1/n \sum_{i=1}^{n} [(x_i - \bar{x})/s]^3 \quad (10)$$

The kurtosis is also a nondimensional quantity. It measures the relative peakedness or flatness of a distribution relative to a normal distribution with an identical mean and standard deviation. The conventional defintion of kurtosis is:

$$\text{Kurt}(x_1 \ldots x_n) = \{1/n \sum_{i=1}^{n} [(x_i - \bar{x})/s]^4\} - 3 \quad (11)$$

The coefficient of variation is a dimensionless measure of dispersion calculated by dividing the standard deviation by the mean:

$$c_v = s / \bar{x} \quad (12)$$

The chi-square statistic, as used here, is a statistical comparison between the distribution of the variable and a normal distribution when each are arranged into identical discrete categories of value ranges. The chi-square is calculated by:

$$\chi^2 = \sum_{i=1}^{n} (N_i - n_i)^2 / n_i \quad (13)$$

Where N_i is the number of occurrences observed in bin i and n_i is the number expected according to a normal distribution. A chi-square value of zero indicates that the distribution is precisely normally distributed while a large chi-square indicates that the variable's distribution is very dissimilar to a normal distribution with the same mean and standard deviation.

The univariate statistical properties of the total magnetic field

intensity and vertical magnetic gradient have been calculated. They are displayed in Table I.

TABLE I

UNIVARIATE STATISTICAL PROPERTIES OF THE TOTAL MAGNETIC INTENSITY AND VERTICAL MAGNETIC GRADIENT DATA

Statistical Property	Total Field Intensity (gammas)	Vertical Gradient (gammas/meter)
Sample Size	576	576
Range of Values	139.10	485.0
Mean	196.81	-10.25
Median	196.70	-14.00
Standard Deviation	23.06	81.08
Standard Error	2.250	7.910
Skewness	0.326	0.566
Kurtosis	1.003	1.556
Coeff. of Variation	0.117	-7.91
Chi-Square Statistic (w.r.t. Normal Distribution)	134.9	231.2

Stationarity of a Regionalized Variable

It often happens that regionalized variables exhibit significant degrees of non-stationary behaviour, i.e. spatial variations in its first two moments throughout the sampled support. When this can be demonstrated, it is necessary to decompose the regional variable into two components, referred to as the drift and the residual. The drift is the non-stationary component of the regional variable. The residual is regarded as the component of the regional variable which can be considered stationary after the drift is removed.

$$\text{original data} = \text{residual} + \text{drift} \qquad (14)$$

[non-stationary] [stationary] [non-stationary]

In an operational sense, drift is usually represented by finite order polynomials (rarely greater than second order), and its determination in other than the simplest situations, such as in areas where the drift component of the regional variable can be mathematically characterized as a tilted plane, is very difficult and is rarely any better than a guess.

Stationary Determination in the Measured Samples

For the Western Processing geophysical data, determination of the degree of dependence between two regional variables, represented by $r_{X,Y}$, and calculated by:

$$r_{X,Y} = s_{X,Y} / s_X s_Y \qquad (15)$$

where $s_{X,Y}$ is the sample covariance between variables X and Y given by (6), and s_X and s_Y are the corresponding standard deviations of those variables calculated by taking the square root of (4). The correlation coefficients, as defined by (11), assume values between -1.0 and 1.0. When $r_{X,Y}$ assumes a value of 0.0, then the two variables X and Y are considered linearly independent (Haan, 1977). Linear independence between the regional variables (total magnetic field intensity and vertical magnetic gradient) with the north and east coordinates of the sampled support can be demonstrated by examination of their correlation coefficients. If the correlations are reasonably small, then it can be assumed that there is little or no statistical dependence of the variables with respect to the coordinates of the sampling grid. Under these circumstances the assumption of stationarity could be considered statistically valid. Scatterplots of the variables with respect to

the support coordinates and each other (Appendix A) indicated that non-linear correlation forms did not exist. Table II displays the correlation matrix of the total magnetic intensity and vertical magnetic gradient data relative to the north and east coordinates for the Western Processing surveys.

TABLE II

CORRELATION MATRIX FOR THE WESTERN PROCESSING GEOPHYSICAL DATA

NUMBER OF OBSERVATIONS: 576

	North	East	Total Field	Gradient
North	1.000			
East	0.003	1.000		
Total Field	0.102	0.116	1.000	
Gradient	-0.041	0.049	0.625	1.000

Several important conclusions were reached from examination of the correlation matrix:

1) The linear correlation between the total magnetic field intensity and the vertical magnetic gradient was moderately high (0.625). This indicated that these regional variables display moderate degrees of linear correlation, but any attempt to characterize one of the variables in terms of the other by way of a regression analysis would probably result in unsatisfactory results.

2) The total magnetic field intensity and vertical magnetic gradient variables had very small correlations with the north and east coordinates of the survey ($r_{\text{Total Field - North}} = -0.102$, $r_{\text{Total Field - East}} = 0.116$, and $r_{\text{Gradient - North}} = -0.041$, $r_{\text{Gradient - East}} = 0.049$).

This indicated that these variables can be considered statistically stationary in the mean. This conclusion became important when considering the most

appropriate type of kriging technique to be used (Davis, 1982; Journel and Huijbregts, 1978).

3) It has been asserted in the literature (Hood et al., 1979; Barongo, 1985) that vertical gradient data have an intrinsic advantage over total field intensity data because the regional gradient, i.e. statistical non-stationarity, is suppressed. This claim seemed to be validated in this particular case. The extremely small correlation coefficients of the vertical magnetic gradient with the north and east coordinates of the survey suggested linear statistical stationarity.

4) The total field intensity data displayed somewhat larger degrees of drift relative to the north and east survey coordinates than the vertical gradient data. The drift was still within levels that could be considered insignificant (spurious correlation effect). It is has been shown, by a world-wide network of geophysical observatories and magnetic surveys performed for mineral exploration purposes, that the total magnetic field intensity has spatial variations which range from a few hundred meters to several hundred kilometers (Nettleton, 1976; Dobrin, 1976; Telford et al., 1982). These variations result from changes in the magnetite and/or iron concentrations in the underlying crystalline rock formations. Even though drift in the mean was not a significant consideration in this particular case due to the relatively small areal extent of the survey (1.322 acres), other situations could present significant drift components in the mean and should be tested for individually using these techniques.

Semivariance

The assumption of second order stationarity, i.e. the mean and standard deviation are invariant throughout the support of the regionalized variables, implies the existence of a finite variance of the measured values which can be estimated by the variance of the sample. Even if the variance of Z(x) is not finite, the intrinsic hypothesis assumes that the incremental variances of Z(x) are finite and that these increments are second order stationary as defined by (8) and (9). This incremental variance in the spatial domain permits the definition of a new function, the semivariance (Journel and Huijbregts, 1978). Semivariance is denoted by the symbol γ (gamma) and is defined as:

$$\gamma(h) = 1/2 \text{ Var } [Z(x_{i+h}) - Z(x_i)] \tag{22}$$

Using the definition of variance given by (3):

$$\gamma(h) = 1/2 \; E[\{Z(x_{i+h}) - Z(x_i)\} - \{E[Z(x_{i+h}) - Z(x_i)]\}^2 \tag{23}$$

Now utilizing the assumption of second order stationarity, i.e.:

$$E[Z(x_i)] = E[Z(x_{i+h})] \tag{24}$$

and combining (13) and (14) yields:

$$\gamma(h) = 1/2 \; E[\{Z(x_{i+h}) - Z(x_i)\}^2] \tag{25}$$

Under this definition, the sample estimate of the population semivariance or experimental semivariance, denoted by the symbol $\gamma^*(h)$, can be calculated by:

$$\gamma^*(h) = 1/2n(h) \sum_{i=1}^{n} [Z(x_{i+h}) - Z(x_i)]^2 \tag{26}$$

where n(h) is defined as the number of samples separated by a distance h.

The relationship between the semivariance, which is a measurement of the variability of the regional variable in a spatial sense, and the covariance, which is a measure of its similarity, can be derived mathematically by

expanding (15) with the inclusion of (8).

$$\gamma(h) = 1/2\ E[Z(x_{i+h})^2 - E[Z(x_{i+h})Z(x_i)] + 1/2\ E[Z(x_i)]^2$$

which yields: $$\gamma(h) = C(0) - C(h) \qquad (27)$$

Therefore, the semivariogram is the reflection of the covariance and the sum of the semivariance and the covariance at any distance h is equal to the population variance. Figure 2 graphically shows this relationship.

If the experimental semivariances $\gamma^*(h)$ are calculated for all separation distances h, as defined by (16) and plotted as a linear graph of $\gamma(h)$ (ordinate) versus the separation distance h (abscissa), the result is the experimental semivariogram. The experimental semivariogram is a graphic estimate of the spatial behavior of the regional variable. In most cases, only

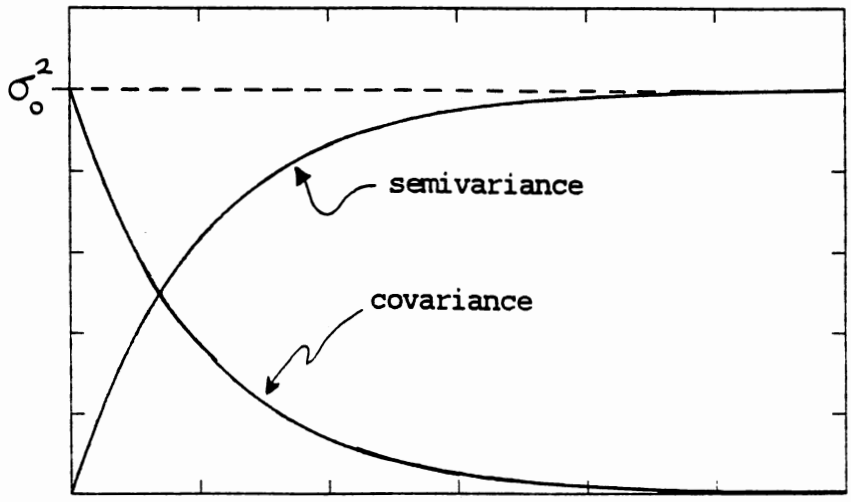

Figure 2 - Relationship between the semivariance and covariance. σ^2 represents the population variance.

discrete values of h and consequently $\gamma(h)$ are generated. The total number

of semivariance values that can be generated for a sample space of n observations in a support is (n)(n-1)/2. For use in the kriging equations, interpolation or extrapolation was required at distances that were not discretely sampled. This required that the semivariance values be defined over the continuous range of distances. In order to do this, it is necessary to mathematically "model" the semivariogram, permitting the derivation of semivariance values at any separation distance. In practice, the modeling procedure is a labor intensive process involving iterative model generation and comparisons to the experimental data points of the semivariogram.

Typically, when dealing with experimentally derived data, the semivariogram is a complex assemblage of data points which are not easily quantified by a continuous mathematical function. There are several features, however, which tend to be representative of many semivariograms. A discontinuity at the origin (an intercept value greater than zero) is commonly referred to as the "nugget effect". This can be interpreted as either: 1) variation on a scale smaller than the minimum separation distance, or; 2) variance in the value of $Z(x_i)$ arising from uncertainties or errors introduced in the measurement process.

In many cases, when the separation distance h becomes very large, the sample values will become statistically independent of each other. The semivariogram will then become parallel to the abscissa at a value which is indicative of the population variance. The value of h at this point is called the "range of influence" of a sample. Separation distances less than the range of influence are said to be within in the "neighborhood" or distance within which all locations are correlated. Values of the regionalized variable separated by distances outside the neighborhood are considered independent

of the location and are ignored in the estimation procedure. The semivariance value at which the curve becomes parallel with the x-axis is referred to as the "sill" of the semivariogram. Figure 3 shows these features which are typical of ideal semivariograms. While the shape of the

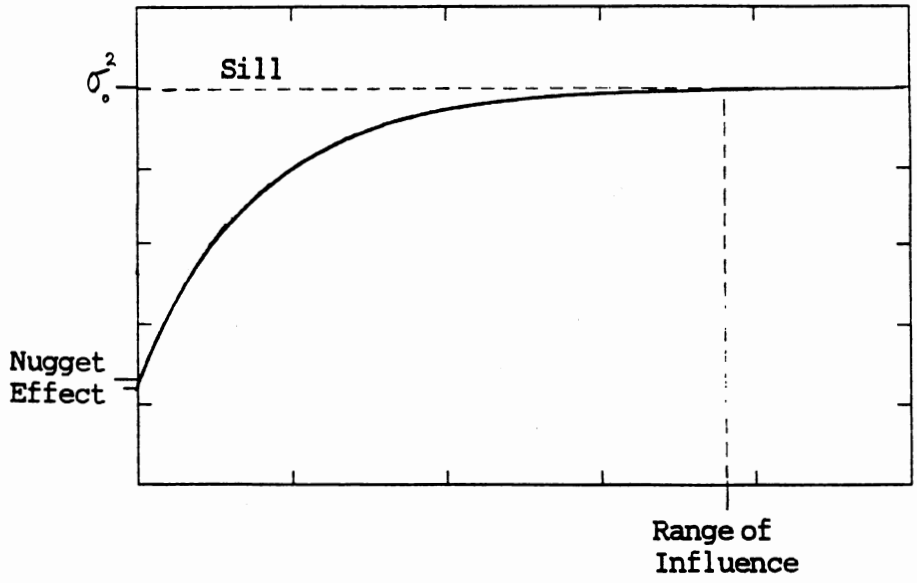

Figure 3 - Typical Semivariogram Features - Nugget Effect, Range of Influence, and Sill.

semivariogram can be modeled by any continuous function, several models are commonly used. The software used in this study, STATPAC, which was developed by the United States Geologic Survey, included four models used in this study:

1) The spherical model is usually regarded as the "ideal" shape for the semivariogram, and is to geostatistics what the normal distribution is to ordinary statistical analysis. It is defined by:

$$\gamma(h) = C[(3h/2a)-(h^3/2a^3) + C_0, \quad @\ h<a \qquad (28)$$

$$\gamma(h) = C, \quad @\ h>a$$

where: h = separation distance

C = semivariance at the sill

a = range of influence

C_0 = nugget effect

This model has the characteristics of rising quickly from the origin (or nugget) and intersecting directly with the sill.

2) The exponential model is described by:

$$\gamma(h) = C[1-\exp(-h/a')] + C^0, \quad @\ h<a \qquad (29)$$

$$\gamma(h) = C, \quad @\ h>a$$

where: $a' = a/3.0$ (approximately)

The exponential model rises more slowly from the origin than the spherical model and never quite reaches the sill. The spherical and exponential models have been the most commonly used when describing experimental semivariograms which characterize the variability of soil, geologic, hydrologic, and other regional variables which are generally characterized as being lognormally distributed (Freeze, 1975; Russo and Bresler, 1980).

3) The linear model is given by:

$$\gamma(h) = ph^T + C_0 \quad @\ h<a \qquad (30)$$

$$\gamma(h) = C, \quad @\ h>a$$

where: p = slope of the line

$0.0 <= y <= 2.0$

When the y parameter assumes some value other than 1.0, then this is considered a 'generalized linear' model.

4) The Gaussian model is described:

$$\gamma(h) = C[1-\exp(-h^2/a'^2) + C_0 \qquad (31)$$

where: $a' = a/1.7$ to $a/2.3$

There are other functional forms which can be used to model semivariograms, but equations (28), (29), (30), (31), and nested forms (linear combinations) of these equations have been sufficient for this effort.

Experimental Semivariances for the Western Processing Magnetometer Surveys

The Western Processing magnetometer surveys, with 576 sampled points, produced a total of 331,200 individual semivariance values in all directions. In addition, because of the redundancy of the survey grid, the resultant semivariogram has a great many values at identical separation distances. Any attempt to analyze an experimental semivariogram (or any graph) with that many data points would be confusing and impractical. To accommodate the multiplicity at many separations, experimental semivariances were averaged over ranges of separations. The average experimental semivariance over that range was plotted against the average separation distance for the same conditions. Using this technique with (16), the experimental semivariance relationships were developed. Tables III and IV show the results for the experimental semivariances for the total magnetic field intensity and the vertical magnetic gradient in tabular form whereas Figures 4 and 5 display the same data in graphical form. These semivariances are "all directional", calculated regardless of the direction of the displacement vector **h**. It needs to be pointed out at this point that the units commonly used to represent magnetic field intensity is the 'gamma', which is equivalent to 1 nanotesla, 10^{-5} oersteds, or 7.958×10^{-4} ampere-turn/meter (Telford et al., 1982). Semivariance is also commonly referred to as a 'gamma'

parameter, as previously noted. To eliminate confusion, it is noted here that the calculated units for semivariance when dealing with total magnetic field intensity are in [gammas^2], and the semivariance units for vertical magnetic field gradient are in [gammas^2/meter].

TABLE III

SEMIVARIANCE ANALYSIS OF TOTAL MAGNETIC FIELD INTENSITY

Distance Range (ft.)	Number of Semivariance Pairs	Gamma $\gamma(h)$	Average Distance (ft.)
7 - 14	1555	172	10.78
14 - 21	1991	379	19.02
21 - 28	1902	483	24.65
28 - 35	3197	490	30.61
35 - 42	4389	668	38.51
42 - 49	3350	822	45.42
49 - 56	5977	810	52.94
56 - 63	3747	827	60.20
63 - 70	4364	918	65.07
70 - 77	6619	898	72.60
77 - 84	6426	892	80.85
84 - 91	5844	891	88.31
91 - 98	4600	851	93.85
98 - 10	6563	817	100.65

The semivariogram for the total magnetic field intensity (Figure 4) displayed many of the "classic" features of semivariograms previously described. There appeared to be a distinct sill at separation distances slightly greater than 60 feet (the range of influence) and a semivariance level of approximately 900 (the sill). At separations less than 60 feet, the individual semivariances assumed the form of a monotonically increasing function and suggests that little (apparent) nugget effect exists. The parameters for continuous functions that adequately model the total magnetic field data set were determined and are documented in the next section.

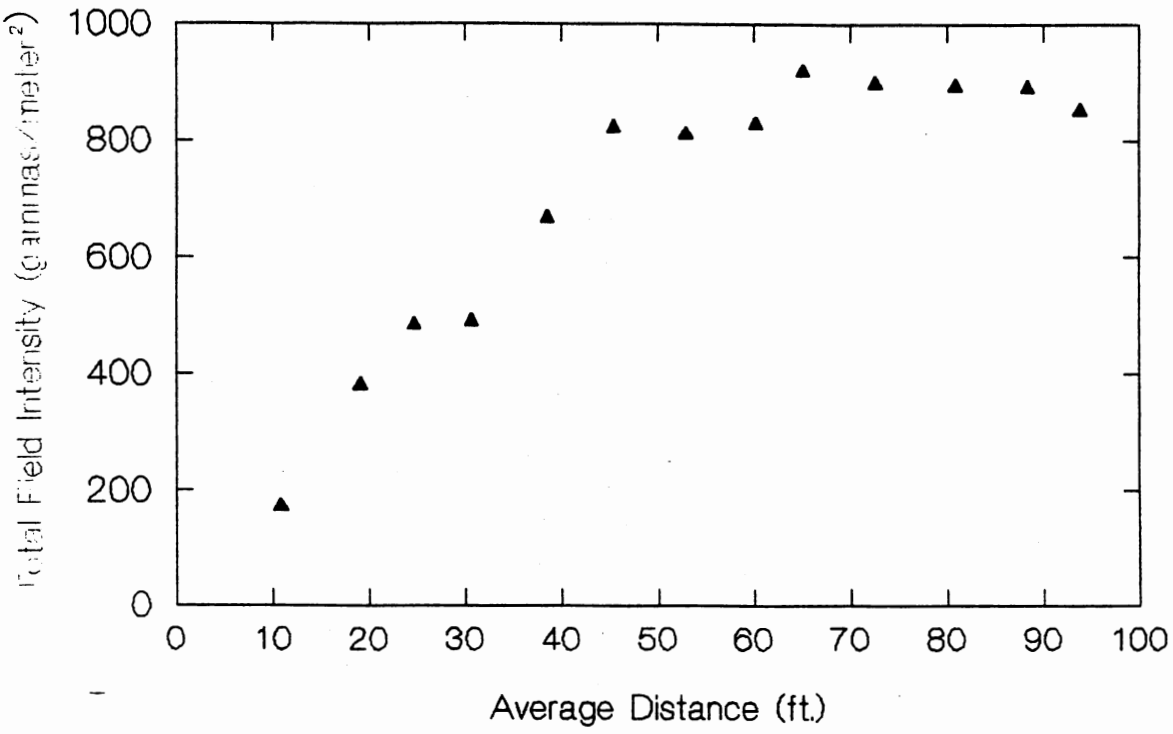

Figure 4 - Semivariogram for the Total Magnetic Field Intensity

TABLE IV

SEMIVARIANCE ANALYSIS OF VERTICAL MAGNETIC GRADIENT

Distance Range (ft.)	Number of Semivariance Pairs	Gamma $\gamma(h)$	Average Distance (ft.)
7 - 14	1633	2960	10.78
14 - 21	2091	4120	19.02
21 - 28	2001	4250	24.62
28 - 35	3404	4250	30.61
35 - 42	4650	4320	38.55
42 - 49	3518	4560	45.41
49 - 56	6367	4350	52.91
56 - 63	4048	4270	60.20
63 - 70	4646	4430	65.08
70 - 77	7088	4360	72.57
77 - 84	6994	4200	80.84
84 - 91	6285	4120	88.31
91 - 98	5077	4190	93.84
98 - 105	7232	4020	100.72

The semivariogram of the vertical magnetic gradient data, displayed in Figure 5, had distinctly different features from that of the idealized semivariogram form. The most prominent feature was the dominance of the sill feature. With the exception of one or two of the semivariance points at the

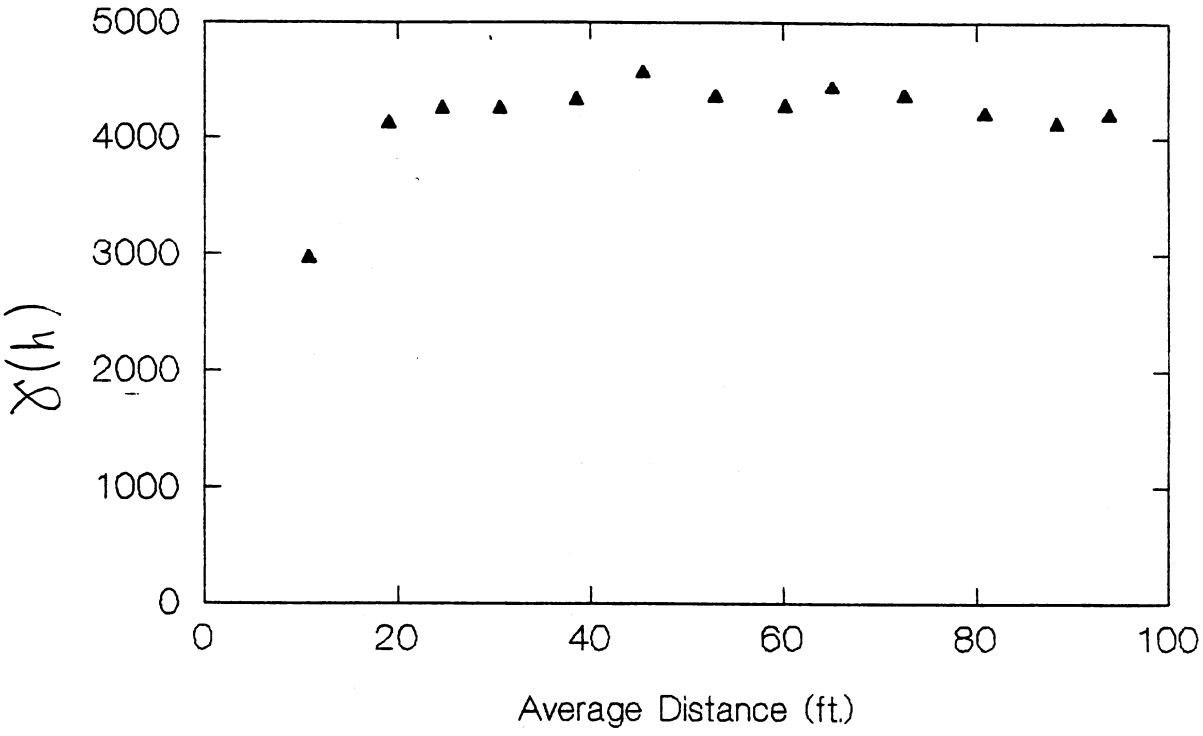

Figure 5 - Semivariogram for Vertical Magnetic Gradient

shortest separation intervals (10.78 and 19.02 ft respectively), the entire semivariogram appeared to reside at or near the sill (the 4300 level). This is commonly referred as "pure nugget effect". The implications from analysis of this semivariogram are as follows:

1) The range of influence for the vertical magnetic gradient was very short. Measured semivariance values that were separated by more than approximately 20 feet were statistically independent.

2) With this particular sampling support, about 2960/4300 or 69% of the

semivariance (covariance) was unaccounted for at the smallest discrete semivariance, indicating that this proportion of the semivariance occurred at separation distances less than 10.78 feet. This implies that the 10 foot sample spacing used for the support system was inadequate to define a significant portion of the spatial structure of the vertical gradient. A survey with a shorter incremental spacing was necessary to define the spatial structure.

3) In an operational sense, any attempt to find a unique solution for the semivariogram of the vertical magnetic gradient was impossible using the available information. Because the spatial structure at distances less than the range of influence was defined only by one or two discrete data points, an infinite number of mathematical functions could be devised to fit them. It was possible however, to treat the uncertainty and variability of the parameters characterizing the semivariogram structure as parameters of a random function in a recursive quasi-Bayesian methodology. Chapter 2 deals with the viability of this approach.

Anisotropy of the Semivariograms

An isotropic medium or model will exhibit the same behavior regardless of its directionality. The medium is said to be anisotropic when its variability is not equal in every direction. If x represents a point in the two dimensional space (x_u, x_v), and $|h|$ is the scalar value of a displacement vector h, then this system can be transformed to a polar coordinate system $(|h|, 0)$, where 0 is the counter clockwise angular rotation from due east. Determination of the degree of anisotropy of the semivariogram of both total magnetic field

intensity and vertical magnetic gradient has been accomplished by the construction of an anisotropy ellipse (Journel and Huijbregts, 1978).

The anisotropy ellipse was generated by the observation of directional semivariograms. Directional semivariograms were developed by calculating the directional experimental semivariances by using (16) at 30 degree angular increments from due east and within angular windows of 15 degrees. From each of these directional semivariograms the range of influence parameter was estimated. They are listed in Table V and show the ranges of influence for each angular increment with the uncertainty factor associated with the estimates.

The estimated range of influence parameters were plotted on a polar coordinate graph of range of influence vs. 0 for both regional variables (reference Appendix B). There was an intrinsic uncertainty associated with the estimation of the range of influence parameters, due to the discrete nature of the individual semivariance values. The value of the range of influence parameter could have been chosen at any point between the two discrete semivariances nearest the apparent sill. An example of this uncertainty is illustrated in Figure 6. Figure 6 shows the directional semivariogram for the 60^0 direction counterclockwise from due east. This semivariogram displays a sill at distances greater than the discretely sampled 63.63 foot separation distance. The uncertainty inherent in determining the "actual" range of influence for this case is the distance between the 63.63 distance and the next lowest discretely sampled point, which is at 58.57 feet. Therefore the uncertainty in the range of influence for this semivariogram is 4.06 feet, which is shown in Figure 6 as the bracketed space.

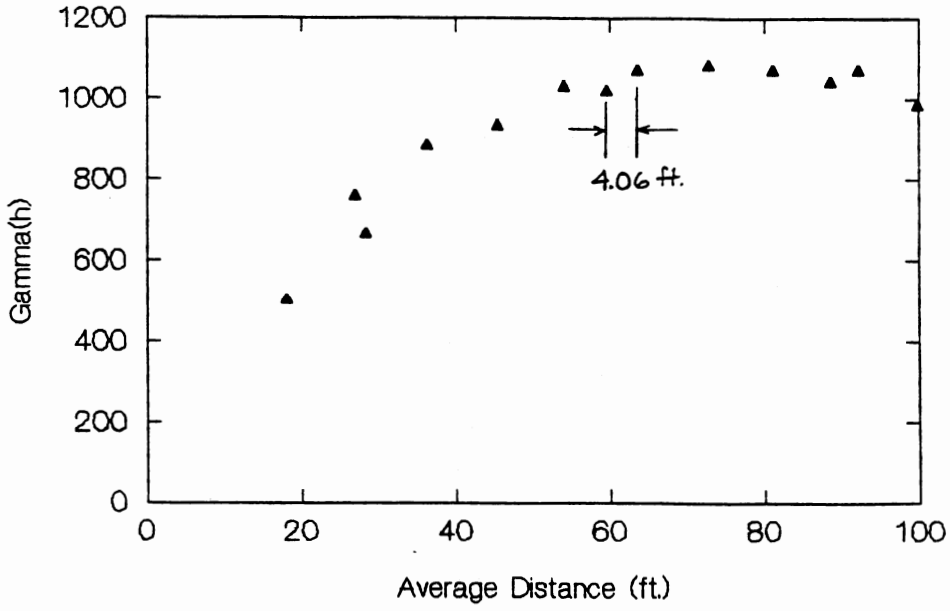

Figure 6 - Directional Semivariogram for the 60^0 Direction Counterclockwise from Due East.

TABLE V

RANGES OF INFLUENCE FOR THE DIRECTIONAL SEMIVARIOGRAMS

Angle (degrees)	Total Field Intensity		Vertical Gradient	
	Range of Influence (ft.)	Uncertainty (ft.)	Range of Influence (ft.)	Uncertainty (ft.)
30	58.77	6.10	30.88	8.52
60	63.63	4.06	26.93	8.90
90	65.08	4.88	24.62	5.50
120	63.63	4.08	26.93	8.90
150	58.77	6.10	30.88	8.52
210	58.77	6.10	30.88	8.52
240	62.65	8.68	26.93	8.90
300	62.65	8.68	26.93	8.90
330	58.77	6.10	30.88	8.52

The ratios of the semi-major to the semi-minor axes of the ellipses are 1.107 for the total magnetic intensity data and 1.254 for the vertical magnetic gradient data. The inherent uncertainty of the estimates would permit the construction of anisotropy ellipses for both variables that each had a ratio of 1.0 (circular), indicating isotropic conditions. Therefore the total field intensity and vertical gradient variables were considered isotropic.

Estimation by Kriging

Kriging is a mathematical procedure used to estimate the value of a regional variable at any unsampled location. Kriging utilizes the information provided by the semivariogram model to establish a linear estimator. The mathematics leads to a set of simultaneous equations, similar in form to a multiple linear regression. Punctual or ordinary kriging is the simplest form of the procedure, where second order stationarity or the intrinsic hypothesis is assumed. Universal kriging refers to the same process except that a non-stationary component is present in the regional variable. When this occurs it is necessary to estimate the drift and remove it mathematically from the original data to produce a stationary residual. The estimation process can then use the punctual kriging procedure to produce an estimate of the stationary surface. The kriged estimate is then added to the drift function to produce the non-stationary estimate.

Kriging uses the assumption that the value of a regional variable at an unsampled location may be estimated by a weighted average of the known observations that are within the neighborhood of the unsampled location. That is, the value at a point p is based on a weighted average of a small set of nearby known control points:

$$Y'_p = w_1 Y_1 + w_2 Y_2 + w_3 Y_3 + \ldots + w_n Y_n \qquad (32)$$

where Y'_p is the estimated value for the regional variable at point p; Y_1, Y_2, Y_3, ... Y_n are the individual values for the regional variable at the measured observations; while w_1, w_2, w_3, ... w_n are the individual weighting factors. The estimate that this procedure provides will differ from the actual, but unknown, value Y_p by an amount which is called the estimation error:

$$\text{Estimation error} = e'_p = (Y_p - Y'_p) \qquad (33)$$

If the weights used in the estimation of Y'_p sum to one, i.e. $w_i = 1.0$, then the resulting estimates are unbiased when order 2 stationarity applies. This means that in a statistical sense, the <u>average</u> estimation error will sum to zero, as the cumulative overestimates and underestimates tend to cancel each other out. That is, if numerous estimations were made using the same procedure, the average error will be zero: $\sum e'_p = 0 \qquad (34)$

The reliability of the estimation process can be measured by examining the distribution of the resulting errors. If the errors are consistently close to zero, then the estimation process is good. Conversely, if the spread of the errors is large (approaching the standard deviation of the variable), the estimator will be less reliable. This spread or scatter can be defined by examining the variance of the error parameter (Clark, 1979)

$$\begin{aligned} \text{Variance of the errors} &= \sigma_e^2 \\ &= \text{average squared deviation from the mean error} \\ &= \text{average of } (e_p - e'_p)^2 \\ &= \text{average of } (Y_p - Y'_p)^2 = 2\gamma(h) \qquad (35) \end{aligned}$$

Therefore we can use the previously derived semivariance to define the error variance as twice the value of the spatial semivariance function at that separation distance.

There are an infinite number of combinations of weights that could be chosen to calculate an estimate. Each assemblage of weights will yield a different estimate and error variance. The key precept in the kriging procedure hinges on the fact that only one combination of weights will yield a minimum error variance. Kriging is referred to as a best linear unbiased estimate. The derived weights are "best" in the sense that the resulting estimates are unbiased (given second order stationarity) and will results in a minimum estimation variance. The optimal values for the weights can be found by solving a set of simultaneous equations which incorporates values from the structural model of the semivariogram. The expression for the error variance depends on three factors:

{error variance of the estimate} = f(support, model, weights) (36)

For any given support and with the semivariogram model determined, the error variance can only change by altering the values of the assigned weights. To minimize the error variance the error variance function is differentiated with respect to the weighting factors:

$$\partial(\sigma_e^2)/\partial w_i = 0 \qquad (37)$$

Completing the differentiation process yields n equations of the form:

$$\begin{aligned}
&w_1\gamma(h_{11}) + w_2\gamma(h_{12}) + w_3\gamma(h_{13}) + \ldots + w_n\gamma(h_{1n}) = \gamma(h_{1p})\\
&w_1\gamma(h_{21}) + w_2\gamma(h_{22}) + w_3\gamma(h_{23}) + \ldots + w_n\gamma(h_{2n}) = \gamma(h_{2p})\\
&w_1\gamma(h_{31}) + w_2\gamma(h_{32}) + w_3\gamma(h_{33}) + \ldots + w_n\gamma(h_{3n}) = \gamma(h_{3p})\\
&\quad\vdots\qquad\quad\vdots\qquad\quad\vdots\qquad\quad\vdots\qquad\quad\vdots\\
&w_1\gamma(h_{n1}) + w_2\gamma(h_{n2}) + w_3\gamma(h_{n3}) + \ldots + w_n\gamma(h_{nn}) = \gamma(h_{np})
\end{aligned} \qquad (38)$$

At this point, there are n equations to calculate for the n number of weighting factors. Another equation is needed to incorporate the constraint of the unbiased estimate: $w_1 + w_2 + w_3 + \ldots + w_n = 1.0$ (39)

Thus, to obtain the "best linear unbiased estimate" it is necessary to to minimize the equation $o_e^2 - \lambda(\sum w_i - 1)$ with respect to $w_1 \ldots w_n$, and λ, where λ is the Lagrange multiplier. The complete set of kriging equations can be rearranged into a generalized matrix of the form:

$$\begin{bmatrix} 0 & \gamma(h_{12}) & \gamma(h_{13}) & \ldots & \gamma(h_{1n}) & 1 \\ \gamma(h_{21}) & 0 & \gamma(h_{23}) & \ldots & \gamma(h_{2n}) & 1 \\ \gamma(h_{31}) & \gamma(h_{32}) & 0 & \ldots & \gamma(h_{3n}) & 1 \\ \ldots & \ldots & \ldots & \ldots & \ldots & \ldots \\ \gamma(h_{n1}) & \gamma(h_{n2}) & \gamma(h_{n3}) & \ldots & 0 & 1 \\ 1 & 1 & 1 & \ldots & 1 & 0 \end{bmatrix} \begin{bmatrix} w_1 \\ w_2 \\ w_3 \\ \ldots \\ w_n \\ \lambda \end{bmatrix} = \begin{bmatrix} \gamma(h_{1p}) \\ \gamma(h_{2p}) \\ \gamma(h_{3p}) \\ \ldots \\ \gamma(h_{np}) \\ 1 \end{bmatrix} \quad (40)$$

which can also expressed as: $[A][w] = [B]$ (41)

The weighting factor vector can be solved via:

$$[w] = [A]^{-1}[B] \quad (42)$$

The diagonal terms in the matrix [A] are all equal to zero because the semivariance of a point with respect to itself is zero by definition. The gamma terms in the matrices are taken directly from the semivariogram or covariogram model. Once the weights have been determined by the solution of the equation (31), the value of the regional variable at location p can be estimated by (22). The estimation variance is determined by (25) as twice the weighted summed semivariance at point p, i.e.

$$s_e^2 = 2[w_1\gamma(h_{1p}) + w_2\gamma(h_{2p}) + \ldots + w_n\gamma(h_{np})] \quad (43)$$

Kriging not only produces estimates which have the smallest possible squared error, but also produces an explicit determination of the magnitude of this estimation error. The generation of the error variance is the feature of kriging which makes it preferable to other interpolation methods.

The key variable in deriving the kriging estimator and the error

variance of the estimate is the semivariogram model. A poorly devised or incorrectly chosen semivariogram model will produce unreliable estimates. Fortunately, since kriging uses only a specified number of the nearest neighboring samples in the estimation, the semivariogram needs to be accurate only within the first few lag distances that encompass the range of influence. A missing element in the kriging methodology lies in the assumption that no error or variance is present at the sampled points within the support of the regional variable. In actuality there is some error inherent in measuring the regional variable or the regional variable may possess temporal stochastic qualities at defined points in the spatial sampling space. Meteorological variables such as rainfall, barometric pressure, humidity, et.al. are prime examples of regional variables which possess both spatial and temporal stochastic properties.

The process of kriging estimation for interpolation of a regionalized variable includes:

1) definition of the regionalized variable and its support;

2) calculation of the experimental semivariogram values;

3) development of a suitable model for the semivariance to account for all separation distances within the range of influence;

4) application of the semivariogram model to develop the kriging equations in matrix form to obtain the values of an optimum set of weighting factors which minimize the estimation variance;

5) from the derived weights, determination of the estimates and error variances at interpolated points within the support.

Structural Analysis of the Total Magnetic Field Intensity Semivariogram

The next step in the kriging procedure was to define a suitable semivariogram model for the total magnetic field intensity (the analysis of the spatial structure of the vertical gradient semivariance will be treated with a Bayesian type analysis in Chapter 2). The structural model $\gamma(h)$ was made up of the nested sum of N isotropic individual structures:

$$\gamma(h) = \sum_i \gamma(|h_i|), \quad i = 1 \text{ to } N \tag{44}$$

where each of the nested structures were described by equations (28) through (31). In practice, it is unusual that more than two nested structures are necessary to provide a workable spatial structure for the semivariogram. As before, this approach required stationarity of order 2 or the intrinsic hypothesis to be valid for interpolation via kriging. The previous analysis verified a statistical basis for the stationarity of the regional variables.

The derivation of a suitable structural model has been accomplished using the following methodology:

1) assumption of a model using the equations (16) through (20);

2) estimation of the parameters of some semivariance models by visual comparison with experimental semivariance data. This process resulted in some approximate solutions which were then subjected to more rigorous quantitative validation techniques, and;

3) estimation of the "goodness of fit", of the model / parameter set through cross-validation procedures, comparative statistical tests, and diagnostic tests.

The cross-validation procedures were made by a point-by-point suppression technique. In this method a point was removed from the data set, and its value was estimated by kriging the remaining data. The deleted point was

then replaced in the data set, and another point deleted and estimated as before. This procedure was repeated until all data points were predicted using this method. A statistical comparison between the original data points and the kriged estimates of these data points was then performed. The following criteria (as suggested by the STATPAC software) were used to evaluate the viability of individual model.

1) The mean kriging error (observed value - estimated value) should be close to zero (cumulative under and overestimates cancel).

2) The standard deviation of the kriging errors should be lower than the standard deviation of the regional variable.

3) The standard deviation of the standardized errors should be close to 1 plus or minus a factor of 2*sqrt(2/n). (Delhomme, 1978)

4) The standardized errors should be independent of their kriged estimates (Journel and Huijbregts, 1978).

5) a) The kriged estimates should be relatively free of drift, i.e. should be non-correlated (correlation coefficients close to zero) with the east and north coordinates of the grid.

b) The kriging errors should also be free of drift.

6. The kriged estimates should have high correlation coefficients (close to 1.0) with the original observed values.

After many iterative attempts to arrive at reasonably viable models for estimating the total magnetic field intensity experimental semivariogram by visual inspection alone, 3 models (2 of the spherical type, 1 of the gaussian type) were chosen for the quantitative cross-validation procedures summarized above. Table VI details the model and parameter specifications. The C_0, C, and <a or a'> parameters in Table VI refer to the nugget effect,

sill, and range of influence parameters from equations (28) through (31). Appendix C presents the graphical relationships of the individual models with respect to the experimental semivariance values.

TABLE VI

MODEL PARAMETERS FOR THE TOTAL FIELD INTENSITY SEMIVARIOGRAM

Model Number	Model Type	Model Parameters		
		C_o	C	a or a'
1	Spherical	0	935	75
2	Spherical	0	910	75
3	Gaussian	80	910	33

Table VII lists the cross-validation statistics for the model forms specified in Table VI. Listed next to the heading for each of the statistical parameters is the "ideal" value for that particular statistic as outlined above, which was used for the evaluation process of the individual models. This analysis was used to choose the semivariance model which best condensed the structural features of the total magnetic field intensity regional variable into an operational form to be used in the kriging procedure.

As shown by Table VII, Model 1 had the superior overall cross validation statistics of the three. It was chosen to represent the semivariance structure for the total magnetic field intensity. The mathematical representation of this model was:

$$\gamma(h) = 935\{(3/2)(h/75)-(1/2)(h^3/(75)^3)\} \qquad (45)$$

Notable is the fact that all three models produced estimates which were very highly correlated with the measured values of the regional variable. This

TABLE VII

CROSS-VALIDATION STATISTICS FOR TOTAL FIELD INTENSITY SEMIVARIOGRAM MODELS

Statistic	Ideal Value	Model 1	Model 2	Model 3
Mean Kriging Error	0.0	-0.0046	0.0325	-0.0867
Standard Deviation of the Errors	< 29.242	9.928	10.753	11.195
Standard Deviation of the Standard Error	< 1.1179 and > 0.8821	0.8086	0.8882	1.1139
Standard Error / Estimate Correlation Coefficient	0.00	0.09	0.14	0.01
Kriged Estimate / East Correlation Coefficient	0.00	-0.01	0.13	-0.01
Kriged Estimate / North Correlation Coefficient	0.00	-0.01	-0.12	-0.01
Kriging Error / East Correlation Coefficient	0.00	0.00	0.00	0.00
Kriging Error / North Correlation Coefficient	0.00	0.00	0.00	0.00
Measured Value / Kriged Estimate Correlation Coeff.	1.00	0.93	0.92	0.91

indicated, in a preliminary sense, that the probabilities of producing reliable estimates at interpolated locations within the sampling support were quite good. Now that proof of a homogenous, stationary, isotropic data set has been

verified, and a semivariogram model which satisfactorily estimated the experimental data has been established, the creation of an interpolation grid within the Western Processing total field intensity magnetometer survey was achievable.

Kriging of the Total Field Intensity Data

The measured grid of the magnetometer surveys were spaced at 10 foot separation distances in repeating triangular patterns, as previously explained. The grid of estimated total magnetic field intensity within the measured grid was chosen as to provide a 5 foot homogenous orthogonal spacing. This arrangement provided 3 kriged estimates for every 1 measured data point. One of the primary objectives for the implementation of the magnetometer surveys were to help delineate possible locations of the buried steel drums within the site. The original locations of the drums were located by way of (unspecified) soil sampling techniques. The depths of the individual drums, an important consideration in the consideration of the magnetic responses, were unrecorded at the time. Comparisons between these drum locations and the kriged estimates were attempted to measure the effectiveness of the estimation procedure. Figure 7 shows the locations of the measured data points of the magnetometer surveys, the kriged estimates, and the drums. In order to examine the effectiveness of the kriged estimates in a detailed manner, the areas that are within the vicinity of the drum caches were detailed. Areas 1 and 2, where the detailed examinations occurred, are also captioned in Figure 7.

The kriged estimates for the each of the individual points were calculated by (32), with the weights determined by (42) and utilized

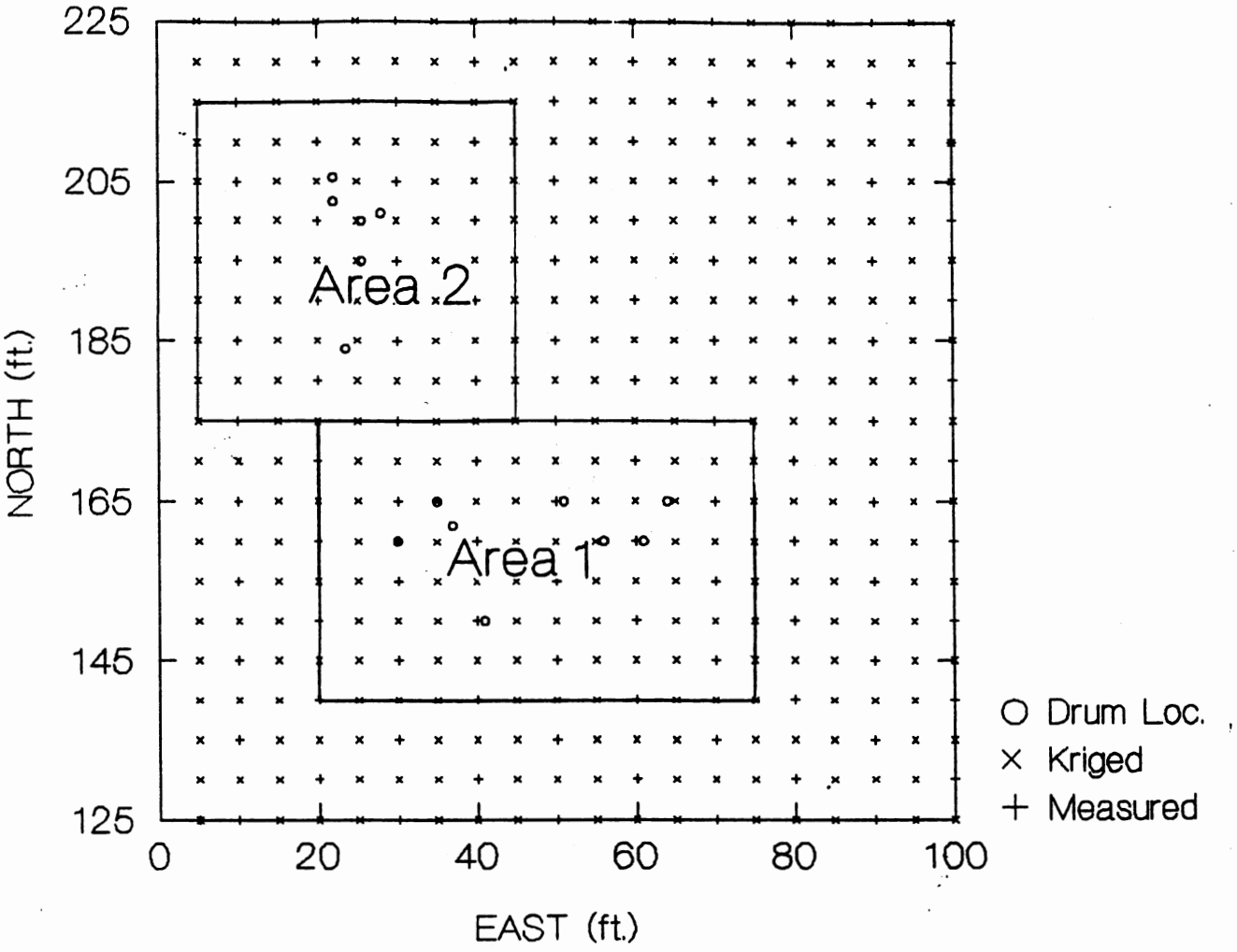

Figure 7 - Western Processing Superfund site / locations of measured values and kriged estimates for the magnetometer surveys and buried drum locations.

semivariance values derived from the model function (45). The estimation variances for the individual kriged estimates were determined by (43) which also employed (34). Figure 8 presents a shaded block map of the total magnetic field intensities for the measured data only, using a block density centered on the measured samples. Figure 9 displays a shaded block map using both measured and kriged values over the same portion of the Western Processing site. The increased block density for Figure 9 directly reflects

the increased density of spatial interpolations provided by the kriged estimates.

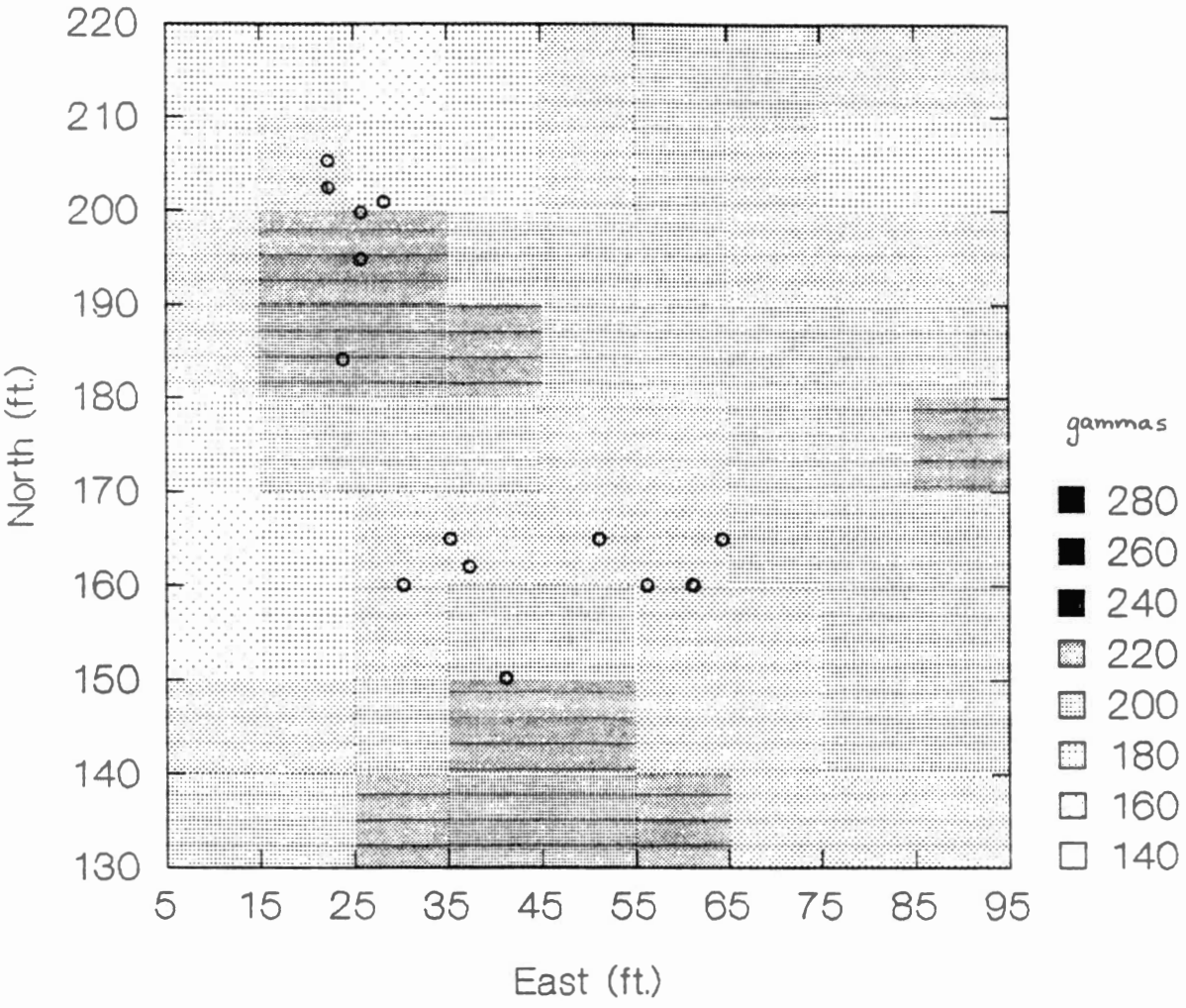

Figure 8 - Total magnetic field intensity shaded block map using the measured values only

The most distinctive features in Figures 8 and 9 were the presence of two anomalous areas of unusually high total magnetic intensity values. These total field intensity anomalies were located relatively close to the drum caches that were discovered. Note that individual drums could not be

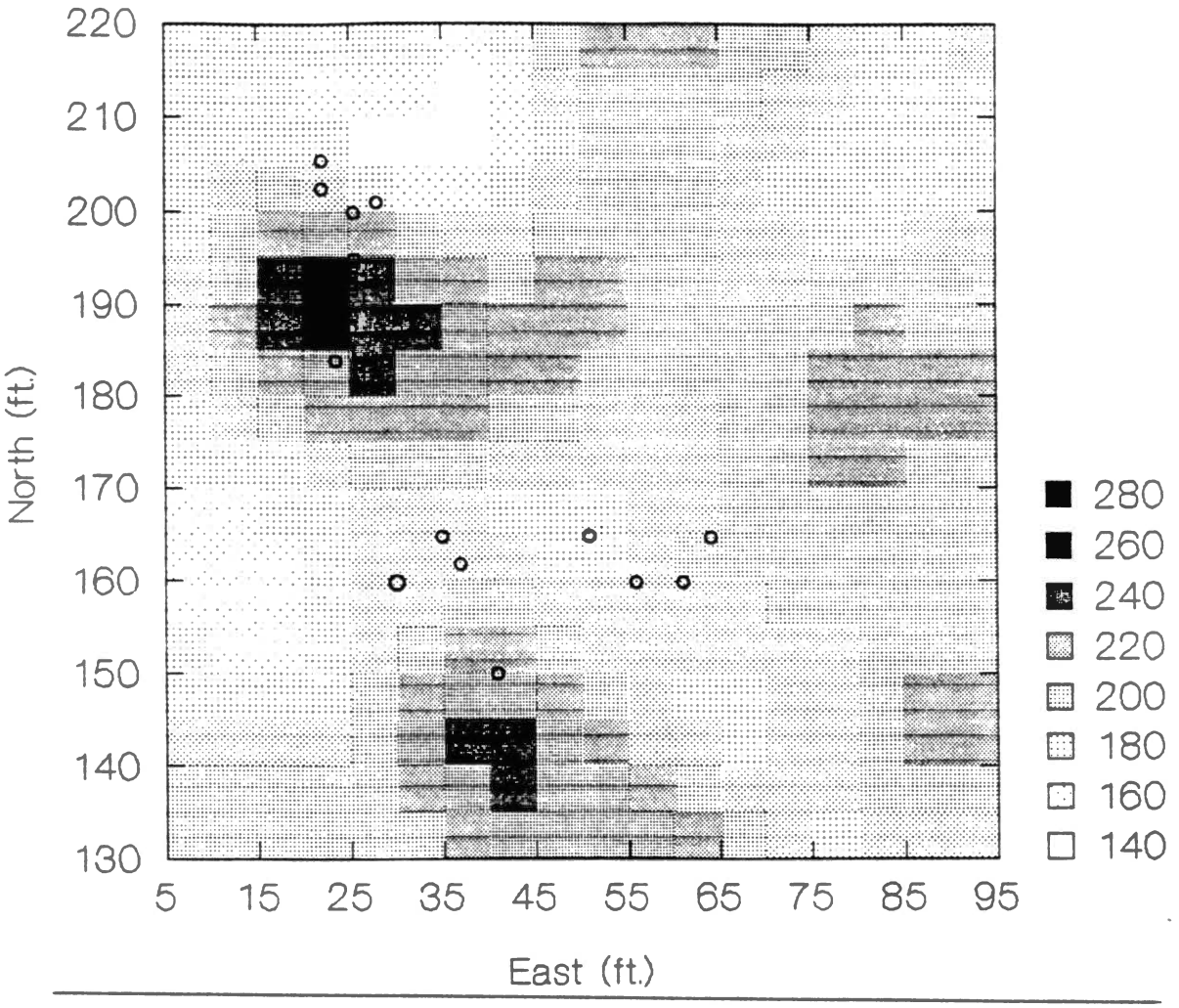

Figure 9 - Total magnetic field intensity shaded block map using both measured and kriged values

identified and that the drums seem to produce a "composite" response in total magnetic field intensity when displayed in this manner. Also notable was the observation that the anomalies seemed to be skewed to the south of the actual drum locations. As it may be expected, Figure 9 showed a more "detailed", i.e. spatially complex, picture of the potential field surface because of the increased spatial density of data points (4 times as many). The degree of validity of the kriged estimates relative to the measured data required quantitative verification. In order to obtain a more complete

evaluation of the effectiveness of the kriged estimates within this support, the following procedure was used.

1) The kriged and measured values were inspected in terms of their statistical parameters (mean, variance, et.al.) and their probability density functions to see if they preserved the statistical characteristics of the regional variable;

2) The individual kriged and measured values relative to the positions of the buried drums were examined in detail. Some generalized expectations of induced magnetic anomalies from buried drums were derived from independent empirical studies. The expected characteristics of the anomalies were compared to the configuration of the resultant anomalies using the composite map made up of the measured and kriged values (Figure 9).

Statistical Properties of the Kriged Values of the Total Magnetic Field Intensity

The univariate statistical properties of the measured total magnetic field intensity measurements and the kriged estimates used to interpolate between the measured values are presented in Table VIII. The key assumption made was that the set of measured values of the total magnetic field intensity accurately represented the population statistics of that variable (central limit theorem). The validity of any set of estimated values which interpolate between measured values should preserve the inherent statistical properties of the regional variable. Conversely, if the estimated values differed significantly in their univariate statistical properties relative to the measured values, then the effectiveness and validity of those

estimated values must be questioned.

TABLE VIII

UNIVARIATE STATISTICAL PARAMETERS OF TOTAL MAGNETIC FIELD INTENSITIES AND ITS KRIGED ESTIMATES

Statistical Parameter	Measured	Kriged	% Difference
Range of Values	139.10	117.43	15.6
Mean	196.81	196.23	0.30
Median	196.70	196.75	0.02
Standard Deviation	23.06	19.91	13.6
Standard Error	2.250	1.122	50.2
Skewness	0.326	0.254	22.0
Kurtosis	1.003	0.088	91.2
Coeff. of Variation	0.117	0.101	13.7

The comparison between the measured vs. kriged statistical properties shows that the indicators of central tendency (mean and median) were virtually identical for both measured and kriged data. Antithesis to this were the measures of dispersion of the probability distributions (standard deviation and standard error). The dispersion properties of the kriged estimates were all less than that of the measured samples. Skewness, the measure of symmetry of the distribution, was slightly positive in each of the data sets. The kurtosis statistics indicated that both the measured and estimated values displayed platykurtic characteristics, i.e. "flatter" than a normal distribution with the same mean and variance (the criteria being <3.0). The kriged estimations magnified this effect when compared to the measured data. The net result is that the kriged estimations displayed a probability distribution which emulated the characteristics of a uniform distribution. The kriged estimates maintained the central tendencies very well and reduced the dispersivity characteristics. This "smoothing" effect on

the distribution of the estimates appeared to result from the use of the linear weighted estimator in the kriging process. The kriged estimates seemed to be more likely to provide interpolated values which reside near the center tendency and less likely to provide values at the extreme ends of the original probability distributions for the measured regional variable. The probability distributions for the measured and kriged estimates for the total magnetic field intensity are shown in Appendix D.

Results of the Measured and Kriged Total Magnetic Field Intensity with Respect to Analytic and Empirical Geophysical Models

Since the effectiveness of the kriged estimates can be evaluated in a retrospective manner, by knowing the locations of the buried drums which were found within the Western Processing site, it was important at this point to explain the analytical factors involved in the expression of the earth's geomagnetic field. Several empirical studies have been found which had the purpose of identifying the magnetic expressions of 55 gallon steel drums in the ambient geomagnetic field.

In a worldwide scope, the geomagnetic field resembles a single axial dipole with the North and South magnetic poles acting as the positive and negative poles of the magnetic dipole. The average strength of this field varies from 60,000 gammas near the poles, where the direction of the magnetic vector is nearly vertical, to approximately 25,000 gammas near the equator where its direction parallels the earth's surface. The cause of the geomagnetic field is not precisely known but is speculated to result from electrical currents derived from convection occurring in the earth's outer core (Telford, et.al, 1982). At any locality the geomagnetic field can be

completely described by 4 parameters, its intensity, gradient, inclination (angular component from the horizontal), and declination (azimuthal deviation from geographic north). Magnetic fields are vector fields and proton precession magnetometers, the type used in the Western Processing survey, have the ability to measure the maximum intensity of the geomagnetic field regardless of its inclination and declination. Magnetic induction is the physical process by which a body, placed in an external magnetic field, is itself magnetized by induction. The induced field is oriented parallel to the external or ambient magnetic field. The degree to which a body is magnetized by induction is a complex function with many factors, but is dominated by its mass and a material property known as the magnetic susceptibility. The effective magnetic susceptibility, k_{eff}, is a dimensionless proportionality constant which relates the magnitude of the induced magnetization, I, to that of the external field, E, where:

$$I = E\, k_{eff} \tag{46}$$

The effective susceptibility is related to the material susceptibility, k_{mat} by:

$$k_{eff} = k_{mat} / (1 + \sigma k_{mat}) \tag{47}$$

where the factor σ, is known as the demagnetization factor (Grant and West, 1965). The demagnetization factor is a function of the shape and orientation of the object in the external field. For an object with a defined geometry and orientation relative to the external field, the relationship between the effective and material susceptibilities yields a unique functional curve (Strangway, 1967). When k_{mat} is very low (< 0.05), as is typical for almost all soils and rock units (with the exception of certain metallic ore bodies), the material and effective susceptibilities are essentially equal. However, ferrous materials such as steel or iron typically have material susceptiblilties which

are in the tens or hundreds, which has the net effect of limiting the effective susceptibilities of 55 gallon steel drums by demagnetization to a few tenths (Barrows and Rocchio, 1990). There are other factors which further limit the ability to model the magnetic response of buried drums. Algorithms are usually designed or built on the assumption that magnetization is uniform throughout easily definable geometric patterns, such as prisms, spheres, cylinders, etc., a situation that is unrealistic in landfill or hazardous waste studies. Many buried drums in landfills are also subject to physical deterioration and corrosion because of overburden pressure and chemical interactions with soil moisture. These factors reduce the effective susceptibility through the dual effects of both reducing the net material susceptibility and altering the geometric configuration of the individual drums. Another potentially significant complicating factor in the analysis of magnetic signatures is remnant magnetism. Remnant magnetism is a permanent magnetic moment per unit volume imparted to the steel during the manufacturing process. Therefore, buried steel drums will possess two magnetic fields which are superimposed on the geomagnetic field:

1) the induced magnetic field, which is proportional to the external field with the effective susceptibility being the proportionality constant, which in itself is a function of the object's geometry and orientation to the external field, and;

2) The remnant magnetic field, a permanent field which will vectorially be added to the induced magnetic and may have the net effect of adding to or reducing the anomaly from induction, depending on its orientation.

The mass is another significant factor in the magnetic response of buried

objects, being proportional to the overall strength of the resulting magnetic anomaly. Fifty five gallon steel drums uniformly weigh approximately 40 lbs. and the total mass of ferrous material in a drum cache could be approximated by some multiple of this amount. The most influential factor affecting the magnetic intensity, measured at the earth's surface, from an anomaly caused by buried drums is the depth of burial. The magnitude of a total field intensity anomaly decreases by the reciprocal of the depth to the center of mass cubed ($1/d^3$) and the magnitude of the vertical gradient anomaly decreases over the depth of burial to the fourth power ($1/d^4$) (Benson, Glaccum, and Noel, 1983).

A factor which influences the expression of magnetic anomalies in map view is the inclination of the geomagnetic field. The induced field produced from a buried steel drum is magnetized in the same vectorial direction as the geomagnetic field. The inclination of the geomagnetic field in the Western Processing area was approximately 69^0 from the horizontal and points toward the magnetic north pole. An anomaly caused by the induced field from a buried drum, measured at the earth's surface, will be located to the south of the actual location of the drums in a map view of the surveyed area. For a single discrete object, the lateral distance that the anomaly is skewed to the south, commonly referred to as "polar migration" by geophysicists (Spector, 1968), is equal to the distance between the magnetometer and the center of the inducing object divided by the tangent of the inclination of the geomagnetic field.

Magnetic "noise", or sources of magnetic flux due to factors other than the anticipated or expected targets (steel drums), is another compounding problem associated with the resolution of magnetic surveys.

Some sources of noise may include: miscellaneous metallic debris, buried pipes, electrical or telephone lines, fences, metallic sludges in soils, and others. In some cases the noise contamination in urban areas may seriously limit or totally obscure the resolution capability for locating buried drums. Fortunately, the Western Processing survey this did not appear to have a significant noise problem.

Obviously, the number of factors which affect the magnetic response of buried steel drums make it difficult if not impossible to evaluate magnetic anomalies through analytically derived deterministic models. For any given measured anomaly, a multitude of parameter configurations can be devised that will duplicate that anomaly. For hazardous waste investigations there is a future need to investigate modeling techniques which accommodate the range of variations (sensitivity analysis, Monte Carlo methods) displayed by the critical parameters in deterministic analysis, such as demagnetization. Until this is done, deterministic models for locating buried drums should be interpreted cautiously. The problem of non-uniqueness in inversion modeling can be somewhat mitigated by integrating analyses from other geophysical methods, such as inphase electromagnetic induction or ground penetrating radar surveys, which can also be used for drum detection (Benson, et.al., 1983).

The difficulties in ascertaining accurate deterministic models, for the reasons outlined above, has led to some empirical studies of the magnetic responses of buried steel drums. Tyagi and Lord (1983) studied the effects of orientation (demagnetization), drum density (number of drums in a cluster) at uniform depths of 4.5 feet, drum sizes at a uniform depth of 3.5 ft, and depth of burial for steel drums. The conclusions pertinent to this study were

that: 1) the depth detection limit for single drums was somewhere between 6 and 11 feet, 2) single drums had a lateral resolution limit of between 6 and 10 feet while a 3 drum cluster produced a single anomaly and had a lateral resolution of greater than 12 feet, 3) inclined drums produce anomalies that were 40-70% stronger than vertically oriented drums (demagnetization effect), and 4) the entire size range (2 - 55 gallons) of steel drums tested could be detected when zero offset data (survey transect passed directly over the drum) were used in the experimental procedure.

Barrows and Rocchio (1990) compared the magnetic signal of a 55 gallon steel drum to analytical models at an equivalent burial depth of 3 feet. The influence of demagnetization on the effective susceptibility of a steel drum under optimum conditions (drift and diurnal effects mathematically removed) was also investigated. The conclusions of their studies were: 1) anomalies from a single 55 gallon drum had a mean maximum intensity due to induction of about 50 gammas, 2) the effects of orientation of the drum altered the intensity of the anomaly by approximately 40%, 3) the mean total anomaly width was 22 feet, 4) crushing the drum to 1.1 ft^3 produced an anomaly only 30% as strong as the intact drum, and 5) the intact drums had a measured remanent magnetization which could be as large as the induced magnetization or as small as 40% while the crushed drum had negligible amount of remanent magnetization.

Benson, Glaccum, and Noel (1983) concluded that individual drums could be detected at distances up to 6 meters. This resulted in a burial depth of 12 feet because magnetometers are routinely suspended on 8 foot high aluminum poles to reduce the effects of soil variations and small metallic objects on the ground. Large piles of drums were found to be detectable at

depths exceeding 60 feet.

The relevant conclusions from these empirical studies were:

1) single drum anomaly width was approximately 22 feet under optimum conditions, i.e. tight clusters of drums had anomaly widths in excess of 30 feet,

2) closely clustered drums were represented magnetically by a single composite anomaly,

3) orientation of a drum (demagnetization effect) could cause a 40% change in anomaly strength,

4) single drums could be detected at depths up to 12 feet, large drum clusters at 60 feet, and

5) using a detectable range of burial depths of 0 to 60 feet, as indicated by the empirical studies, the polar migration distances of magnetic anomalies from vertical location of the buried drums would range from 3 to 23 feet at the Western Processing site.

This would account for the apparent separation between the maxima of the total field intensity anomalies and the locations of the discovered drums shown in Figure 9. The quantitative determinations of polar migration at the site are discussed in the next section. Since the drums were clustered at the Western Processing site, and consequently produced a single composite anomaly per cluster, a more reliable reference point would be that of the center of mass of the drum clusters. The precise information on depth of burial, orientation, remanent magnetism, and state of deterioration of the individual drums were not recorded upon discovery and removal actions at the Western Processing site. The only information recorded was the spatial distribution of the individual drums in map view. This permitted the

calculation of the center of mass for the drum caches. With the available information, the areal configurations of the magnetic anomalies were compared to the center of mass calculations.

Using the general expectations of steel drum magnetic anomalies from the empirical studies, a basis for comparison was established for evaluating the characteristics of the resultant anomalies detailed by the kriged estimates. The characteristics of the anomalies in terms of anomaly widths, maximum amplitudes, and polar migrations were computed. A key assumption used in the comparisons was that the sole source of ferrometallic materials at this site was the steel composition of the buried drums.

Comparisons of Total Magnetic Intensity Data Anomalies with the Centers of Mass of the Buried Drum Caches

Figure 7 showed Areas 1 and 2 captioned within the boundaries of the survey which have been examined in detail for location of the magnetic anomalies relative to the centers of mass for the drum caches that were present in each of these areas. Figures 10 and 11 represent maps of Areas 1 and 2 respectively. The individual measured and kriged values of the total magnetic field intensity were posted next to their locations. The drum locations and the center of mass were also plotted on these figures. The distances between the center of mass of the drum caches and the peak values in the anomalous region, identified by areas which have significant degrees of statistically deviant values, were used as the criteria for evaluating the relative value of the kriging process in extending the measured data set.

Observing the Area 1 map (Figure 10), it can be seen that the area

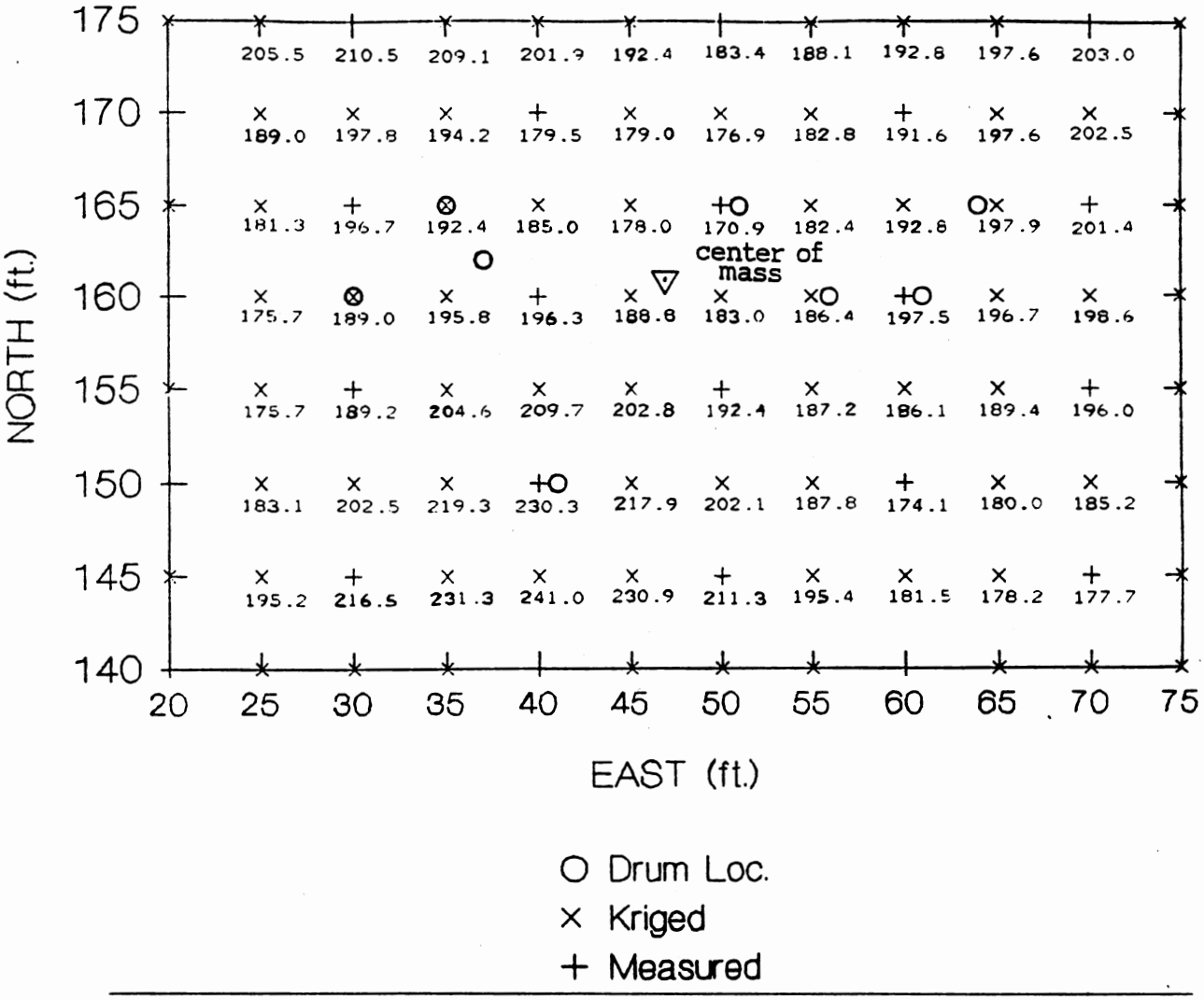

Figure 10 - Area 1 Total Magnetic Field Intensity Measured & Kriged Individual Values.

directly over the buried drums displays values which were equal or slightly less than the mean (within the range 170.9 to 197.9 gammas) with the exception of the drum located at (41,150), the southernmost drum in the cache. The highest measured value for the total field intensity occurred at (40,145) with a value of 241.0. This corresponded to 2.15 standard deviations above than the mean, greater than a 95% confidence limit for normally distributed data (Haan, 1977). This means that the maxima in Area 1 is

greater than approximately 95% of all of the values. This peak measured value was separated from the center of mass (as indicated by the inverted triangle) by a separation distance of 17.3 ft. This is the amount of polar migration of the anomaly in Area 1. It falls within the acceptable migration range of 3 to 23 feet. With a magnetic inclination of 69^0, this corresponds to an average depth of 37.06 feet. The highest kriged estimates had values of 231.3 and 230.9, nearly identical in value to the measured intensities and were located at (35,145) and (45,145), adjacent to the largest measured value by one sample space on its east and west sides. The separation between the largest kriged values and the center of mass of the Area 1 drum cache were 19.8 feet and 16.0 feet respectively. Again, these migration values are within the acceptable range (3 to 23 feet).

The closest measured and kriged values which are greater than one standard deviation (68% confidence limit) to the center of mass were used to indicate the location of the "flank" of the total field anomaly. For Area 1, these values were located at (40,150) and (45,150) respectively. This corresponds to 12.14 and 10.17 foot separations from the center of mass. These separation distances between the peak intensities and flanks of the anomaly with respect to the actual center of mass were due to the polar migration effect. They are all within the established acceptable ranges.

The Area 2 map (Figure 11), produced a more tightly clustered assemblage of buried drums and consequently a smaller, higher amplitude anomaly was observed. The drum cache area was transitional, with relatively low values trending (south) into an extremely high amplitude anomaly. The highest measured total field intensity value was 273.5 which occurred at (20,190). This value was the highest in the entire total magnetic intensity

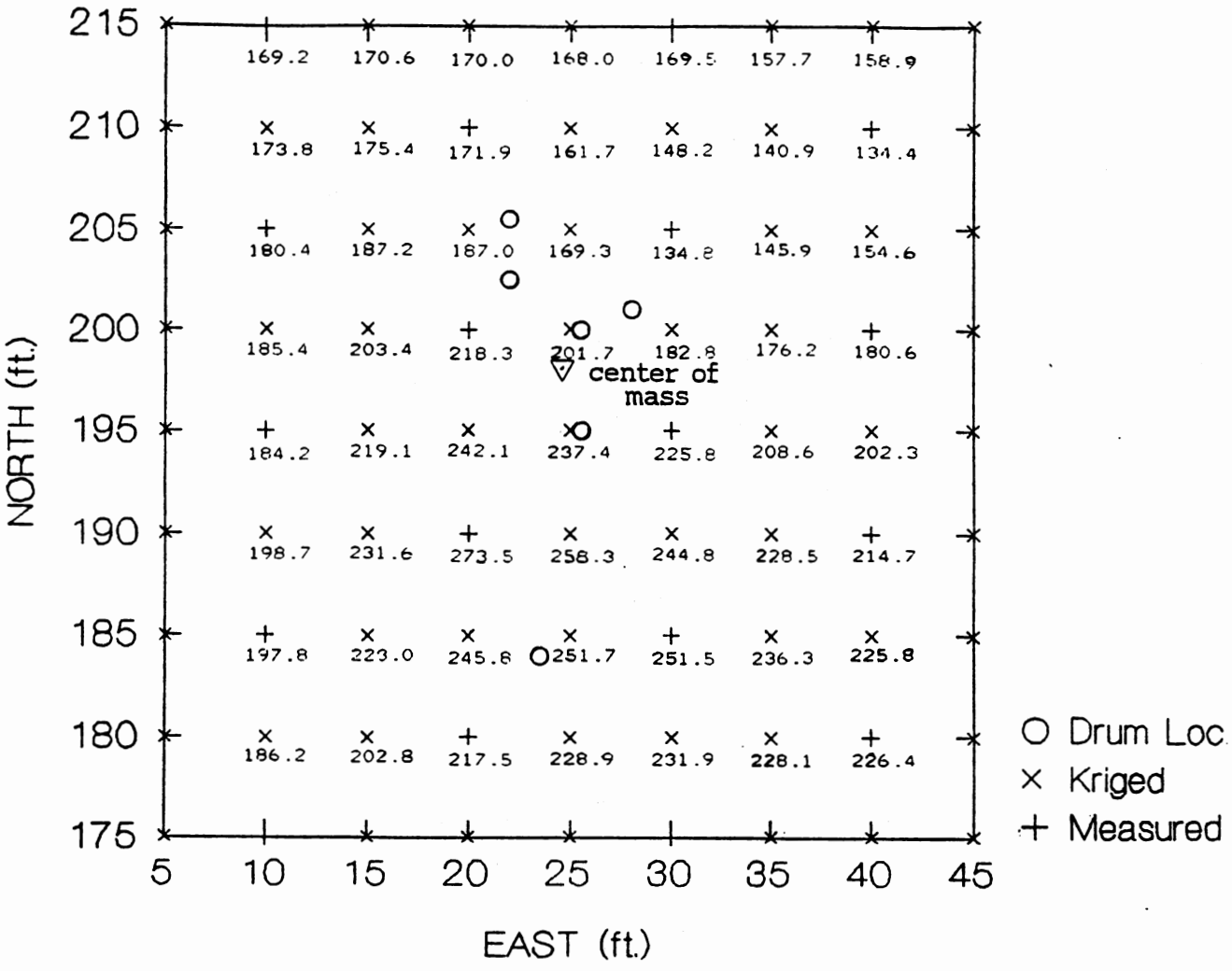

Figure 11 - Area 2 Total Magnetic Field Intensity Map of Measured and Kriged Values.

survey at 3.72 standard deviations greater than the mean. The separation distance between this point and the center of mass, at (24.4,198.0) was 9.13 feet. This was considerably closer than the corresponding 17.3 feet separation (polar migration) in Area 1. This value suggested an average depth of 15.9 feet for the buried drums in Area 2. The highest kriged estimate in Area 2 was located at (25,190), with a value of 258.3. The kriged estimates produced values which resided at less extreme values, i.e. closer

to the central tendency. The distance separating the highest kriged estimate from the center of mass of the drum cache in Area 2 was 8.0 feet, again considerably closer than the corresponding 16.0 feet separation in Area 1. The highest kriged estimates in Area 2 were at (20,195) and (25,195), with values of 242.1 and 237.4, and were 2.20 and 1.98 standard deviations greater than the mean. The closest measured and kriged estimates with values greater than one standard deviation above the mean (68% confidence interval) were located at (20,200) and (25,195). This corresponded to separation distances of 4.83 and 3.06 feet from the center of mass. Again, the location of kriged estimates with similar statistical properties resided slightly closer to the actual center of mass as compared to Area 1. Without knowing the depths, orientations, and remnant magnetizations of the individual drums, there is no way to determine whether the kriged values are more or less accurate than the measured data.

In both Area 1 and 2 the kriged interpolations had the net effect of shifting the center of the overall anomaly to a position which was closer to due south of the mass center, which would be expected to be the magnetic anomaly configuration via purely analytical considerations. The net result was that the kriged interpolation had the effect of "extending" the magnetic anomaly in the direction of the center of mass of the drum cache. The kriged estimates (compare Figures 8 and 9) provided an additional level of detail which allowed the size and shape of the anomalies to be determined.

Recall that the best fitting semivariance model used for the kriging estimator used a range of influence parameter of about 75 feet, which inferred that the values for total magnetic field intensity, where separated by less than this distance, were statistically correlated. Using the spherical

model, the estimates were highly correlated only at distances less than about 60 feet. Conversely, the magnetic anomalies in Areas 1 and 2, presumably caused by induced responses corresponding to the drum caches, displayed anomaly widths in the range of 30 to 35 feet. This may appear to be conflicting, but can be explained from the recognition that the experimental semivariogram was calculated from the entire support, not just the anomalous areas. From Figure 9 it can be seen that the anomalously high areas and the corresponding magnetic lows flanking them had similar values separated by approximately 50 to 65 feet. These separations appeared to be dominate the experimental semivariogram response.

The experimental semivariogram determined for the total magnetic field intensity (Figure 4) revealed a small nested structure at the 30.61 foot average separation distance. This point had statistical significance, being the mean of 3197 individual semivariances. This event possibly was a result of the expression of the width of the individual magnetic anomalies on the experimental semivariogram. This brings to question whether a model devised from a more "localized" experimental semivariogram, i.e. from a smaller drum containment area, could provide semivariograms which could better identify the spatial characteristics of the individual anomalies.

Methodology for the Evaluation of Localized Semivariance Models

Semivariograms were calculated for 1/2 of the total area (the southern half, containing Area 1). The derived model was used to krige the data for the other 1/2 of the total area (the northern half, containing Area 2). Comparing the estimates from this process with kriged estimates using the localized structural semivariance model for Area 1 and the model from the

entire survey (as previously determined) to krige Area 1 data identified unique semivariance relationships.

Kriging of the Total Magnetic Intensity Data Using Localized Semivariance Models

Experimental semivariances were subsequently calculated for each of the drum cache areas separately. Using the procedures outlined in the previous sections, models were developed to characterize the semivariance structures for use in the equations for kriging estimation (32) and kriging error (43). The model generated to represent the semivariance for the northern half of

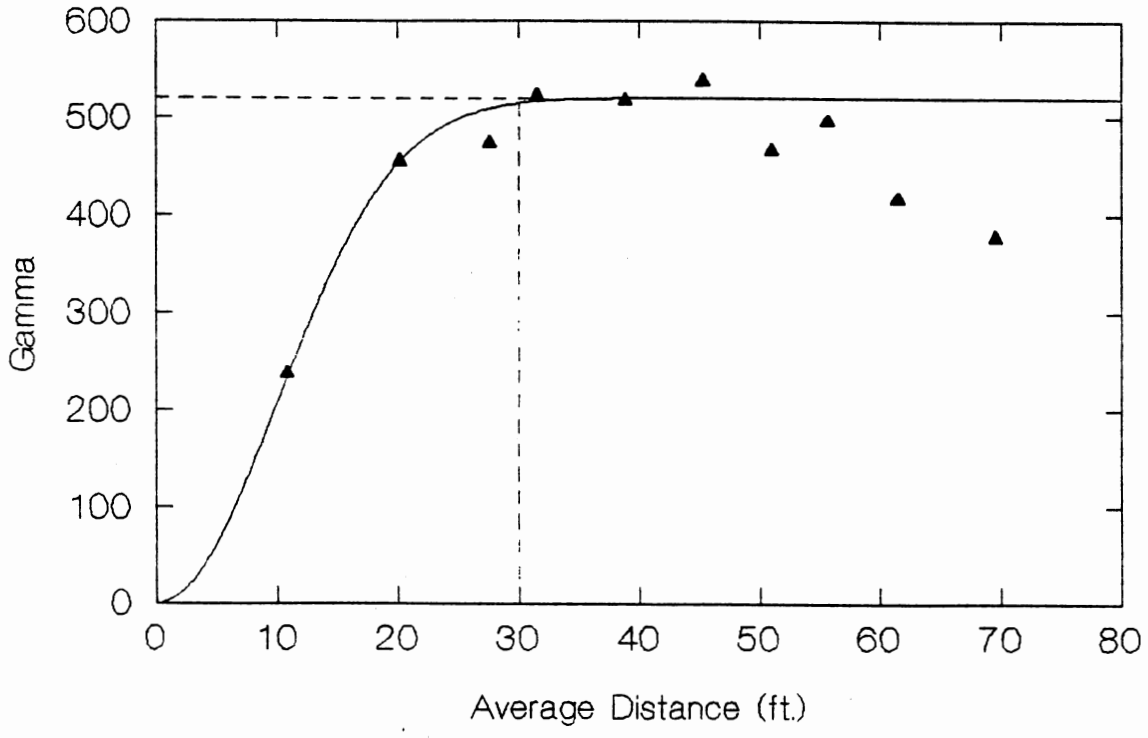

Figure 12 - Experimental Semivariogram for the Northern 1/2 of the Total Magnetic Field Intensity Data with Superimposed Gaussian Structural Model

the survey was the gaussian type (equation 31) and had the form:

$$\gamma(h) = 520(\ 1 - \exp(-h^2/\ (14)^2) \qquad (48)$$

Figure 12 displays the experimental semivariogram for the total magnetic field intensity values which were measured over the north 1/2 of the survey. Notice in particular that the range of influence for the semivariogram was at approximately 30 feet, which was about the same as the width of the magnetic anomalies examined in the previous section. It appeared that when a localized semivariance analysis was performed on the magnetometer survey, the effect of the drum anomalies become more prominent. The width of the magnetic anomaly was very distinctive for this semivariogram, as compared to the semivariogram for the complete data set, where the anomaly was encrypted in a relatively minor nested structure. Also notable was the observation that the sill for the localized northern 1/2 semivariogram was at a significantly lower level (520) relative to the large scale semivariogram (935).

The experimental semivariogram for the southern 1/2 of the survey is shown in Figure 13. The model that was found to best characterize the structure in this area was of the linear type (20) and had the form:

$$\gamma(h) = 60 + 30h^{1.0} \qquad (49)$$

This model included a range of influence parameter of 30 feet and a sill equal to 955, considerably higher than that from the northern 1/2 data set but comparable to the large scale semivariogram. The distinctiveness of the localized semivariogram shape becomes significant despite the fact that both semivariograms displayed a dominant spatial length of 30 feet characteristic of the anomaly widths apparently caused by the buried drums contained in the area. Note that many different functional forms, sill values, and range of

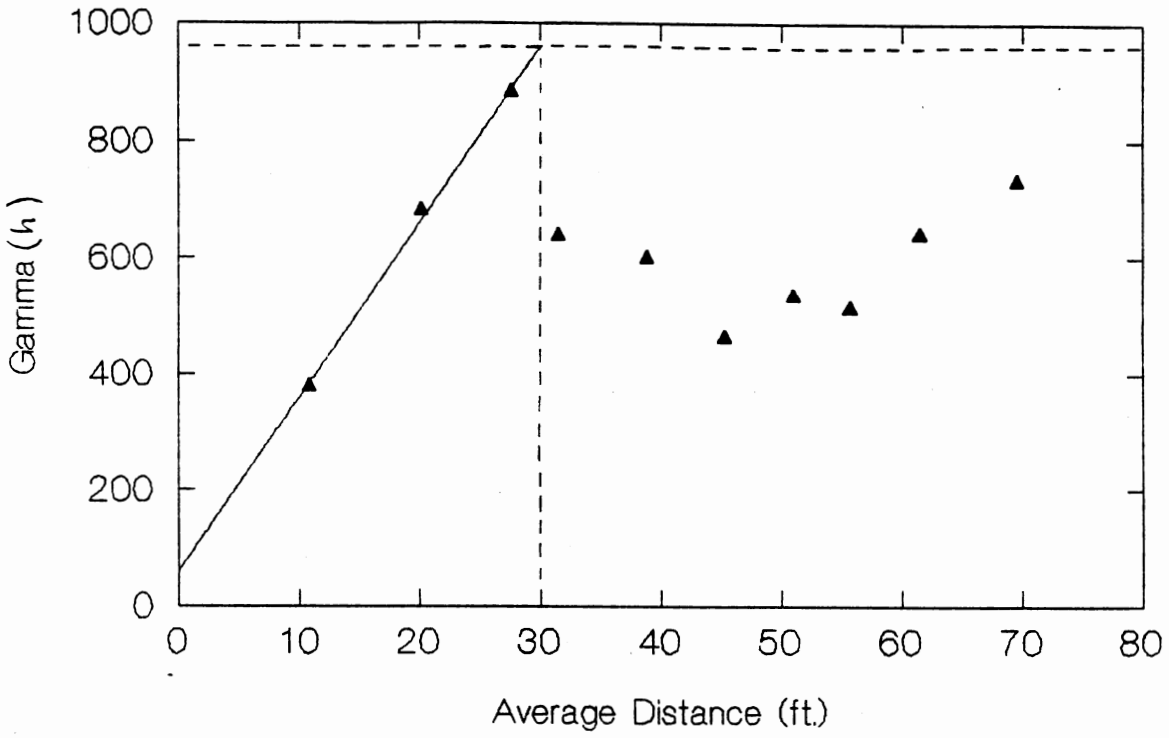

Figure 13 - Experimental Semivariogram for the Southern 1/2 of the Total Magnetic Field Data with Superimposed Linear Structural Model.

influence parameters could have been used to model the experimental semivariogram in Figure 13. Semivariograms are designed to express the dominant spatial wavelengths of a regionalized variable, and reflect the physical dimensions of the variable (Clark, 1979). In this instance the 30 foot range of influence parameter was selected as relevant because it correlated with the width of the anomaly in the area.

The semivariance models (48) and (49) were subsequently cross - validated and kriged over the northern 1/2 of the survey on the previously defined 5 foot support grid. The relative merits of kriging using these structural model were determined from:

a) a localized area which contained buried drums, i.e the northern half

of the survey which contained Area 2,

b) some other localized area which also contained buried drums, i.e. the southern half of the survey which contained Area 1, and

c) the large scale survey of the entire site, which contained buried drums but was generally magnetically "quiet", i.e. dominated by very low amplitude variations typical of soils containing little or no ferromagnetic material.

The individual models were evaluated by the cross-validation statistics, the statistical parameters of the kriged estimates relative to the measured data, the kriging error variances, and the location of the maxima of the kriged estimates within the magnetic anomalies relative to the centers of mass of the drum cache in Area 1. The model parameters used in this part of this study are listed in Table IX and the listing of the cross-validation statistics for each of these models are listed in Table X.

TABLE IX

MODEL PARAMETERS USED TO KRIGE
THE NORTHERN HALF OF THE SURVEY AREA

Model	Source of the Model	Model Form	Model Parameters			
			C 0	C	a or a'	p
1	Entire Survey Area	Spherical	0	935	75	-
2	Southern 1/2	Linear	60	690	1	30
3	Northern 1/2	Gaussian	0	520	14	-

Some notable comparative features of the cross-validations were apparent. The statistics for all the models used, and in all categories, were considerably less robust in all categories than the corresponding statistics in Table VII, which cross-validated the plausible models derived to krige the

entire survey. This was very possibly the effect of an insufficient sample, i.e. deriving sample estimates of the spatial statistics with an inadequate number of observations to accurately describe the actual population attributes of the regionalized variable. It was difficult to definitively choose

TABLE X

CROSS-VALIDATION STATISTICS FOR THE MODELS USED TO KRIGE THE NORTHERN HALF OF THE SURVEY AREA

Statistic	Ideal Value	Model 1 (total)	Model 2 (S/2)	Model 3 (N/2)
Mean Kriging Error	0.0	-0.030	-0.858	-1.336
Standard Deviation of the Errors	< 29.242	13.746	14.417	12.735
Standard Deviation of the Standard Error	< 1.3814 and > 0.6186	1.1292	1.7092	0.7225
Standard Error / Estimate Correlation Coefficient	0.00	0.29	-0.29	0.20
Kriged Estimate / East Correlation Coefficient	0.00	0.11	0.05	0.19
Kriged Estimate / North Correlation Coefficient	0.00	-0.47	-0.30	-0.27
Kriging Error / East Correlation Coefficient	0.00	0.00	0.04	-0.02
Kriging Error / North Correlation Coefficient	0.00	-0.09	-0.11	-0.11
Measured Value / Kriged Estimate Correlation Coeff.	1.00	0.85	0.83	0.80

one of these models over the others based on these analyses although Model 1, derived from the semivariogram of the entire survey would have been preferred, rating superior in 5 of the 9 statistical categories. Model 3, derived from the localized semivariogram, would rate second, being best in 3 of the 9 statistics. Model 2, the semivariogram, obtained from the southern half of the survey, would rank last with superiority in only 1 of the 9 statistics.

The univariate statistical properties of the kriged estimates using Models 1 through 3, compared the statistical properties of the kriged estimates to those of the measured samples within similar areas. The statistical parameters listed in Table XI included a modified chi-square statistic which permitted a measure of the "sameness" of the probability distribution functions (pdf's) resulting from Models 1 through 3 to the pdf of the measured sample. The smallest numerical value for the chi-square statistic indicated the strongest agreements between measured and simulated data. With the pdf's binned, i.e. arranged into identical discrete value ranges for the measured and kriged estimates, the chi-square statistic was determined by :

$$\chi^2 = \sum_{i=1}^{n} [(R_i - S_i)^2 / (R_i + S_i)] \qquad (50)$$

(Press, Flannery, Teukolsky, and Vetterling, 1988)

where R_i was the number of occurrences for the event within bin i for the pdf of kriged estimates and S_i was the number of occurrences expected for the corresponding measured data. The graphical representations of the pdf's for the kriged estimates for all three models and the measured data within the northern half of the survey area are shown in Appendix E. The chi-square statistic contributed a single parameter that provided comparisons to

TABLE XI

STATISTICAL PARAMETERS OF THE MEASURED DATA AND THE ESTIMATES FOR THE MODELS USED TO KRIGE THE NORTHERN HALF OF THE TOTAL MAGNETIC FIELD INTENSITY SURVEY

Statistical Parameter	Measured Data	Model 1 (total)	Model 2 (S/2)	Model 3 (N/2)
Range of Values	134.4	141.0	127.8	104.9
Mean	196.6	195.7	195.8	195.7
Median	197.2	196.5	195.7	196.6
Standard Deviation	24.6	21.0	24.3	19.4
Standard Error	3.32	1.64	1.89	1.52
Skewness	0.15	0.20	0.26	0.18
Kurtosis	1.24	0.12	0.68	-0.04
Coeff. of Variation	0.13	0.11	0.12	0.10
Chi-Square Statistic vs. Measured Data	--	23.51	15.20	23.73

the reference pdf and indicated which particular pdf (of the kriged estimates) was more "similar" statistically to the reference (measured) pdf.

The univariate statistics consistently indicated that Model 2, obtained from the semivariogram projected from the southern half of the survey, produced kriged estimates which more closely approximated the measured data. The ability to replicate the central tendencies of the collected data was very good for all the models. The dispersion, symmetry, and peakedness indicators, however, showed Model 2 (projected from the southern 1/2 to the northern 1/2) to be preferable. Most notable was the modified chi-square statistic, where Model 2 displays superiority over the other two models.

This was somewhat contrary to the results from the cross-validation statistics, which indicated that Model 2 produced the least desirable estimates. This is partially explained by the relationship between the parameters of the semivariance models and the kriging process. The previous

sections showed that the kriging process, when used with an accurately derived semivariance model, produced estimates that were less dispersive and produced more uniform probability distributions than the original measured data. Model 2, projected from the neighboring area to the south, yielded a model which provided for significantly larger semivariance values (higher degrees of spatial variability) at corresponding distances than Model 3 (derived from the localized area) or Model 1 (derived from the entire survey area). Consequently, when the kriged estimates were generated using Model 2, the results showed higher dispersive qualities than the corresponding results from the other two models.

Another method of evaluating the applicability of the individual models was obtained from the kriging errors of the estimates, as determined by equation (45). Recall that the kriging methodology was based upon the assumption that the regional variable, which was the total magnetic field intensity, had zero variance at the measured data points within the support and that the kriging error was determined to be twice the sum of the weighted individual semivariances. The resulting spatial pattern for the kriging errors throughout the grid for all of the models was an orthogonal arrangement, which had maxima at the nodes at the kriged points. The kriged points along the perimeter of the survey had higher error values than the points that were within the interior of the survey. This was due to the larger weighting factors resulting from the solution of the kriging matrix (44) for extrapolation outside of the support. Figure 14 showing the resultant kriging error variances from model 3 illustrates the pervasive spatial pattern of these variances. This pattern was repeated for every model with only the absolute magnitude of the kriging errors changing. Notable in this pattern

was the observation that the north-south columns which did not have any measured sample points, and consisted entirely of kriged points, had slightly higher error variances than the north-south columns in which kriged points alternated with measured data within the grid. The largest values for the kriging error variances that resided within the interior portion of the support (so the "edge effect" does not dominate) were determined and listed in Table XI. This parameter was used to evaluate the relative merit of the estimates calculated from the individual models listed in Table IX.

TABLE XI

MAXIMUM KRIGING ERROR VARIANCES FOR THE MODELS USED TO KRIGE THE NORTHERN HALF OF THE SURVEYED AREA

Model	Maximum Kriging Error Variance
1	96.2355
2	233.3847
3	7.1725

Table XI indicated that Model 2, had the largest inherent error corresponding to the kriging estimates by a significant amount. The cause of this unusually high error variance, relative to the other models, was that the Model 2 semivariogram reached relatively high values for the gamma parameter at short distances, while conversely, Model 3, the localized semivariance model, resulted in very low error variances from the kriging procedure. Although Models 2 and 3 exhibited the same range of influence (30 feet), the difference in the sill values of 83.7% (955 as compared to 520) for these models resulted in kriging error variances which differed by a factor of 32.54. This accounted somewhat for the results derived from the univariate statistics in Table X, where Model 2 displayed considerably higher

dispersivity levels than did the other models. Estimates from Model 1, derived from the entire survey, which had a large sill value (935) and a relatively large range of influence (75 feet), resulted in an kriging error variance which was intermediate to the extremes displayed by Models 2 and 3.

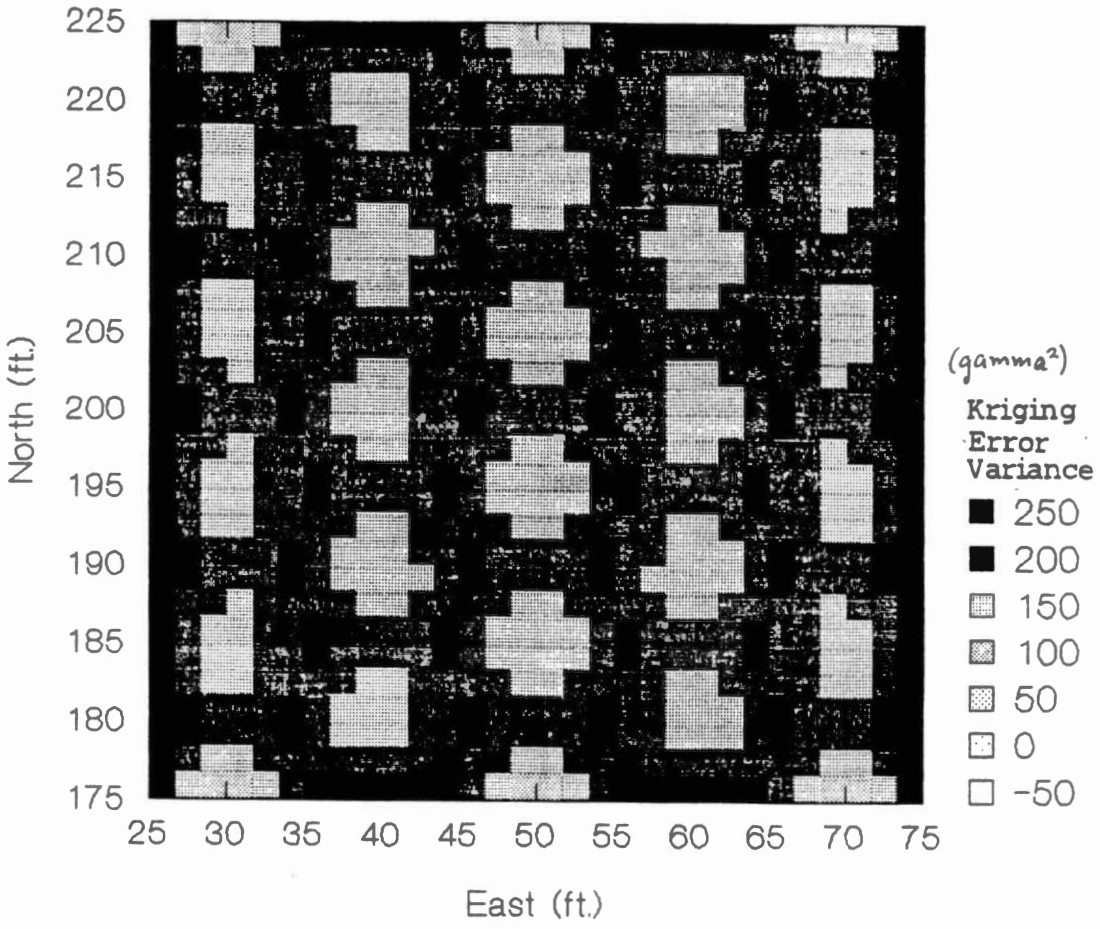

Figure 14 - The Kriging Error Variances Using Model 3 Over a Portion of the Northern Half of the Total Magnetic Field Intensity Survey, Showing the Characteristic Pattern of Kriging Error Variances.

In summary, from the perspective of kriging errors, Model 3, the semivariance/covariance function determined from the localized experimental semivariogram over the northern 1/2 of the site, displayed the best

performance for making estimates of the interpolated total magnetic field intensity over the entire site.

The final criteria in the evaluation of these models were the distances and magnitudes of the maxima of the kriged estimates within the magnetic anomalies with respect to the location of the center of mass for the buried drums. Appendix F shows the maps of the kriged estimates using Models 2 and 3 respectively, along with the individual drum locations and their cumulative centers of mass. Figure 10 presented a similar map for Model 1. Table XIII summarizes the distances and magnitudes of the kriged maxima with respect to the center of mass for each of the semivariance models evaluated here.

TABLE XIII

LOCATION OF THE MAXIMUM KRIGED ESTIMATES WITHIN THE NORTHERN HALF OF THE SURVEY FOR THE TOTAL MAGNETIC FIELD INTENSITY DATA USING SEMIVARIANCE MODELS DESCRIBED IN TABLE IX

Model	Total Magnetic Field Intensity		Distance of Anomaly Apex to the Center of Mass (ft.)
	Kriged Maxima (Gammas)	Location (East,North)	
1	258.3	(25,190)	9.13
2	275.5	(25,190)	8.02
3	251.5	(25,190)	9.13

Recall that the largest measured value within the anomaly in Area 1 occurred at (20,190), with a magnitude of 273.5. The location of the maxima of the magnetic anomaly, when both measured data and kriged estimates were considered, only changed when Model 2 was used. A magnitude of 275.5 at (25,190) moved the "apex" of the total intensity anomaly to the east by 5 feet, resulting in an approximation 12.3% closer to the center of mass. The kriged estimate at this point was larger (by 0.7%) than the largest value that was

directly measured in the original survey. Associated with this estimate was the large (233.38 gammas^2) inherent error variance, which reduced the reliability of the estimate. This shift in the anomaly apex positioned it nearly due south of the center of mass for the buried drums. From theoretical expectations, considering a magnetic declination of 8^0 east of north and assuming that each drum was demagnetized identically, one would expect the apex of the anomaly to lie about 1.7 feet to the west of (25,190). Therefore locating the maxima of the magnetic anomaly caused by the buried drums at (25,190) was plausible.

Conclusions on the Kriging Process as a Method to Extend the Magnetometer Data and the Relative Suitability of the Spatial Functions

In this case, the magnetometer surveys, conducted over reasonably small areas, the total magnetic field intensity and vertical magnetic gradient regional variables could reasonably be assumed to be statistically stationary and isotropic. The total magnetic intensity data had an experimental semivariogram that displayed many typical features and was easily defined mathematically. In contrast, the experimental semivariogram for the vertical magnetic gradient indicated that about 69% of the spatial variation occurred at distances less than those definable with the 10 foot triangular grid at which the original survey was conducted. Only two of the discrete semivariances could be considered to reside at levels less than the sill semivariance, the level of the population variance. The structure of the vertical magnetic gradient could not be rigorously defined with this support. For the application of locating buried drums in hazardous waste sites with

a vertical magnetic gradient survey, a 10 foot triangular grid proved insufficient to define the actual semivariance/covariance surface. Similarly, a 15 or 20 foot grid would have provided vertical magnetic gradient readings that would be statistically uncorrelated at adjacent sampling points, that is, results from such a grid would be undistinguishable from randomly located sample points.

Several models for the semivariogram of the total magnetic field intensity were evaluated via an array of cross-validation statistics by a point-by-point suppression technique after visual inspections for "goodness of fit". All of the chosen model forms produced very high quality cross-validation statistics, all correlation coefficients of the kriged vs. measured values greater than 0.90. A spherical model with a range of influence of 75 feet was chosen as the best structural representation based on consistently superior cross-validation statistics. This model was then used to produce kriged estimates at locations which interpolated between the measured points to produce an orthogonal grid with 5 foot separation distances. These estimates were then evaluated in terms of their univariate statistical properties relative to those of the measured values of total magnetic field intensity. It was found that the kriged estimates reproduced the central tendency statistics extremely well, the dispersion statistics fairly well, and the symmetry and dispersion statistics rather poorly. It was also found that the weighted linear operator of ordinary kriging altered the probability distribution of the regional variable so that it become closer to that of a uniform distribution within approximately one standard deviation of the mean. This was pervasive in all of the cases and appeared to be an intrinsic property of kriged estimates. In general, kriging would consequently provide

more stochastically consistent results when used on regional variables which originally had discrete uniform probability distributions.

The composite maps of measured data and interpolated kriged estimates were then examined for magnetic anomalies which were caused by induced magnetic fields from the buried steel drums. Two prominent anomalies were found. The areal configurations of the two drum clusters that were eventually discovered were considerably different, one being a rather concentrated cluster with the other more scattered in a general east-west direction. Nonetheless, each produced a single magnetic anomaly with similar characteristics. It was found that the magnetic anomalies conformed to the parameters suggested by previously conducted empirical studies on the magnetic responses of buried drums in terms of the anomaly width and the polar migration of the apex of the anomaly relative to the center of mass of the drum caches in both of the areas studied.

The viability of using the semivariance structure of a smaller, more localized area was evaluated relative to a localized structure projected from an adjacent drum storage location as well as from the structure derived from the entire survey area. The semivariograms calculated from the localized areas displayed dominant spatial wavelengths, as indicated by the range of influence parameters, which were much smaller (30 feet) than the semivariogram derived from the entire survey (75 feet). The reason for this difference was that the 30 foot characteristic separation correlated with the dominant width of the magnetic anomalies caused by the induced field of the buried drums. The 75 foot characteristic length from the entire survey appeared to result primarily from the separation distances between the two individual magnetic anomalies. The only indication of the effect of the

magnetic anomalies on this structure was a relatively small nested structure at the 30 foot increment.

The two localized semivariograms, despite the highly similar ranges of influence, had very dissimilar structural forms and representative parameters. The two localized models and the larger scale model were evaluated by cross-validation statistics, univariate statistical properties relative to the measured data, the kriging error variances, and the position of the apex of the magnetic anomaly relative to the centers of mass of the drum cache. The results of these tests did not conclusively demonstrate the superiority of any of the models, but inferences were drawn. The semivariance structure generated from the entire survey produced generally better cross-validation statistics than either of the localized structures when calculated over the smaller area. The kriged to measured correlation coefficients over the smaller area were less robust than over the entire survey. The inference drawn from this is that kriging produced better estimates when applied to areas which had a smaller proportion of the total area with "extreme" values.

The localized model projected from the southern half of the survey produced the best univariate statistics and the most comparable probability distribution function to the distribution of the measured samples. The localized model produced the lowest kriging error associated with the estimations. This was due to the form of its semivariogram, which had a significantly lower sill value relative to the other semivariograms. It appeared that using the localized semivariance structure produced kriged estimates that were unimproved from the estimates produced from the structure derived from the entire survey. Taking all of the evaluation

criteria as an aggregate, the estimates produced from the structure derived from the entire survey seemed to produce the best overall results.

Using the measured geophysical data alone on the original 10 foot triangular sampling grid produced a rather diffuse picture of the surface of the total magnetic field intensity regional variable. The shape and boundaries of the individual anomalies caused by the inducing properties of the buried ferrometallic drums were difficult to discern due to the lack of detail. The measured data did allow for the robust definition of a semivariance / covariance spatial structure that permitted the generation of interpolated values by the kriging process. These kriged interpolations, in a composite map with the original measured data, defined the anomalous features in greater detail (refer to Figures 8 and 9). The resultant composite anomalies were consistent in size, magnitude, and polar migration with those results produced from independent studies of magnetometer responses of buried ferrometallic drums. The interpretation was that kriging produced reasonable interpolations of the measured total field intensity data which assisted in the definition of the target anomalies.

Kriging should be used only when field data is not available. It should not be a substitute for additional measured data. It always would be preferable to have more measured samples at the closer separation distances. Kriging (and any other interpolation method) has utility whenever additional field data cannot be acquired. Kriging has an intrinsic advantage over customary interpolation or averaging techniques in that it's interploated values depend only on a neighborhood of points implied by the semivariance structure, and it also provides the variance of the corresponding errors of estimation. For the Western Processing site total magnetic field intensity

data, it appeared that the kriged interpolations were statistically sound relative to the measured data. The magnetic anomalies that were detailed using the kriged estimates conformed to the expected characteristics. In the absence of additional measured data, kriging apparently produced quality estimates of the configuration of the total magnetic field intensity.

CHAPTER II

ANALYSIS OF UNCERTAIN SPATIAL FUNCTION FORMS FOR THE VERTICAL MAGNETIC GRADIENT DATA

Problem Definition

As part of the remedial investigation of the Western Processing Superfund site, located in Kent, Washington, a vertical gradient magnetic survey was conducted with the objective of locating buried steel drums and utility corridors within the confines of the site (French, Williams, and Foster, 1987). The survey grid was designed as a triangular array of sampled vertical gradient values with a elemental spacing of 10 feet. In an effort to produce interpolated values for the vertical magnetic gradient regional variable, the experimental semivariance / covariance of the measured samples of the survey was examined with the intended purpose of mathematically defining their spatial correlation structure for use in the kriging procedure. The resultant semivariogram, shown in Figure 15, displayed characteristics which could be considered pure "nugget effect". The majority of the semivariances were near the sill (population variance). This means that the vertical magnetic gradient data behaved as if it were randomly generated from its probability distribution. The smallest semivariance / average distance pair was located at (10.78, 2960). This means that 2960/4300 or 68.8% of the total semivariance remained unaccounted for (resided at shorter separation distances). This means that more than two thirds of the spatial semivariance / covariance structure occurred at distances less than 10.78 feet, implying that the vertical magnetic gradient was under-sampled using a 10 foot triangular grid. With only 2 points of the experimental

semivariogram determining any amount of the spatial structure, a great number of functional forms could be devised that conformed with this information. To rigorously define the correlation structure, the vertical

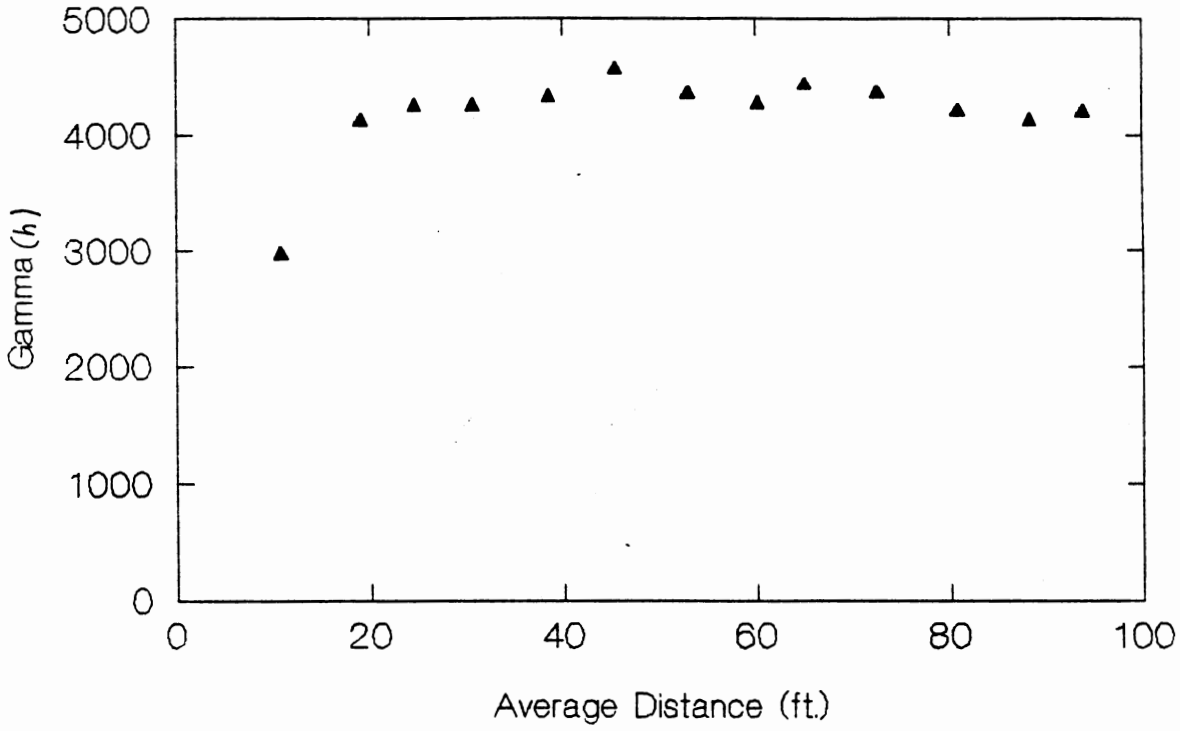

Figure 15 - Experimental Semivariogram for the Vertical Magnetic Data Over the Western Processing Superfund Site.

magnetic gradient variable should be resampled at spacings that are somewhat less than 10 feet. Under these circumstances an attempt was made to answer the following questions;

1) Is there a procedure which can be used to derive a functional form, out of the numerous possibilities that fit the limited information, which defines the correlation structure in a way which produces "better" kriged estimates than the other functions ?

2) If one were to devise a spatial sampling scheme for vertical

magnetic gradient measurements with the purpose of locating buried drums, what would be an acceptable (not necessarily optimum) elemental spacing for the purpose of defining the correlation structure that could subsequently be used in the kriging methodology ?

Structural Analysis and Experimental Procedures

An initial step in defining a plausible structural form that would extend the vertical magnetic gradient survey was to define a suite of mathematical models, each capable of fitting the experimental semivariogram. Subsequently each of these models was evaluated by:

1) calculation of cross-validation statistics using a hole-by-hole suppression technique,

2) comparison of the univariate statistical properties of the kriged estimates to those of the measured samples,

3) calculation of kriging error variances resulting from the estimates, and

4) comparisons of simulated areal configurations of the magnetic anomalies to the buried drum locations.

Using these criteria the best overall model was determined. The parameters from this model could be considered a realization from a stationary stochastic process, further characterized by common univariate statistical properties such as mean, standard deviation, etc. With this assumption a set of model parameters were treated as a prior probability distribution, in a functionally expedient facsimile of Bayes' theorem for continuously distributed parameters. An iterative experimental procedure could be used to produce updated estimates of the model parameters (Press, 1989).

Bayes' theorem states that the probability distribution function of a parameter θ described by some moment of a spatial statistical attribute for a set of observable random variables $(y_1, y_2, \ldots, y_n)$ is given by:

$$f'(\theta) = K\, L(\theta)\, f(\theta) \tag{51}$$

where:

K = normalizing constant

$L(\theta)$ = likelyhood function for the parameter

$f(\theta)$ = prior probability distribution of the parameter

statistical moment or attribute of the model

In a strictly theoretical sense, the posterior expected values for the statistical attribute or moment can be obtained by integrating the equation for the posterior distribution given by (40). An equivalent qualitative statement of Bayes' theorem can be written as:

$$\text{Posterior} \propto \text{Likelyhood} \times \text{Prior}$$

For this experiment, the comparable Bayesian prior, was determined by examining a suite of semivariance models which conformed reasonably to the experimental semivariogram as shown in Figure 15.

Initial Estimate for Semivariance (Prior Distribution) for

the Vertical Magnetic Gradient Data

Four individual model forms were selected (by the methods described on page 37) so that they allowed a sufficient range of model parameters to be evaluated. The models were:

1) linear model - $\gamma(h) = C_0 + ph^{\gamma}$

$$= 1440 + (141)h^{(1.0)} \tag{52}$$

$$C = 2860, \{\text{sill}\} = C + C_0 = 4300$$

range of influence = 20 ft.

2) spherical model - $\gamma(h) = C_0 + C\,(\,3/2(h/a) - 1/2(h/a)^3)$

$= 550 + (3750)(3/2(h/23) - 1/2(h/23)^3)$ (53)

{sill} = 4300, range of influence = 20 ft.

3) gaussian model - $\gamma(h) = C_0 + C\,(\,1 - \exp(-h^2/a'^2)$

$= 730 + (3570)(1 - \exp(-h^2/(11)^2)$ (54)

{sill} = 4300, range of influence = 20 ft.

4) nested exponential + linear model -

$\gamma(h) = C_0 + C_1\,(\,1 - \exp(-h/a')) + ph^J$

$= 0 + (2760)(\,1 - \exp(-h/8)) + (85)h$ (55)

{sill} = $C_0 + C_1 + C_2 = 0 + 2760 + 1540$

= 4300, range of influence = 20 ft.

The graphical configurations of these specific functions relative to the experimental semivariogram are shown in Figure 16. Cross-validation statistics were generated using the hole-by-hole suppression technique to identify which model most closely approximated the observed spatial structure. The significance of the individual cross-validation statistics were discussed in Chapter I. Previous applications of this technique to the total magnetic field intensity data with the same sampled support indicated that the results would have very similar cross-validation statistics, as the removal of an individual point caused the nearest sampled points to assume greater dominance in the revised estimate. Since these distances were discretely sampled at the 10 foot separations, properly configured individual models (ones that conformed well with the experimental data) were expected to generate kriged values that are very close to each other. This would be the predicament encountered with the hole-by-hole suppression cross-validating

technique whenever a repeated, symmetric sampling scheme was used to investigate a regional variable, as is usually the case with geophysical surveys. The resultant statistics of the cross-validations are included in Table XIV.

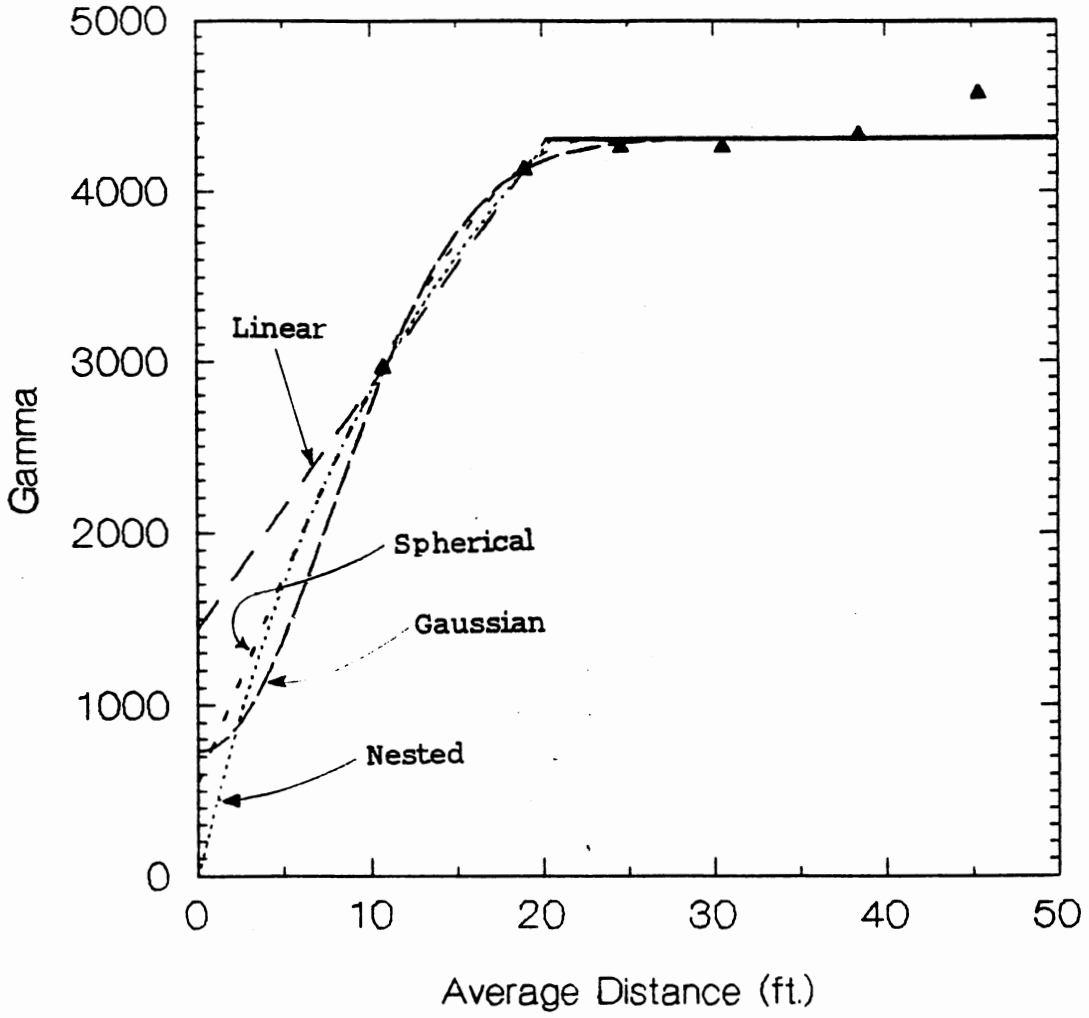

Figure 16 - Spatial Functions Representing the Semivariance of the Vertical Magnetic Gradient Superimposed on the Experimental Semivariogram.

As expected, the cross-validation statistics were very similar for all of the structural forms. In fact, it was difficult to choose or distinguish the

viability of one model relative to the others using these criteria alone. The most notable result was the measured value / kriged estimate correlation coefficients, all of which were in the range 0.50 to 0.54, significantly lower

TABLE XIII

CROSS-VALIDATION STATISTICS FOR THE INITIAL MODELS FOR THE VERTICAL MAGNETIC GRADIENT SEMIVARIANCE

Statistic	Ideal Value	Linear Model	Spherical Model	Gaussian Model	Nested Model
Mean Kriging Error	0.0	0.0527	0.4259	0.4487	0.1890
Standard Deviation of the Errors	< 63.7	55.1	54.6	54.5	54.6
Standard Deviation of the Standard Error	< 1.118 and > 0.882	1.032	1.027	1.051	1.020
Standard Error / Estimate Correlation Coefficient	0.00	0.00	-0.15	-0.16	-0.04
Kriged Estimate / East Correlation Coefficient	0.00	0.10	0.07	0.07	0.09
Kriged Estimate / North Correlation Coefficient	0.00	-0.08	-0.05	-0.05	-0.07
Kriging Error / East Correlation Coefficient	0.00	0.00	0.00	0.00	0.00
Kriging Error / North Correlation Coefficient	0.00	0.00	0.00	-0.01	0.00
Measured Value / Kriged Estimate Correlation Coeff.	1.00	0.50	0.53	0.54	0.52

than the equivalent statistics for the total magnetic field intensity data. With

this exception, the cross-validation statistics were within the "acceptable" ranges of values previously outlined. In an attempt to more definitively distinguish which of these structures produced enhanced kriged estimates, the vertical gradient data set was kriged on a 5 foot orthogonal grid, using each of the models listed above. The univariate statistical properties of those kriged estimates were subsequently calculated. The objective was to compare these statistics to those of the measured values in the survey. Accurate interpolated estimates or any stochastic model representative of a random process should emulate the statistical properties of the regional variable (Haan, 1977). Table XIV registers these results.

TABLE XV

UNIVARIATE STATISTICAL PARAMETERS FOR MEASURED AND KRIGED VERTICAL MAGNETIC GRADIENT DATA FOR SEVERAL SEMIVARIANCE MODELS

Statistical Parameter	Measured Data	Linear Model	Spherical Model	Gaussian Model	Nested Model
Range of Values	485.0	237.0	344.0	414.0	335.2
Mean	-10.25	-11.17	-11.42	-11.45	-11.38
Median	-14.00	-11.33	-15.08	-17.22	-13.78
Standard Deviation	81.08	43.91	59.70	67.12	56.52
Standard Error	7.91	2.47	3.36	3.78	3.18
Skewness	0.566	0.322	0.447	0.476	0.445
Kurtosis	1.556	0.026	0.418	0.716	0.480
Coeff.of Variation	-7.91	-3.93	-5.23	-5.86	-4.97
Chi-Square Statistic vs. Measured Data	----	57.70	36.81	35.09	42.60

The univariate statistical comparisons showed that the gaussian model provided the estimates which more closely emulated those of the measured data relative to the other models. Again the kriging method preserved the central tendency, reduced the dispersion and asymmetry, and flattened the probability distribution of the measured regional variable. The

gaussian model distorted the statistical characteristics of the input data to a lesser degree than the others. The chi-square statistic, which was indicative of the degree of similarity between the kriged estimates and the original measurements (0.0 denoting perfect correlation), also implied that the gaussian model had the best statistical agreement with the measured data. From these results it was inferred that the gaussian model had the spatial characteristics which were the closest to the "actual" spatial structure of the vertical gradient data. The histogram probability distributions for the kriged estimates of each model are presented in Appendix G.

Another factor used to evaluate the comparative effectiveness of the semivariance models (41) through (44) was the kriging error variances. The spatial pattern of the variance of the kriging error variances, as calculated by equation (45), was characterized by a repeating pattern further defined by the sampling grid of the survey. The maximum kriging variances within this pattern were used as a relative indicator of model effectiveness. The maximum kriging error variances occurred along the north-south rows comprised entirely of kriged locations. The values of the maximum kriged error variances for each model are listed in Table XVI.

TABLE XVI

MAXIMUM KRIGING ERROR VARIANCES

Model	Maximum Kriging Error Variance
Linear	2504.17
Spherical	2025.05
Gaussian	1392.67
Nested Exp/Lin	2028.82

The results from this table show that estimates produced using the

gaussian model had the lowest error variance estimate by at most a margin of ~2/3. This may be attributable to the dominant weighting factor generated from the kriging matrix, which would have occurred at the closest separation distance (5 feet). Consequently, when the kriging error variance was calculated via (32), the semivariance at the 5 foot separation distance became the critical parameter because of the dominant weight at this separation. The semivariances at the 5 foot separation distance and the nugget effects for each of the models are listed in Table XVII.

TABLE XVII

SEMIVARIANCE VALUES AT THE 5 FOOT SEPARATION DISTANCE FOR THE VERTICAL GRADIENT STRUCTURAL MODELS

Model	Semivariance @ 5 foot Separation	Nugget Effect
Linear	2145.0	1440
Spherical	1753.6	550
Gaussian	1396.4	730
Nested Exp/Lin	1707.7	0

Note the correspondence between the semivariances at the 5 foot separation and the resultant kriging error variances from Table XVI. The spherical and nested models have produced very similar results in all of the tests despite very distinct functional forms. The coincidence of their semivariance values at the critical 5 foot separation distance is probably the cause.

The final determination of the validity of the individual models was made from a comparison of the resultant maps of the vertical magnetic gradient values for the measured and kriged values relative to the areal configurations of the buried drums at the site. Appendix H displays these maps over the two areas which contained buried drums. Unfortunately, there

is a dearth of empirical studies on the expression of buried steel drums on the vertical magnetic gradient of the earth's magnetic field. However, some theoretical studies have been performed examining the vertical gradient expression over simple prismatic shapes. Nelson (1988b) suggested that an inductive prism has a resultant vertical gradient anomaly that exhibits the polar migration phenomena (maxima skewed to the south). An associated area of anomalous negative values should be positioned to the north of the prism with a extrema that is approximately 1/2 the magnitude of the positive maxima. The area directly above the center of mass of an object can be expected to be transitional between the positive and negative anomalies. With this in mind, the location of the "zero" contour marking the transitional boundary relative to the center of mass of the drum caches, becomes a relevant parameter. Since determining the precise location of a zero contour is highly unlikely, a reasonable surrogate parameter is the distance between the center of mass and the nearest positive value associated with the positive anomalies. Table XVIII summarizes these results.

A comparison of the maps of the kriged and measured values showed that the locations of the individual anomaly boundaries were generally the same regardless of which model was used. The extrema of the resultant estimates, and consequently the shape of the anomaly were significantly affected by the structural model used. The gaussian model produced the best estimates relative to the measured values, as indicated by the univariate statistics.

From all of the criteria used to evaluate the viability of the individual semivariance models, the gaussian model appeared to produce the best estimates. The resultant univariate statistics of the estimates and the

kriging error estimates were most indicative of the superiority of the gaussian model relative to the others.

The intent has been to provide a structural semivariance form for the vertical gradient which would improve the estimates produced by kriging procedure. With this in mind, the gaussian model, described by (43), can be regarded as the prior distribution to produce a posterior distribution by methods similar to updating probability distributions by Bayes' theorem.

TABLE XVIII

ATTRIBUTES OF THE POSITIVE VERTICAL MAGNETIC GRADIENT ANOMALY RELATIVE TO THE CENTER OF MASS OF THE DRUM CACHES

Model	Area 1 Anomaly		
	Closest Non-Negative to Center of Mass	Largest Kriged Value	Largest Kriged to Center of Mass
Linear	11.035 ft.	113.03	26.77 ft.
Spherical	11.035 ft.	163.00	26.77 ft.
Gaussian	9.043 ft.	187.17	26.77 ft.
Nested	11.035 ft.	160.22	26.77 ft.

Model	Area 2 Anomaly		
	Closest Non-Negative to Center of Mass	Largest Kriged Value	Largest Kriged to Center of Mass
Linear	3.06 ft.	91.8	13.01 ft.
Spherical	3.06 ft.	144.9	13.01 ft.
Gaussian	3.06 ft.	157.3	13.01 ft.
Nested	3.06 ft.	128.2	13.01 ft.

Updating Procedure for Semivariance of the Vertical Magnetic Gradient Data

Updating the semivariance estimator was completed by assuming that the gaussian model (43) gave or described the "correct" form for the semivariances at distances less than the 10 foot separations at which the

survey was originally sampled. The resultant kriged estimates, using (43), at the 5 foot separation distances were then used, along with the original measured data, to produce a new experimental semivariogram. This semivariogram contained information, at the closer separation distances, that attempted to define the portion of the semivariance structure previously unknown. The experimental semivariograms generated from the measured data and previous estimate for the spatial function were then modeled. The resulting model was then the updated or posterior realization for the vertical magnetic gradient data. This model was subsequently used to provide semivariance values in the kriging equations to provide new, updated estimates. These estimates were then subjected to similar validation procedures as previously described. If the updated estimates improved the quality of the initial estimates, then the process could be repeated once again. When this process failed to produce improved estimates, then the previous spatial structural form could be considered the "best" model that could be derived from the available information.

Updating the Semivariance Function

An initial semivariogram was constructed using the estimates provided by the gaussian model. This provided sufficient delineation of the spatial structure such that a single mathematical function could define the discrete experimental semivariances. This function then became the updated or posterior estimate describing the parameters of the spatial semivariance / covariance structure for the vertical magnetic gradient data. This function was described mathematically as:

$$\gamma(h) = 6450\,[1 - \exp(-h^2 / (12)^2] \qquad (56)$$

Comparison of this function to the previous estimate, the gaussian function described by (54), showed that the range of influence parameter a' increased slightly from 11 to 12, the nugget effect was eliminated, and the sill value was raised considerably from 4300 to 6450. Recall that the most critical portion of the structural model for the interpolations on this grid was the value of the semivariance generated at the 5 foot separation distance. This value decreased from 1396.4 to 1028.0. The graphical representation of the posterior semivariogram and the resultant model with its sill and range of influence are shown in Figure 17.

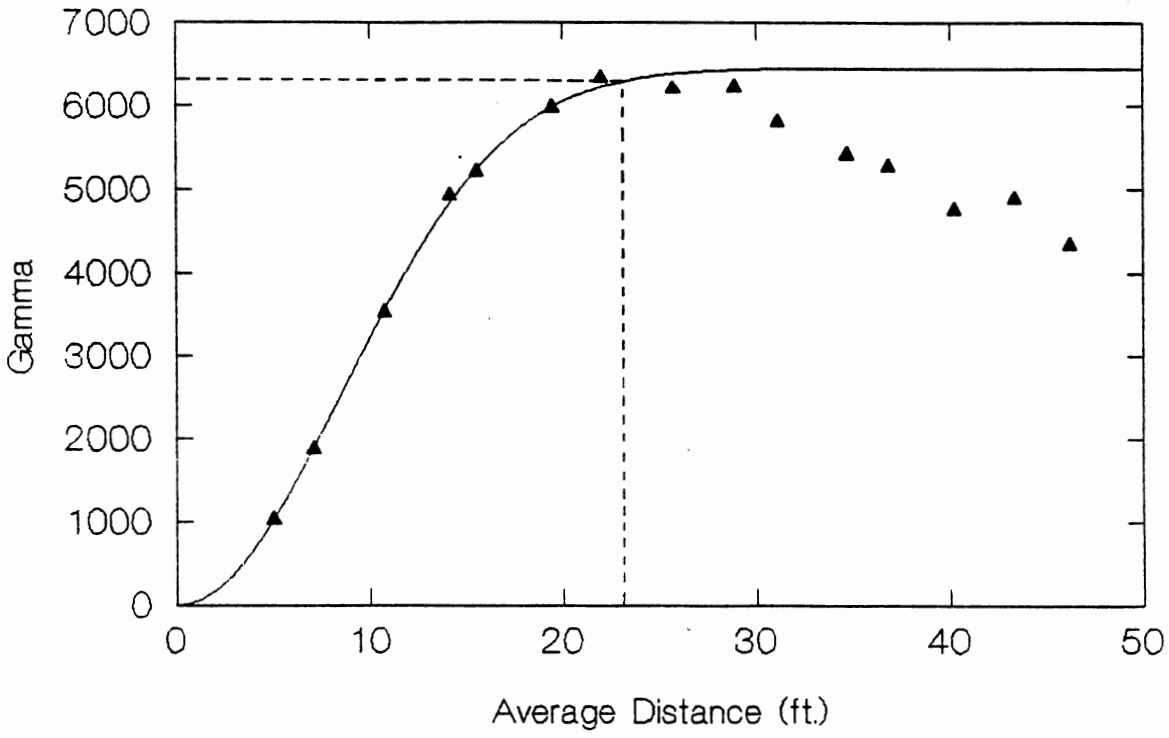

Figure 17 - Experimental Semivariogram and Resultant Structural Model for the First Updated Parameter Estimates.

The next step was to determine whether the new, updated kriged

estimates were an improvement relative to the prior estimates. The univariate statistical properties of the updated kriged estimates, the prior estimates, and the measured data are displayed in Table XIX.

The univariate statistics showed that the updated estimates provided generally better correlations than the prior estimates with the original measured data set, having comparatively improved in 6 of the 9 categories. The statistical categories which did not improve, such as the mean and skewness parameters, decreased only in small increments from the prior estimate.

TABLE XVIII

UNIVARIATE STATISTICAL PROPERTIES OF THE MEASURED DATA, PRIOR, AND UPDATED KRIGED ESTIMATES FOR THE VERTICAL MAGNETIC GRADIENT DATA

Statistical Parameter	Measured Data	Prior Estimate	Updated Estimate
Range of Values	485.0	414.0	513.2
Mean	-10.25	-11.45	-11.56
Median	-14.00	-17.22	-19.01
Standard Deviation	81.08	67.12	78.26
Standard Error	7.91	3.18	4.41
Skewness	0.566	0.476	0.465
Kurtosis	1.566	0.716	0.992
Coeff.of Variation	-7.91	-5.86	-6.77
Chi-Square Statistic vs. Measured Data	----	35.09	29.93

The maximum kriging error variances were then examined for the updated estimate relative to the prior. Examination of these variances associated with the estimating process for the updated structural estimates showed a maximum kriging error of 251.62. This compared favorably to the error variance of 1392.67 provided by the prior estimate, a considerable improvement. The largest kriged estimate within the anomalous areas caused

by the buried drums was located at the same location for both the prior and updated estimates. The magnitudes of the extrema at both areas increased with the updated estimates to values closer to those of the measured data. The kriged maxima for Area 1 improved from 70.6% to 83.9% (13.3% closer) of the measured maxima and from 71.2% to 87.2% (16% closer) for Area 2 when the updated estimates were used relative to the prior. With a statistical improvement in the definition of spatial covariance / semivariance proven by the resultant kriged estimates, the process was repeated to observe whether further improvement was possible. Iterative applications of this technique might result in additional improvement in the kriged estimates.

The updated estimate of the spatial function, considered to be an improvement over the previous estimates, assumed the role of the prior distribution. The process of determining a posterior distribution was then reiterated, using the estimates determined by kriging using equation (45) along with the measured data. The resultant experimental semivariogram was modeled mathematically with a nested gaussian / spherical form:

$$\gamma(h) = 7900(1-\exp(-h^2/(12)^2) + 325(3/2(x/15) - 1/2(x^3/(15)^3) \quad (46)$$

The semivariogram with this model superimposed is shown in Figure 18. The original data set was subsequently kriged using this semivariance function. The univariate statistical parameters for the kriged results are listed in Table XX.

The univariate statistics showed little or no change from the previous estimate and even slightly diminished the correlation with the measured data. The initial updating procedure had a much more pronounced effect on the quality of the estimates than did the second iteration. The resultant maximum kriging error variance for the second iteration was 510.42, compared with the

with the value of 251.62 which resulted during the first iteration

TABLE XX

UNIVARIATE STATISTICAL PROPERTIES FOR THE MEASURED DATA, FIRST AND SECOND ITERATION KRIGED ESTIMATES FOR THE VERTICAL MAGNETIC GRADIENT DATA.

Statistical Parameter	Measured Data	Kriged / First Iteration	Kriged / Second Iteration
Range of Values	485.0	513.2	504.6
Mean	-10.25	-11.56	-11.57
Median	-14.00	-19.01	-18.74
Standard Deviation	81.08	78.26	77.33
Standard Error	7.91	4.41	4.36
Skewness	0.566	0.465	0.469
Kurtosis	1.566	0.992	0.969
Coeff.of Variation	-7.91	-6.77	-6.69
Chi-Square Statistic vs. Measured Data	---	29.93	39.66

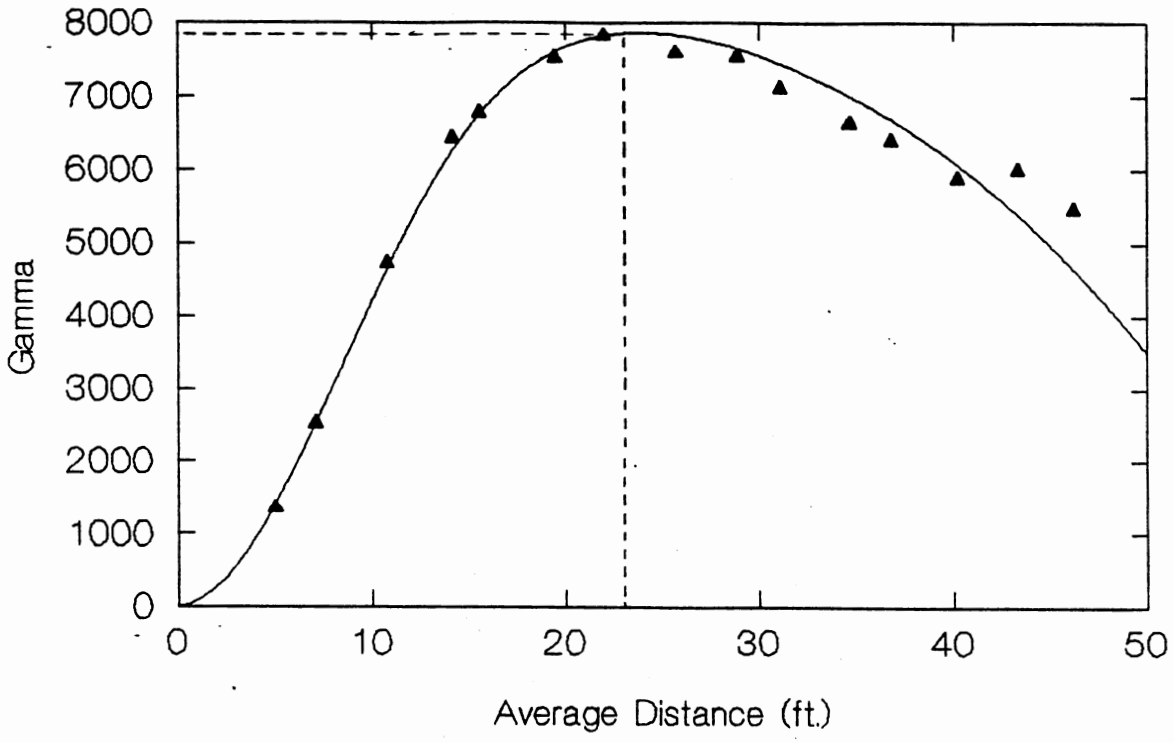

Figure 18 - Experimental Semivariogram and Resultant Model for the Second Updated Parameter Estimates.

The estimates produced from the structural model during the second iteration could be considered to be less accurate and reliable than those from the first iteration. Having reached the point where the procedure did not provide improved spatial semivariance models, the process was considered to have converged and was terminated. The results generated from the first updating procedure were the "best" estimates that could be obtained from the available information.

Conclusions of the Validity and Utility of the Spatial Semivariance Updating Procedure.

In this chapter the viability of recursively updating the parameters of the spatial semivariance function for the vertical magnetic gradient survey performed over the Western Processing superfund site was examined. An analogy to the process of generating posterior distributions for parameters which exhibit the properties of a spatially varying stochastic process using Bayes' theorem was developed. The gradient data, which were employed in locating buried drums within the site, varied spatially (as determined by an experimental semivariogram) in a way that much of its correlation structure resided at sampling separation distances shorter than the 10 foot separations in the triangular sampling array used for the survey. The conclusion was that this 10 foot spacing under sampled the data such that interpolating the data became problematic. The process consisted of developing a suite of structural semivariance models, each of which fit the original data and exhibited distinctly different mathematical forms. These structural models were then used to compute interpolated estimates of the vertical magnetic gradient by kriging on a 5 foot orthogonal grid. The

results for each of the estimations were subsequently evaluated by a variety of methods including comparisons of univariate statistical properties to those of the measured data, kriging error variances. With these evaluations as a guide, the model which exhibited the "best" properties was chosen as a prior estimate for the parameters of the spatial model. The kriged estimates from this "best" structural model were then used, along with the precursor measured vertical gradient data, to generate an experimental semivariogram. This contained information at the shorter spatial separation distances that were absent from the original semivariogram. This revised semivariogram was then modeled mathematically to produce a new spatial structure, which was then analogous to a posterior estimate for the parameters of the "actual" spatial structure. This structure was employed to krige the original data set on the 5 foot orthogonal grid. Evaluation statistics were calculated to compare the revised estimate to measured data and to previous trials. This process could be applied recursively while improvement in the reliability of the kriged estimates resulted. In this case, for the vertical magnetic gradient data, the initial updating procedure provided a significant improvement in the estimates with the second updating yielding little or no additional improvement.

The updating procedure provided rewards in the form of improved statistical correlation with the measured data and greatly reduced kriging error variances. A useful aspect was that all of the improvement in the estimates was derived from the process in only two iterations. This was advantageous because the physical process of fitting mathematical functions to experimental data can be time and labor intensive. The fact that only a few iterations are necessary makes the process more useful in a practical sense.

From the results yielded from this study, it is recommended that sampling schemes be evaluated via the semivariogram prior to the conclusion of field sampling to ensure adequate definition of the spatial structure. Closer sample spacings than 10 feet have been shown to be necessary in this case to adequately define the correlation structure for the vertical magnetic gradient. Future vertical magnetic gradient surveys, with the purpose of delineating buried drum locations in hazardous waste sites, should consider using an isometric triangular sampling pattern with an incremental spacing of 5 feet to ensure the definition of the spatial structure of the vertical gradient data.

Considering the relatively low correlations resulting from the cross - validation procedures, the utility of kriging the vertical magnetic gradient data would be contingent on whether: a) there is a definite need for interpolated values, b) additional vertical gradient field measurements are unavailable and not acquirable, and c) the time required to rigorously perform the necessary analyses is available.

REFERENCES

Barrows, L. and Rocchio, J.E. (1990). Magnetic surveying for buried metal objects. Ground Water Monitoring Review, 10(3), pp. 204-212.

Barongo, J.D. (1985). Method for depth estimation on aeromagnetic vertical gradient anomalies. Geophysics, 50(6), pp. 963-968.

Benson, R.C., Glaccum, R.A. and Noel, M.R. (1983). Geophysical Techniques for Sensing Buried Wastes and Waste Migration. Miami, Florida: U.S. E.P.A. Contract No. 68-03-3050.

Clark, Isobel (1979). Practical Geostatistics. London: Applied Science Publishers Ltd., pp. 1-122.

Davis, J.C. (1982). Statistics and Data Analysis in Geology. New York: John Wiley and Sons, pp. 238-405.

Delhomme, J.P. (1978). Kriging in hydrosciences. Advances in Water Resources, 1(5), pp. 251-266.

De Marsily, G. (1986). Quantitative Hydrogeology. New York: Academic Press, pp. 254-297

Dobrin, M.B. (1976). Introduction to Geophysical Prospecting. New York: McGraw Hill, pp. 574-581.

Easley, D.H., Borgman,L.E., and Shive,P.N. (1990). Geostatistical simulation for geophysical applications - Part I: Simulation. Geophysics, 55(11), pp. 1435-1440.

Freeze, R.A. (1975). A stochastic-conceptual analysis of one-dimensional groundwater flow in nonuniform homogeneous media. Water Resources Research, 11(5), pp. 725-741.

Forrest, A.M. (1991). What is Geophysics? Water Well Journal, 45(7), pp. 32-34.

French R.B., Williams, T.R. and Foster A.R. (1987). Western Processing Remedial Action Site Final Geophysical Survey Report. Seattle, Washington: E.P.A Region 10 Job Number 280-002.

Gilkeson, F.H., Heigold, P.C. and Laymon, D.E. (1986). Practical application of theoretical models to magnetometer surveys on hazardous waste disposal sites - A case history. Ground Water, 28(4), pp. 54-61.

Grant, F.S. and West, G.F. (1965). Interpretation Theory in Applied Geophysics. New York: McGraw-Hill.

Haan, C.T. (1977). Statistical Methods in Hydrology. Ames, Iowa: The Iowa State University Press, 42-80.

REFERENCES

Hood, P.J., Holroyd, M.T., and McGrath P.H. (1979). Magnetic methods applied to base metal exploration. Geol. Survey of Canada, Econ. Geol. Rep., 31, pp.77-104.

Journel, A.G. (1989). Fundamentals of Geostatistics in Five Lessons. Washington, D.C.: American Geophysical Union, pp. 1-11.

Journel, A.G. and Huijbregts, C.J. (1978). Mining Geostatistics. New York: Academic Press, pp. 14-254.

Kitanidis, P.K. (1986). Parameter uncertainty in estimation of spatial functions: Bayesian analysis. Water Resources Research, 22(4), pp. 499-507.

Knighton, R.E. and Wagenet, R.J. (1987). Geostatistical Estimation of Spatial Structure. Ithaca, N.Y., Cornell Univ. Press, pp. 2-16.

Krige, D.G. (1966). Two dimensional weighted moving average trend surfaces for ore evaluation. Journal S. African Inst. Min. Metall., 66, pp. 13-38.

Lord, A.E. and Koerner, R.M. (1988). Nondestructive testing (NDT) techniques to detect conained subsurface hazardous waste. Journal of Hazardous Materials, 19(4), pp. 119-123.

Massman, J.W. and Freeze, R.A. (1989). Updating random hydraulic conductivity fields: a two step procedure. Water Resources Research, 25(7), pp. 1763-1765.

Matheron, G. (1971). The Theory of Regionalized Variables and Its Applications, Fontainebleau, France: Ecole des Mines.

McBratney, A.B., Webster, R. and Burgess, T.M. (1981). The design of optimal sampling schemes for local estimation and mapping of regionalized variables. Computers and Geosciences, 7(4), pp. 331-334.

Nelson, J.B. (1988a). Calculation of the magnetic gradient tensor from total field gradient measurements and its application to geophysical interpretation. Geophysics, 53(7), pp. 957-960.

Nelson, J.B. (1988b). Comparison of gradient analysis techniques for linear two-dimensional magnetic sources. Geophysics, 53(8), pp. 1088-1095.

Nettleton, L.L. (1976). Elementary Gravity and Magnetics for Geologist and Seismologists. Tulsa, Oklahoma: Society of Exploration Geophysics. pp. 88-93.

Parkhurst, D.F. (1984). Optimal sampling geometry for hazardous waste sites. Environmental Science and Technology, 18(7), pp. 521-523.

REFERENCES

Press, S.J. (1989). Bayesian Statistics. New York: John Wiley and Sons, pp. 23-119.

Press, W.H., Flannery, B.P., Teukolsky, S.A. and Vetterling, W.T. (1988). Numerical Recipes in C. New York: Cambridge Univ. Press, pp. 472-490.

Russo, D. and Bresler, E. (1980). Field determination of soil hydraulic properties for statistical analysis. Soil Sci. Soc. Am. Jour., 44, pp. 697-702.

Spector, A. (1968). Spectral Analysis of Aeromagnetic Data. Ph.D. dissertation, University of Toronto . pp. 58-63.

Strangway, D.W. (1967). Magnetic Characteristics of Rocks. Tulsa, Oklahoma: Society of Exploration Geophysics. pp. 454-473.

Struttmann, T. and Anderson T. (1989). Comparison of shallow electromagnetic and the proton precession magnetometer surface geophysical techniques to effectively delineate buried wastes. Metcalf and Eddy technical paper. Columbus, Ohio, pp. 27-34.

Telford, W.M., Geldart, L.P., Sheriff, R.E. and Keys, D.A. (1982). Applied Geophysics: New York: Cambridge Univ. Press, pp. 443-529.

Tyagi, S. and Lord, A.E. (1983). Use of a proton precession magnetometer to detect buried drums in sandy soil. Journal of Hazardous Materials, 8(4), pp. 11-23.

APPENDIX A

SCATTERPLOTS OF TOTAL FIELD INTENSITY AND VERTICAL MAGNETIC GRADIENT RELATIVE TO EACH OTHER AND THE NORTH AND EAST COORDINATES OF THE WESTERN PROCESSING SURVEY GRID

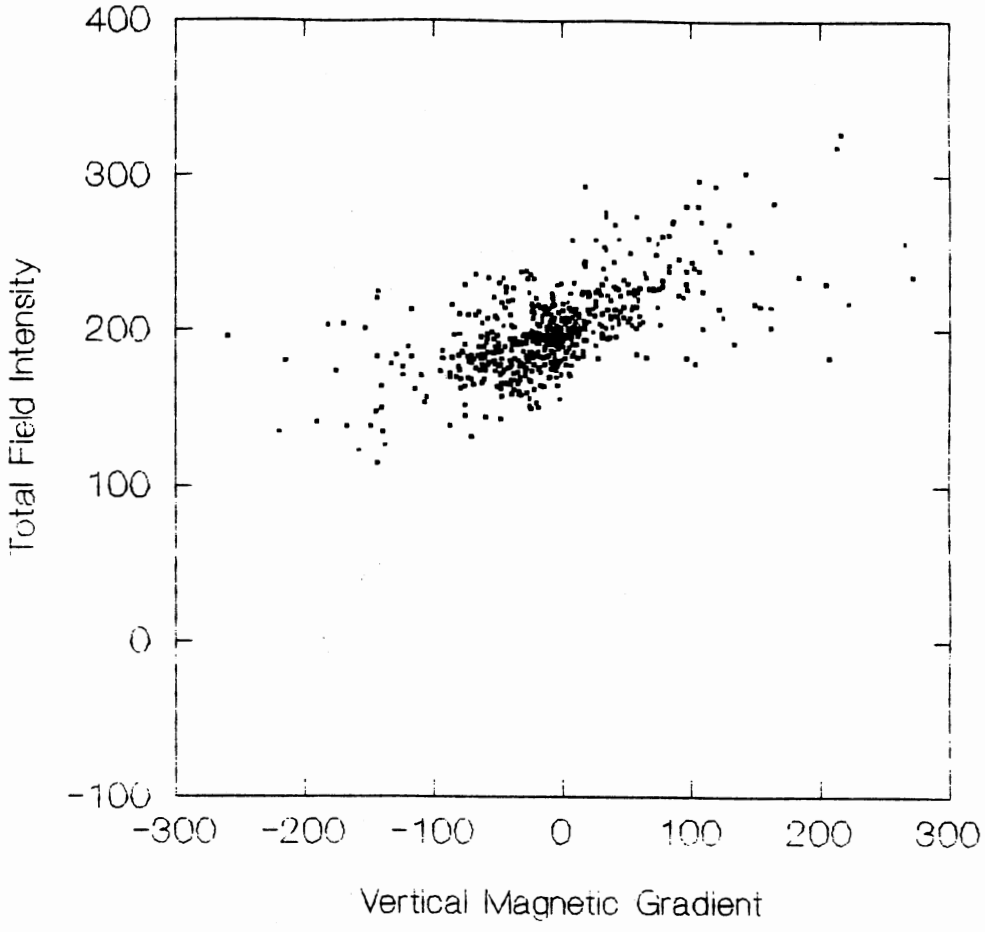
400
300
200
100
0
-100
-300
-200
-100
0
100
200
300
Total Field Intensity
Vertical Magnetic Gradient

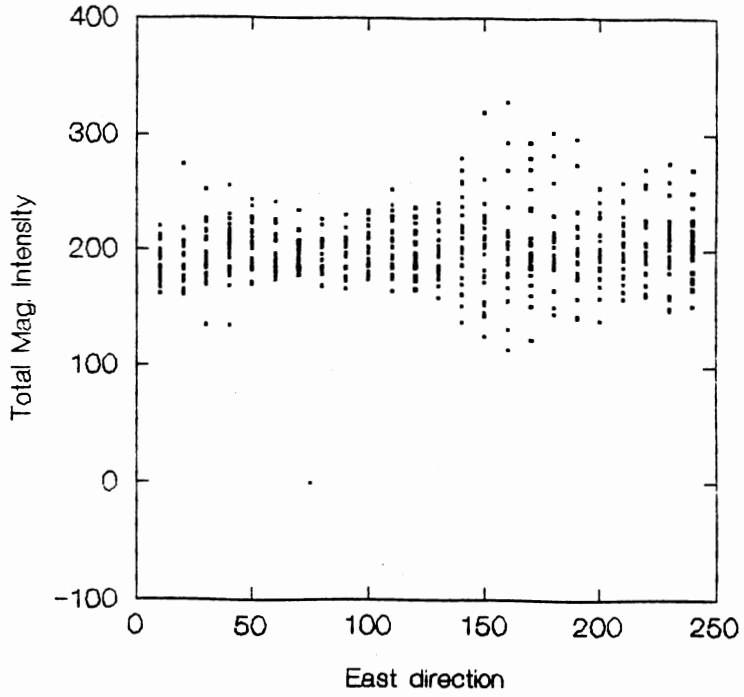
400
300
200
100
0
-100
0
50
100
150
200
250
Total Mag. Intensity
East direction

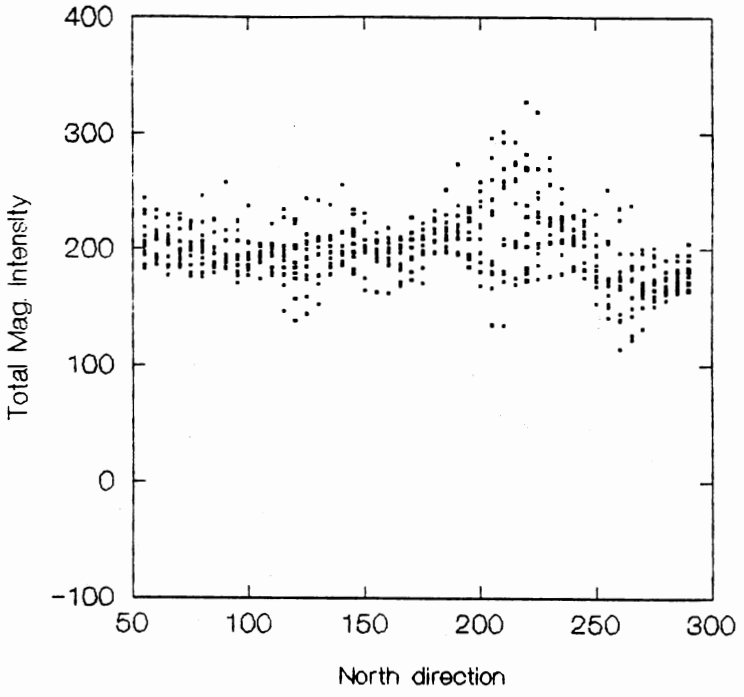
400
300
200
100
0
-100
50
100
150
200
250
300
Total Mag. Intensity
North direction

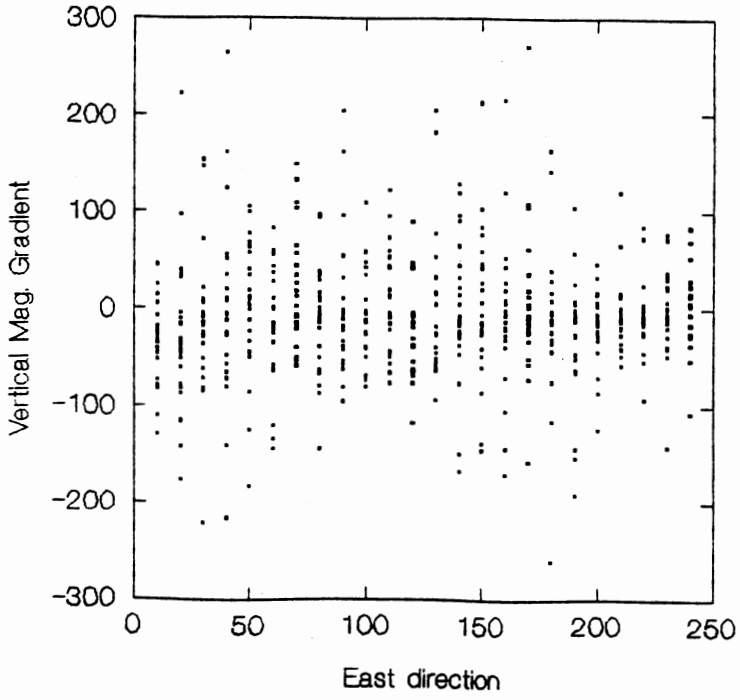
300
200
100
0
-100
-200
-300
0
50
100
150
200
250
Vertical Mag. Gradient
East direction

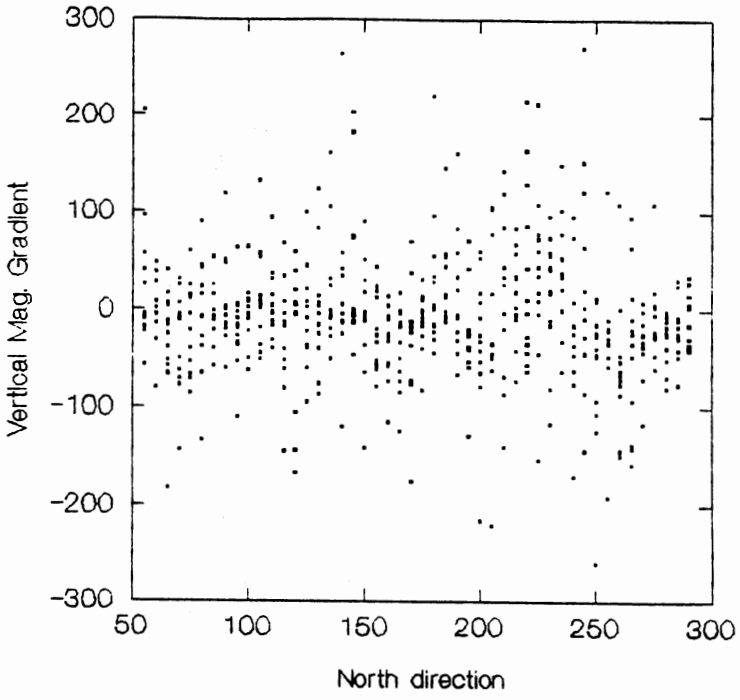
300
200
100
0
-100
-200
-300
50
100
150
200
250
300
Vertical Mag. Gradient
North direction

APPENDIX B

ANISOTROPY ELLIPSES FOR THE TOTAL MAGNETIC FIELD INTENSITY AND VERTICAL MAGNETIC GRADIENT DATA

TOTAL FIELD ANISTROPY

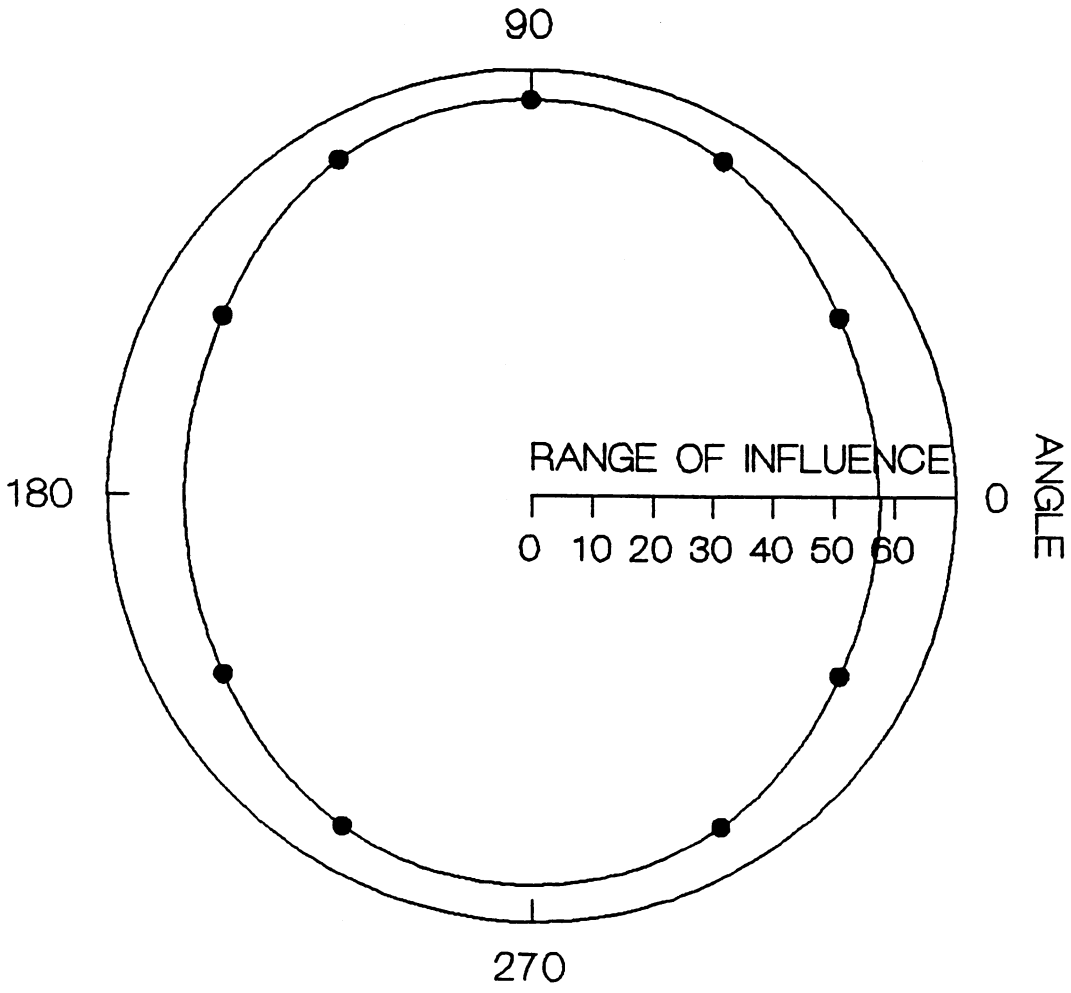

GRADIENT ANISOTROPY

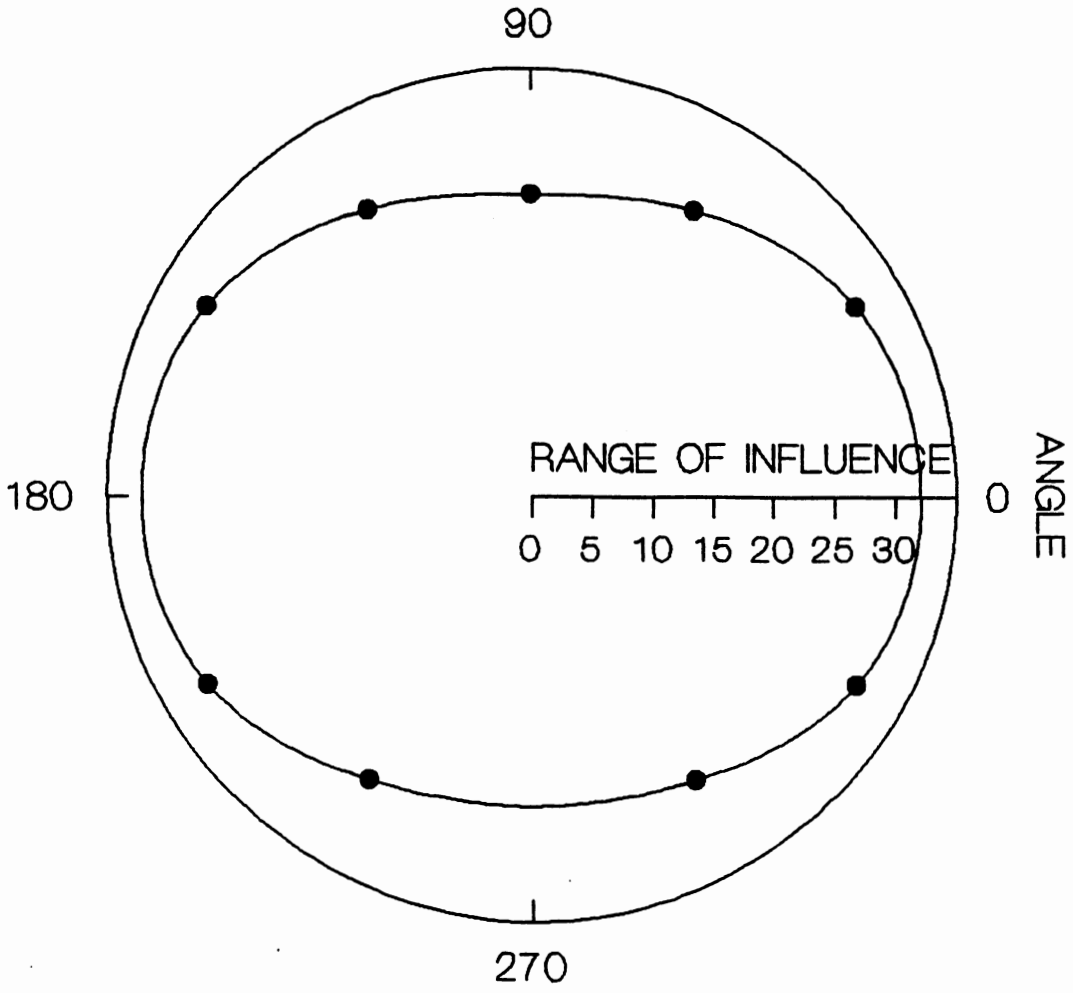

APPENDIX C

GRAPHICAL REPRESENTATIONS OF THE TOTAL MAGNETIC INTENSITY SEMIVARIANCE MODELS WITH SUPERIMPOSED EXPERIMENTAL SEMIVARIANCES

MODEL 1

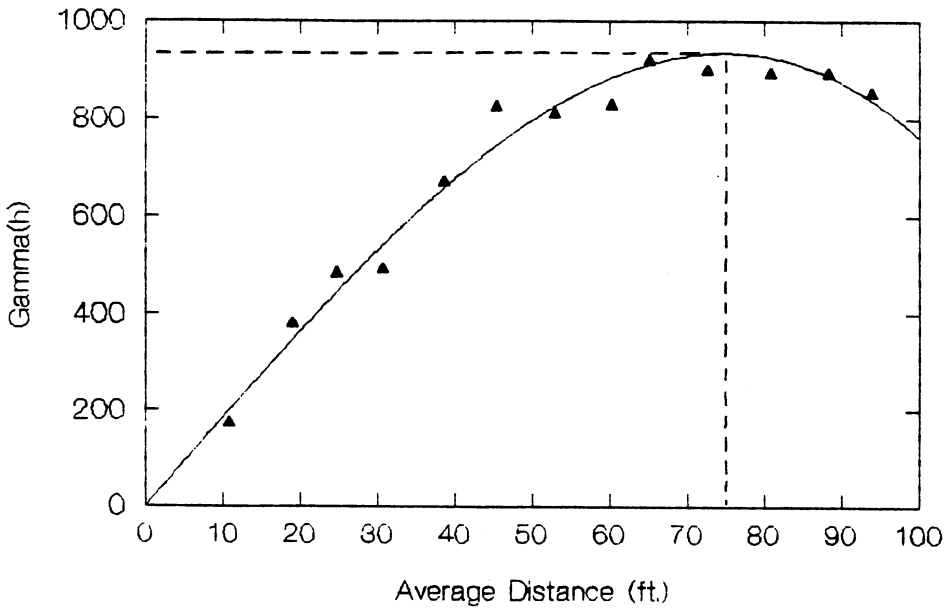
1000
800
600
400
200
0
Gamma(h)
0
10
20
30
40
50
60
70
80
90
100
Average Distance (ft.)

MODEL 2

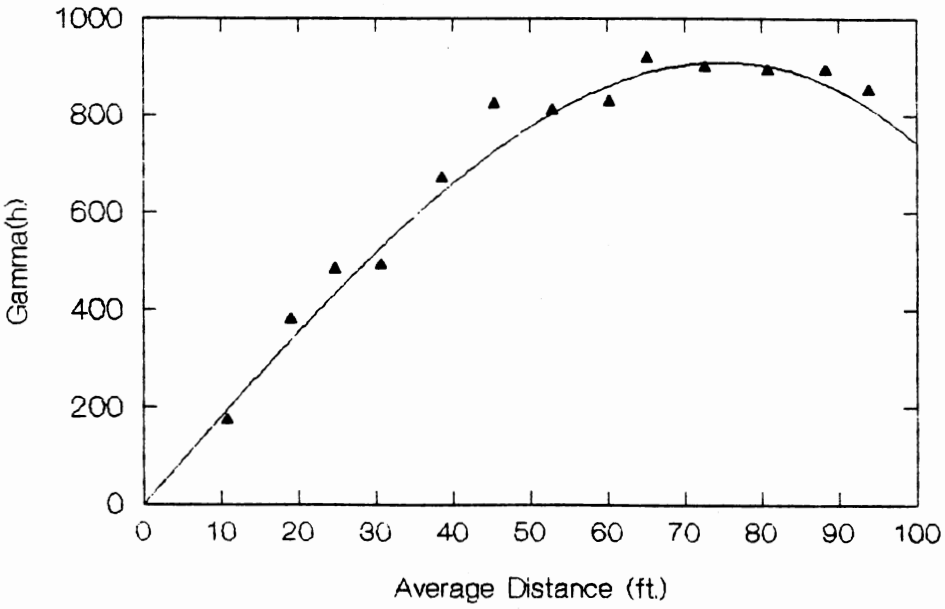
1000
800
600
400
200
0
Gamma(h)
0
10
20
30
40
50
60
70
80
90
100
Average Distance (ft.)

MODEL 3

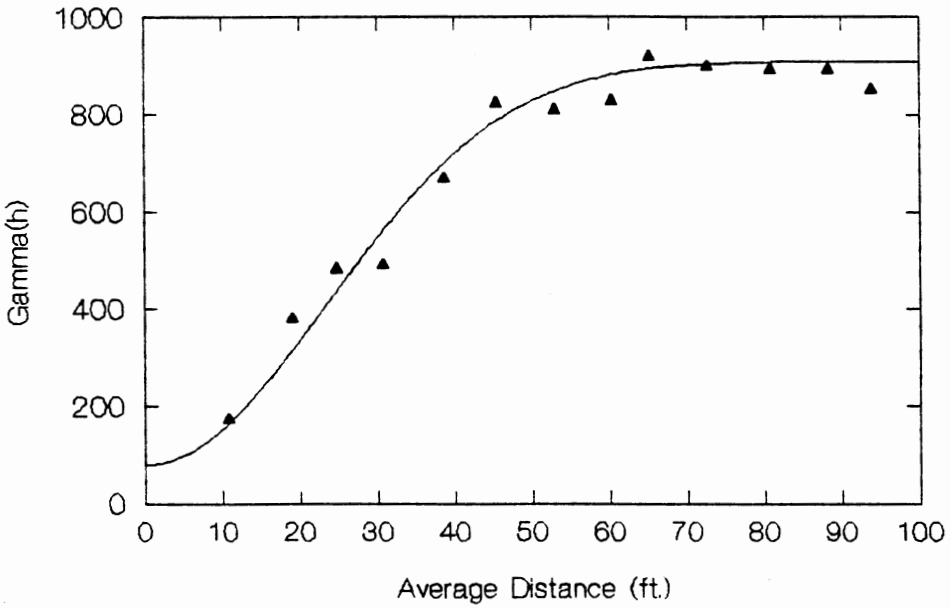
1000
800
600
400
200
0
Gamma(h)
0
10
20
30
40
50
60
70
80
90
100
Average Distance (ft.)

APPENDIX D

PROBABILITY DISTRIBUTION FUNCTIONS FOR THE KRIGED AND MEASURED TOTAL MAGNETIC INTENSITY DATA OVER THE ENTIRE WESTERN PROCESSING SURVEY AREA

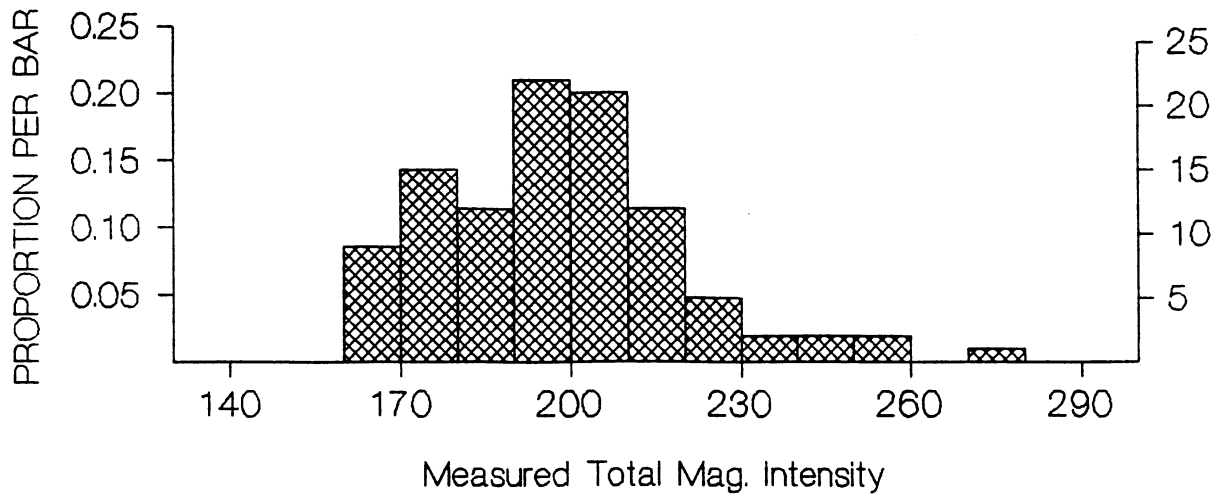
PROPORTION PER BAR
0.25
0.20
0.15
0.10
0.05
25
20
15
10
5
140
170
200
230
260
290
Measured Total Mag. Intensity

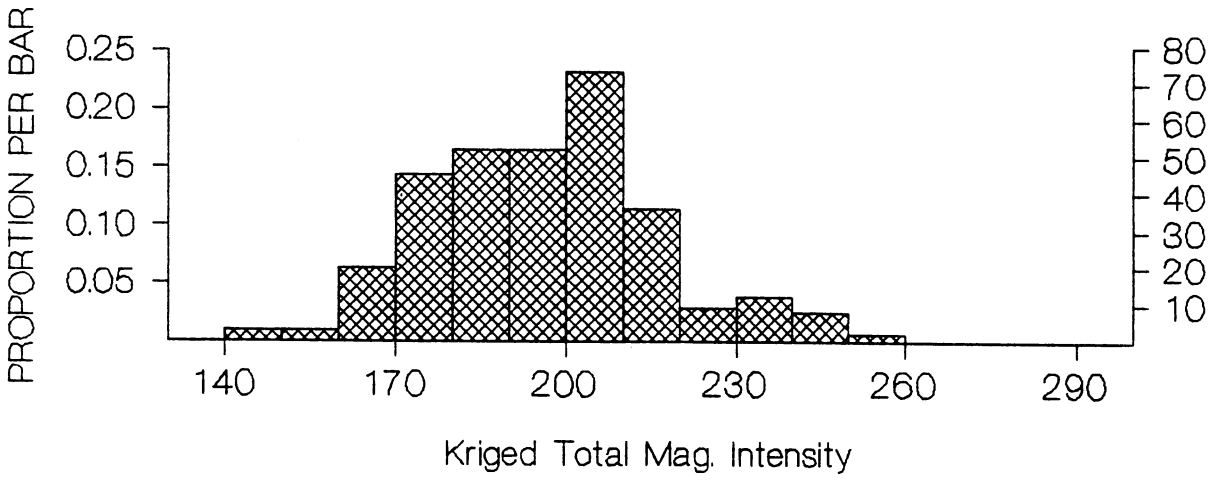
PROPORTION PER BAR
0.25
0.20
0.15
0.10
0.05
80
70
60
50
40
30
20
10
140
170
200
230
260
290
Kriged Total Mag. Intensity

APPENDIX E

PROBALILTITY DISTRIBUTION FUNCTIONS FOR THE KRIGED DATA DERIVED FROM THE LOCALIZED AND PROJEJCTED LOCALIZED SEMIVARIANCE MODELS AND THE MEASURED DATA FOR THE NORTHERN HALF OF THE TOTAL MAGNETIC INTENSITY SURVEY

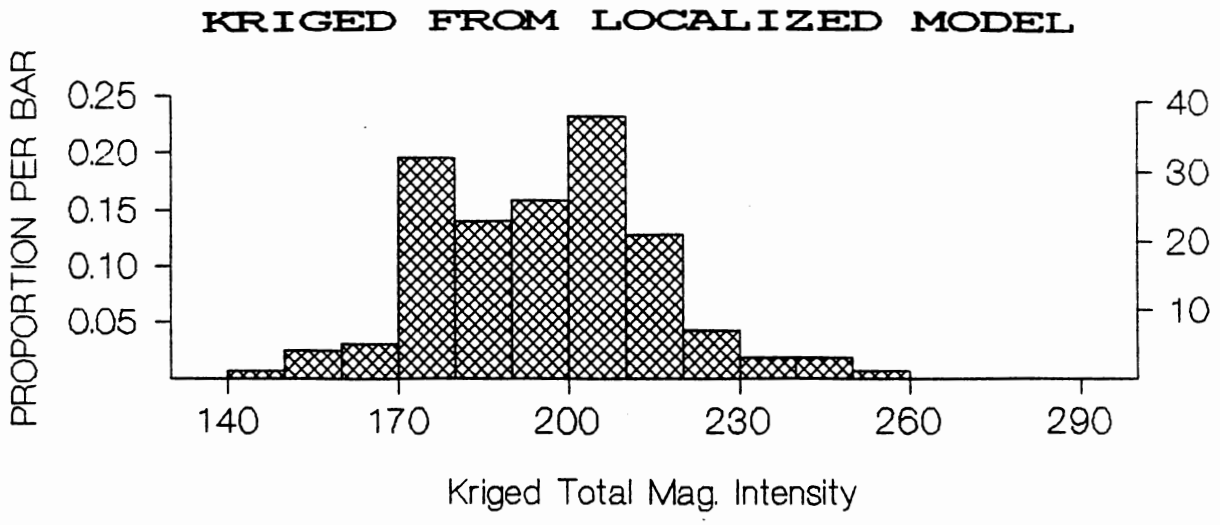
KRIGED FROM LOCALIZED MODEL
PROPORTION PER BAR
0.25
0.20
0.15
0.10
0.05
40
30
20
10
140
170
200
230
260
290
Kriged Total Mag. Intensity

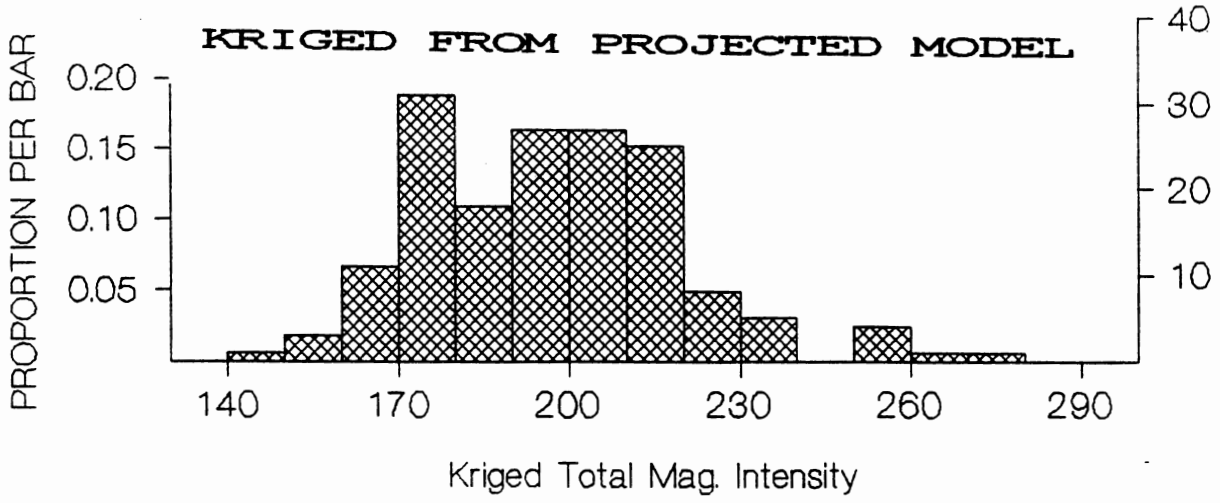
KRIGED FROM PROJECTED MODEL
PROPORTION PER BAR
0.20
0.15
0.10
0.05
40
30
20
10
140
170
200
230
260
290
Kriged Total Mag. Intensity

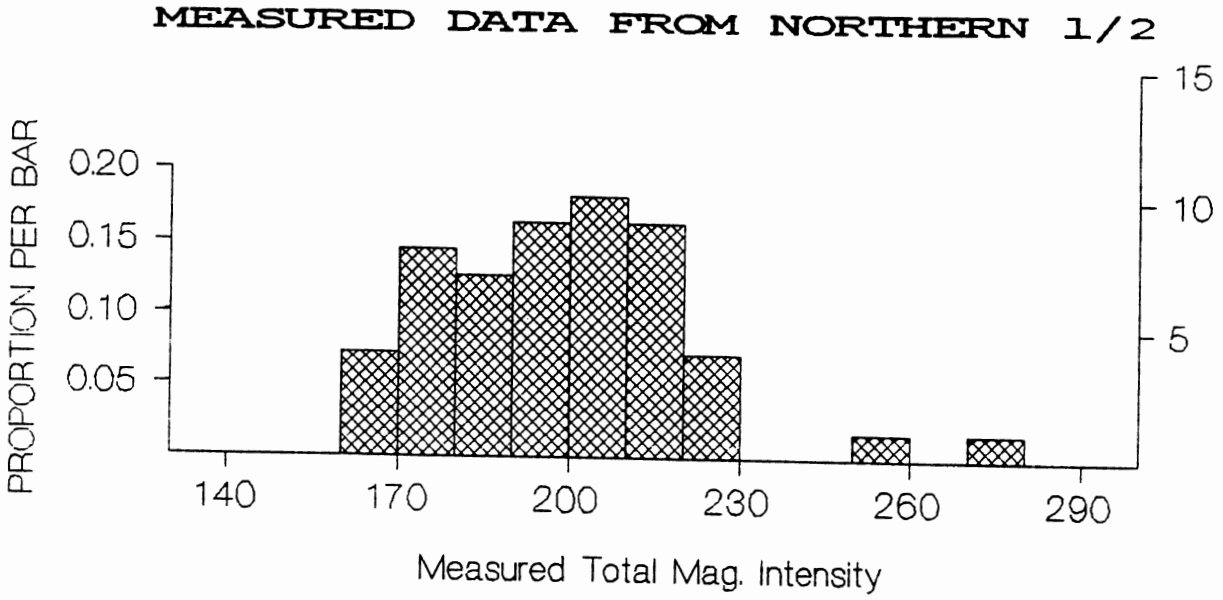
MEASURED DATA FROM NORTHERN 1/2
PROPORTION PER BAR
0.20
0.15
0.10
0.05
15
10
5
140
170
200
230
260
290
Measured Total Mag. Intensity

APPENDIX F

MAPS OF MEASURED AND KRIGED TOTAL MAGNETIC INTENSITY VALUES OVER THE NORTHERN HALF OF THE WESTERN PROCESSING SURVEY GRID

Area 2 - Total Field Kriged / Area 1 Model

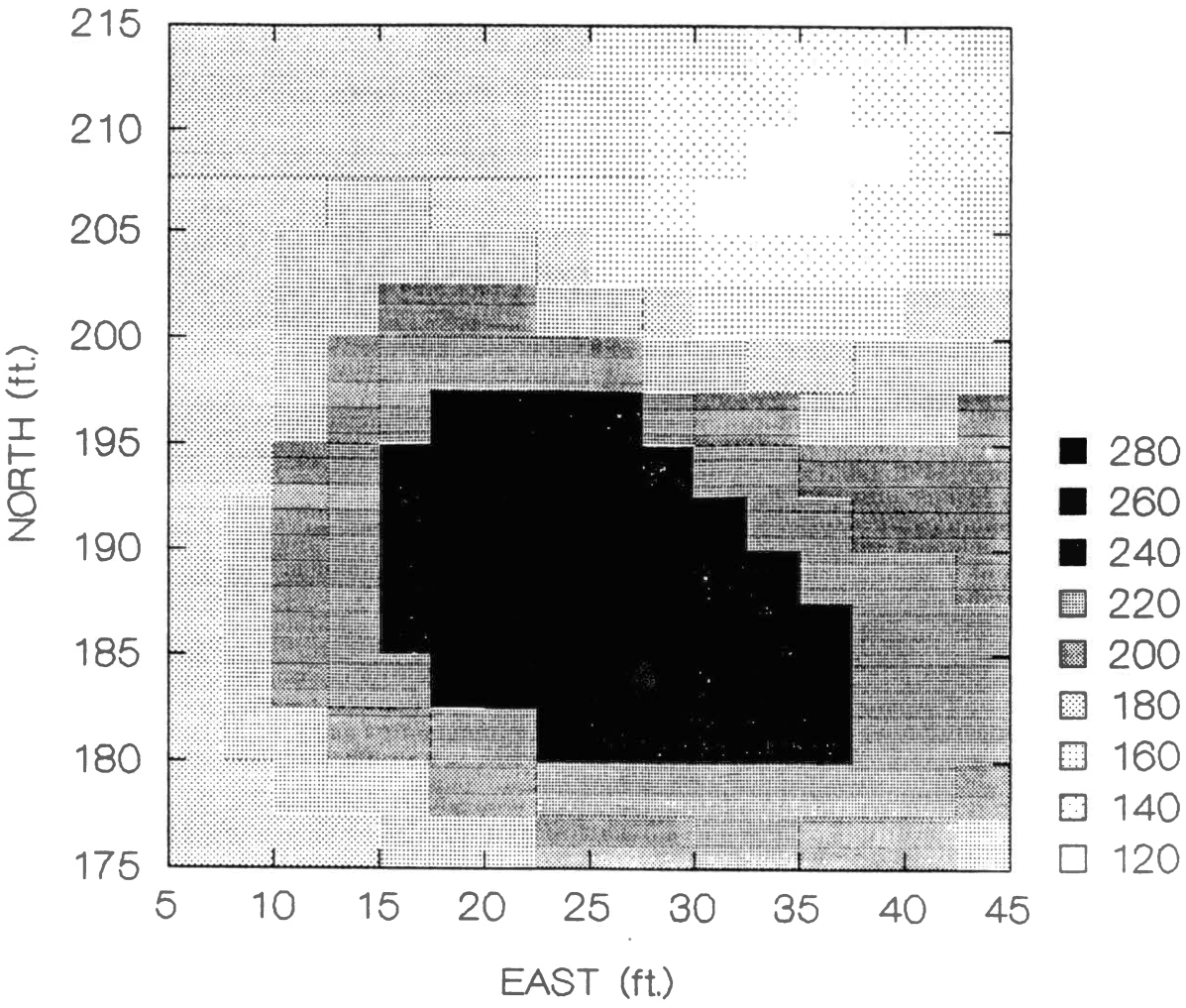

Area 2 - Total Field Kriged / Localized Model

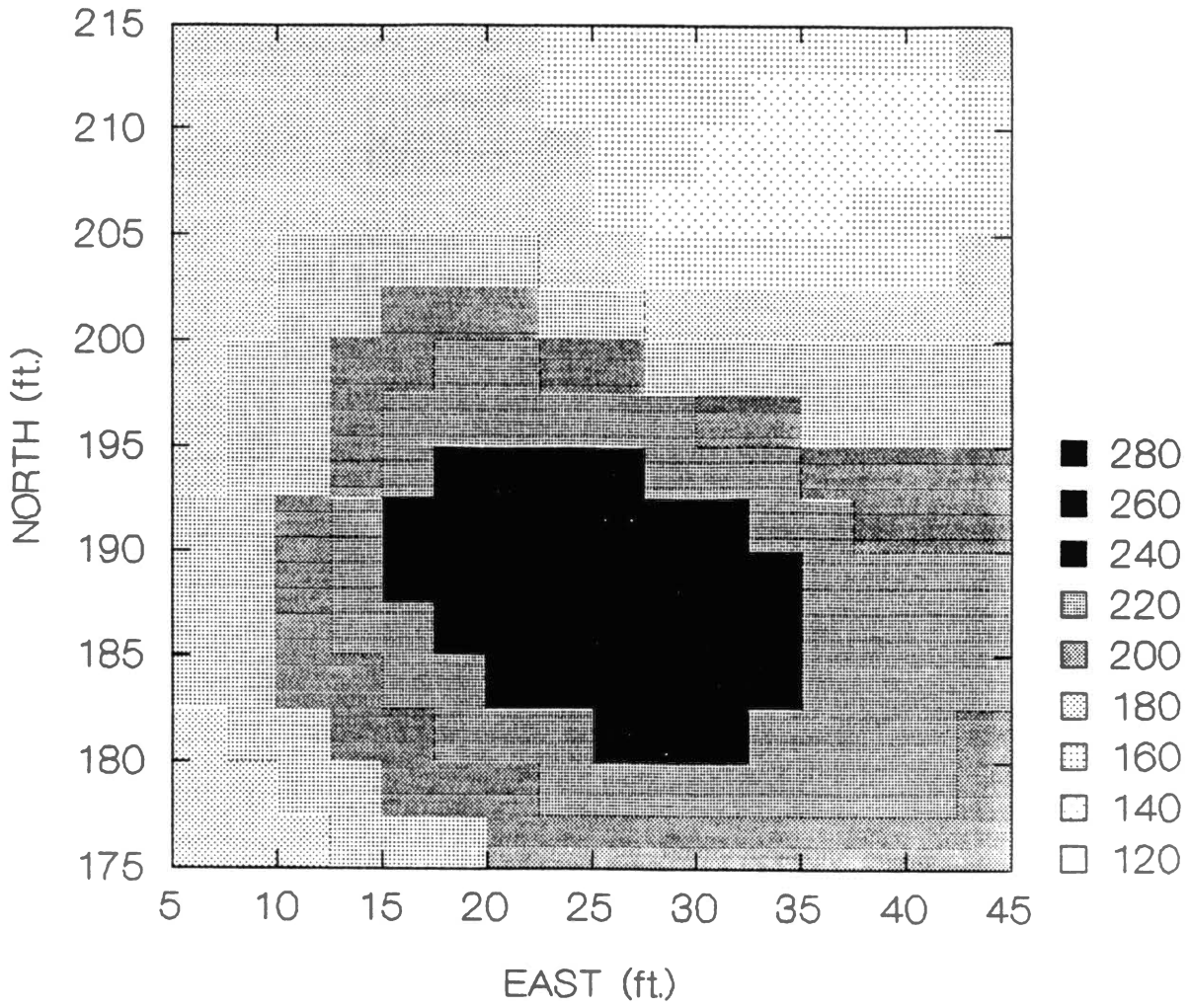

APPENDIX G

PROBABILTITY DISTRIBUTION FUNCTIONS FOR THE MODELS USED TO DETERMINE THE PRIOR ESTIMATE FOR SEMIVARIANCE OF THE VERTICAL MAGNETIC GRADIENT DATA

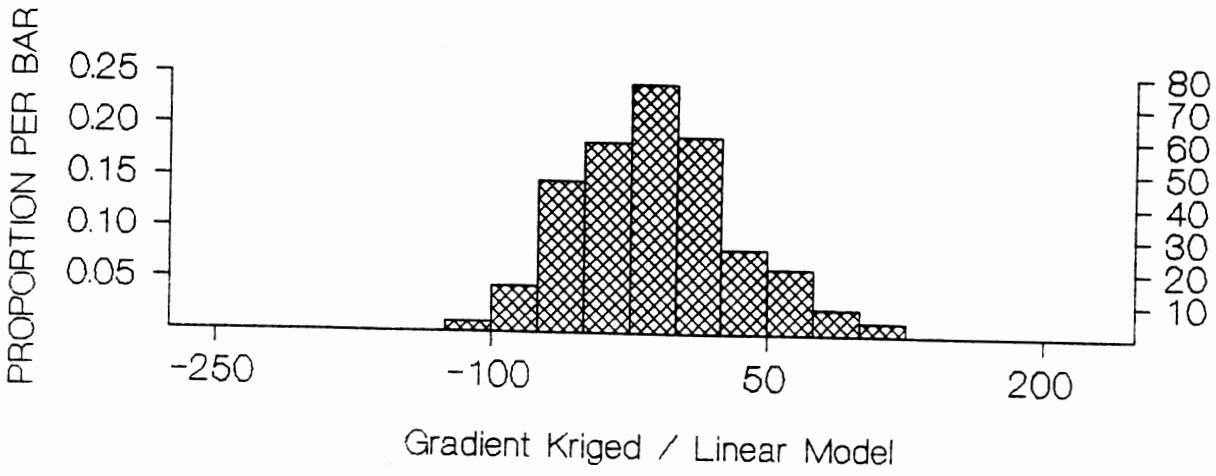
PROPORTION PER BAR
0.25
0.20
0.15
0.10
0.05
80
70
60
50
40
30
20
10
-250
-100
50
200
Gradient Kriged / Linear Model

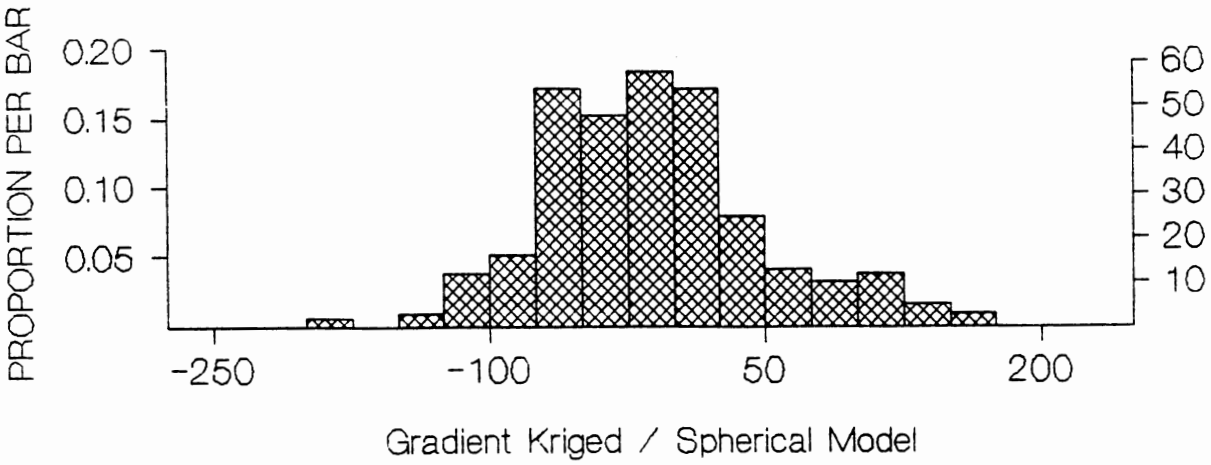
PROPORTION PER BAR
0.20
0.15
0.10
0.05
60
50
40
30
20
10
-250
-100
50
200
Gradient Kriged / Spherical Model

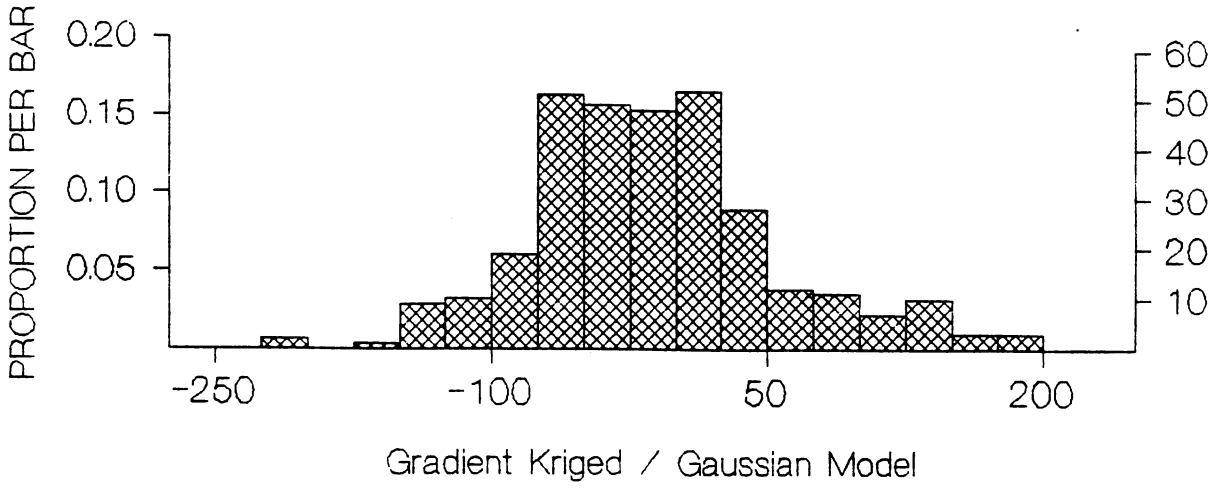
PROPORTION PER BAR
0.20
0.15
0.10
0.05
60
50
40
30
20
10
-250
-100
50
200
Gradient Kriged / Gaussian Model

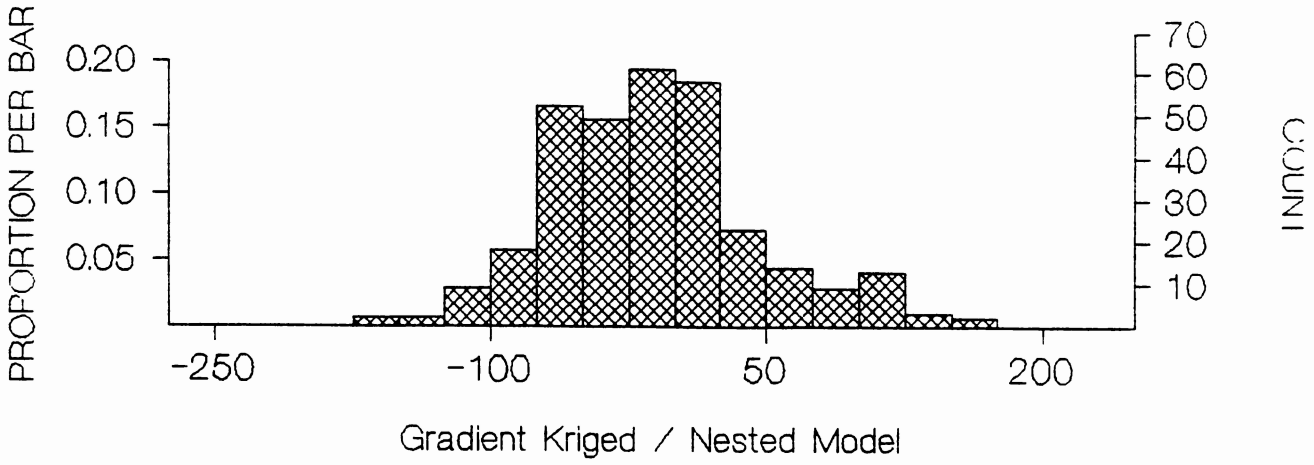
PROPORTION PER BAR
0.20
0.15
0.10
0.05
70
60
50
40
30
20
10
COUNT
-250
-100
50
200
Gradient Kriged / Nested Model

APPENDIX H

COMPOSITE MAPS OF THE VERTICAL MAGNETIC GRADIENT DATA USING MEASURED AND KRIGED DATA USING THE MODELS DEFINED ON PAGES 64 AND 65

Area 1 Drum Cache

KRIGED USING LINEAR MODEL

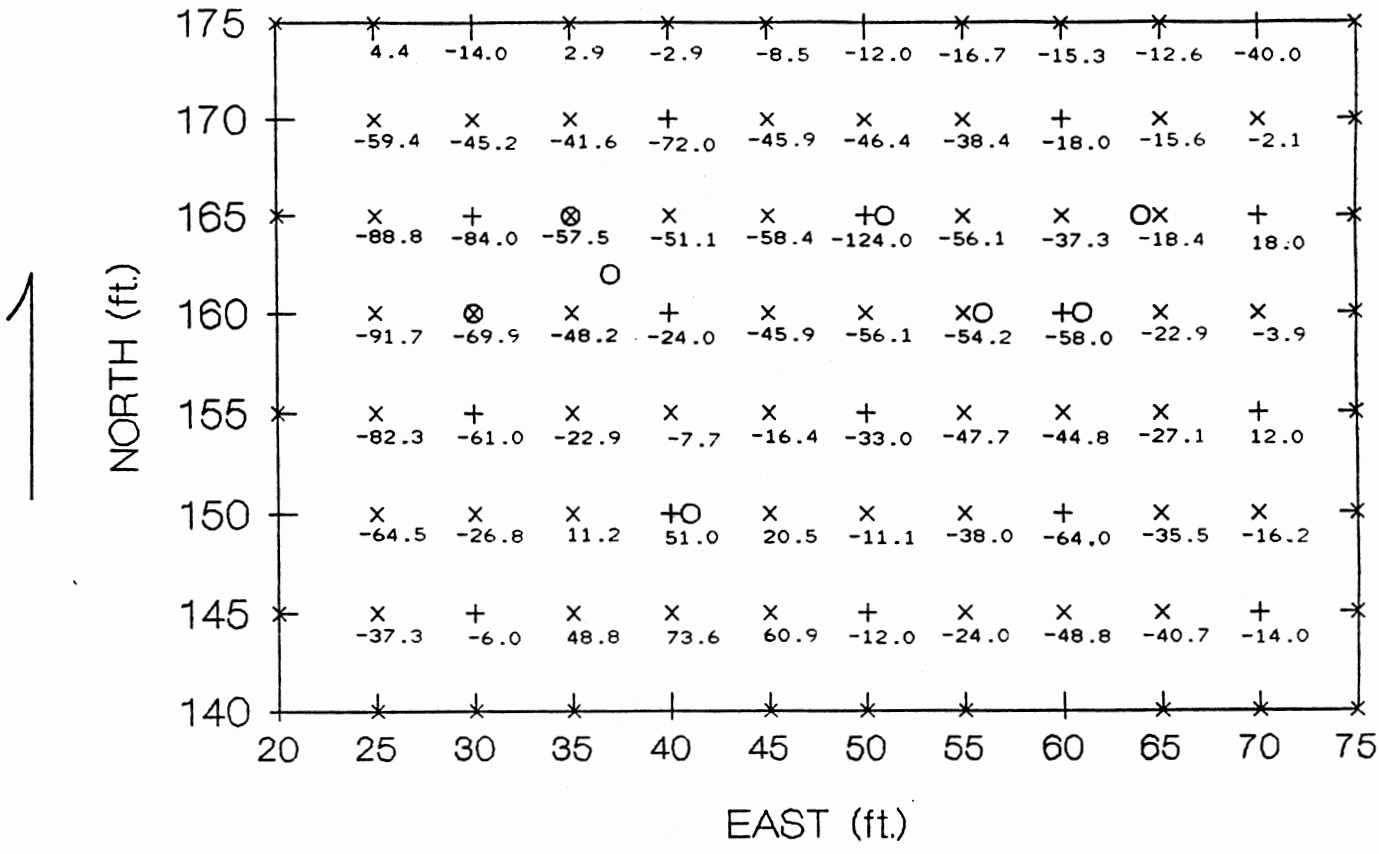

O Drum Loc.
× Kriged
\+ Measured

Area 2 Drum Cache

KRIGED USING LINEAR MODEL

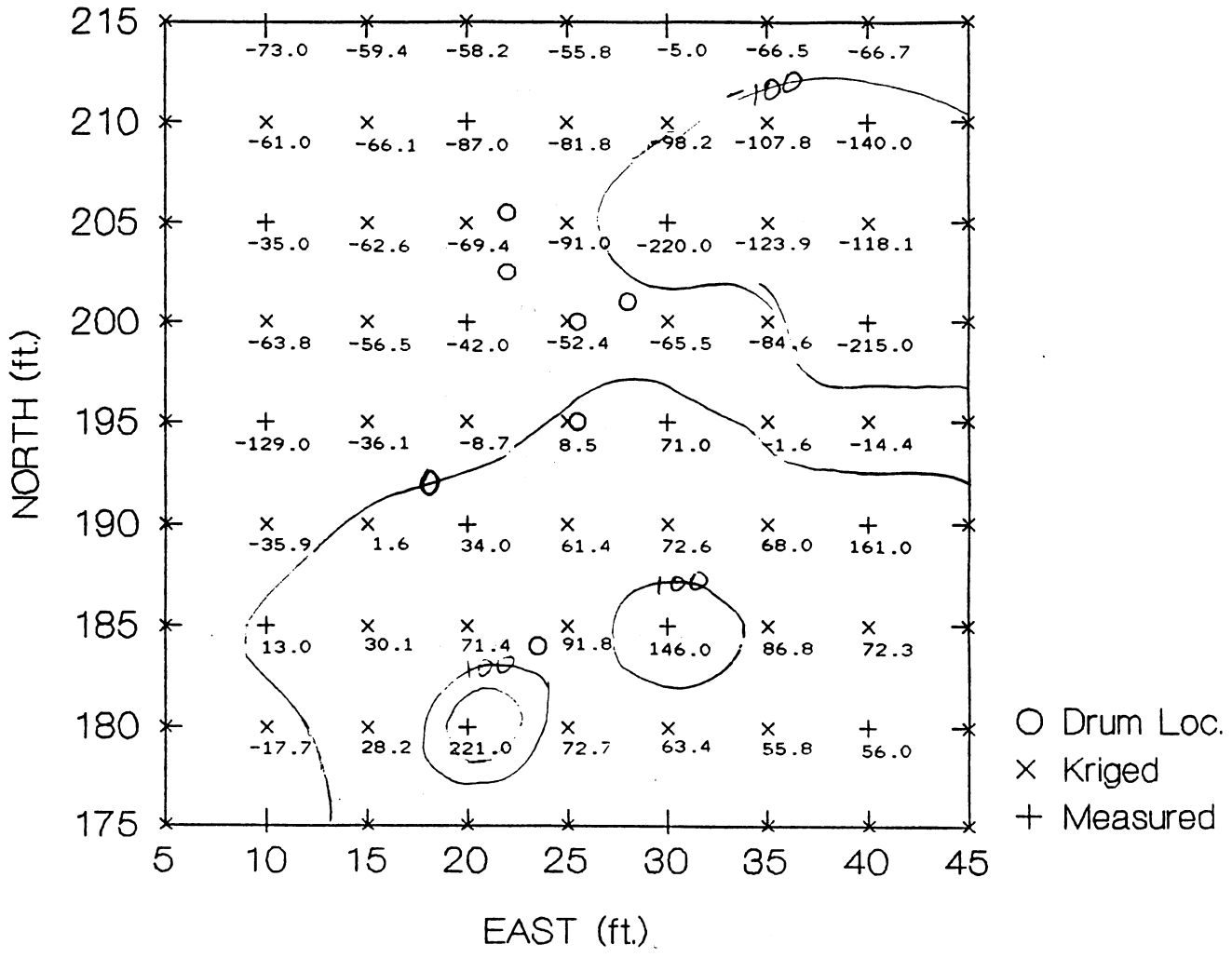

Area 2 Drum Cache

KRIGED USING GAUSSIAN MODEL

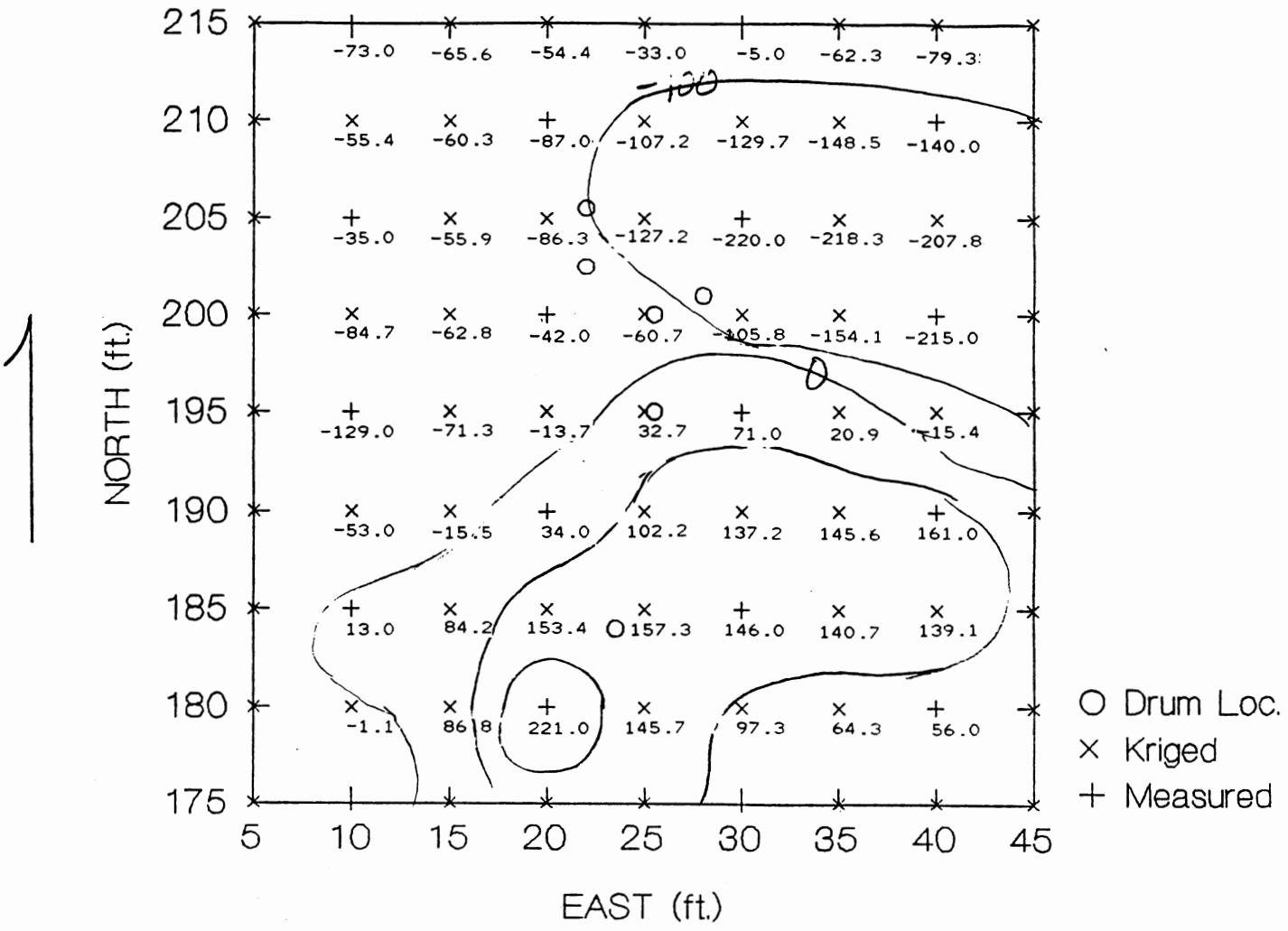

Area 1 Drum Cache

KRIGED USING GAUSSIAN MODEL

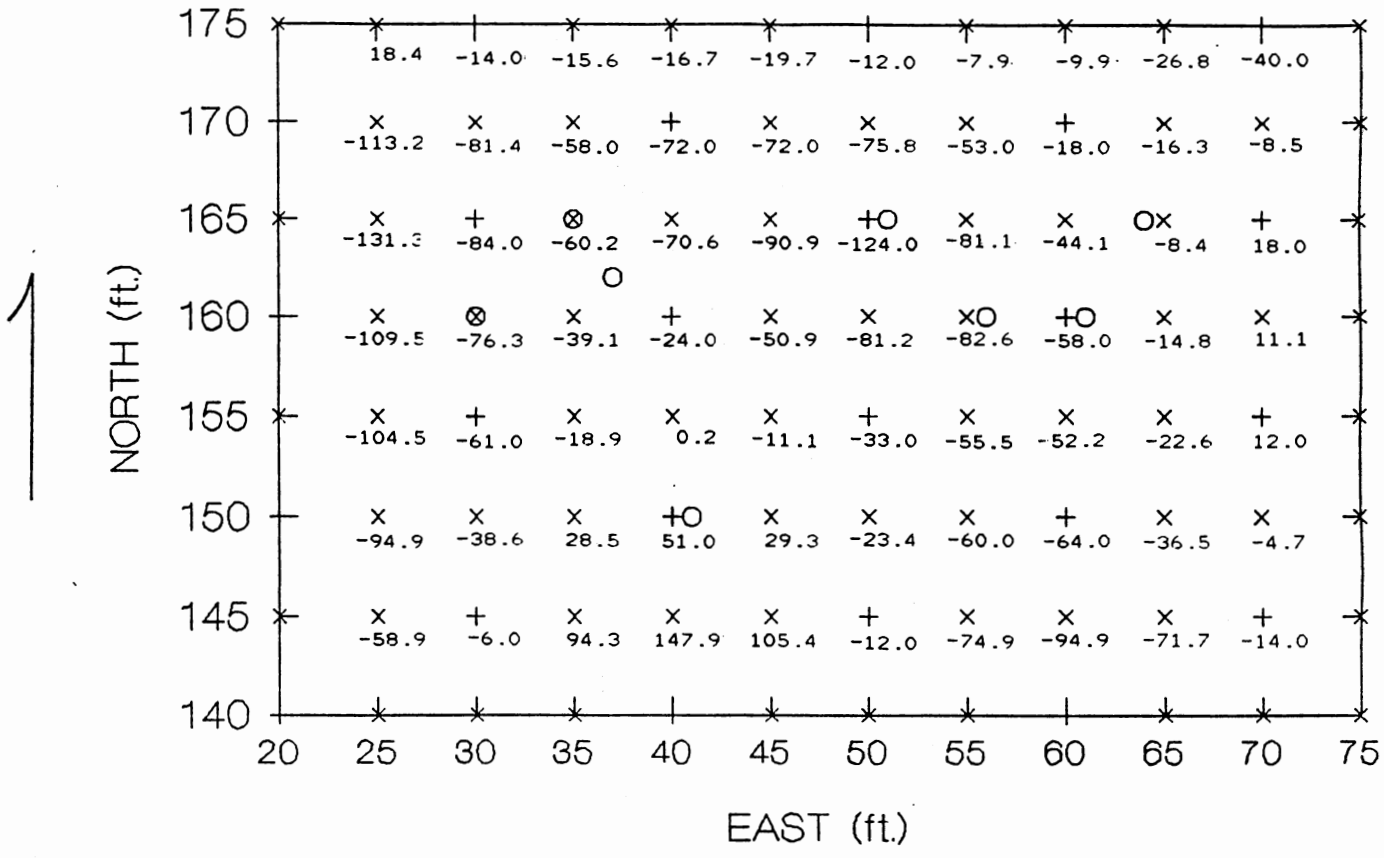

Area 1 Drum Cache

KRIGED USING SPHERICAl MODEL

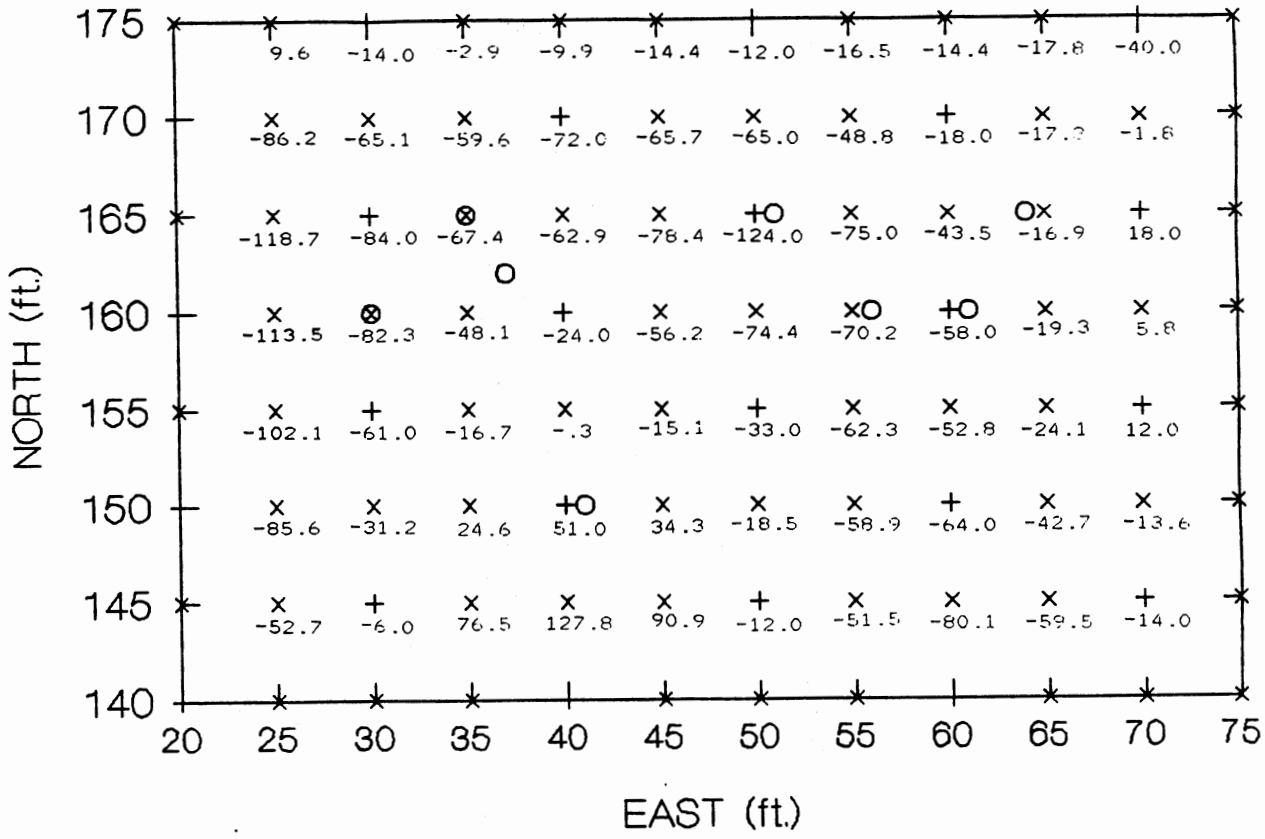

Area 2 Drum Cache

KRIGED USING SPHERICAL MODEL

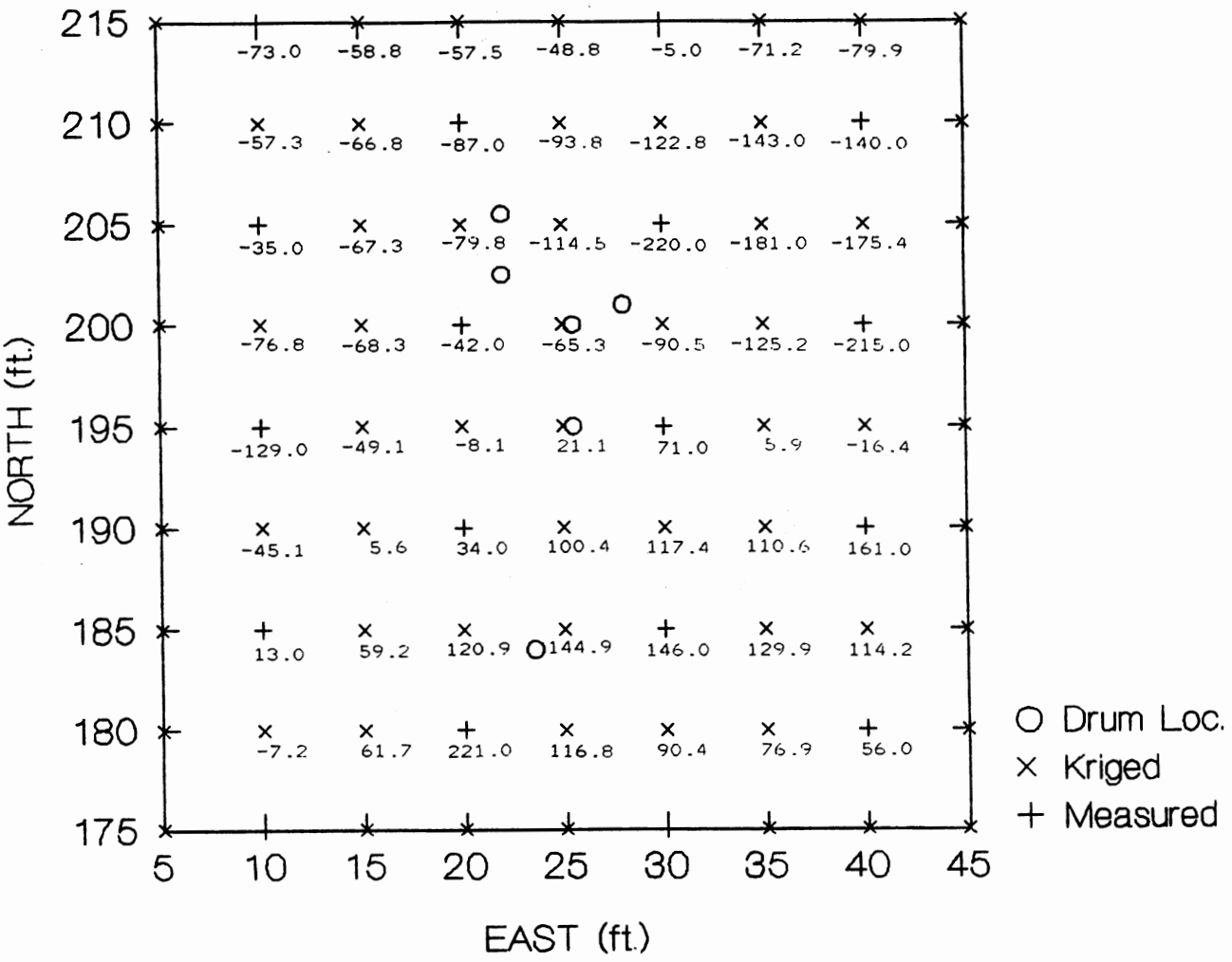

Area 1 Drum Cache

KRIGED USING NESTED LIN/EXP MODEL

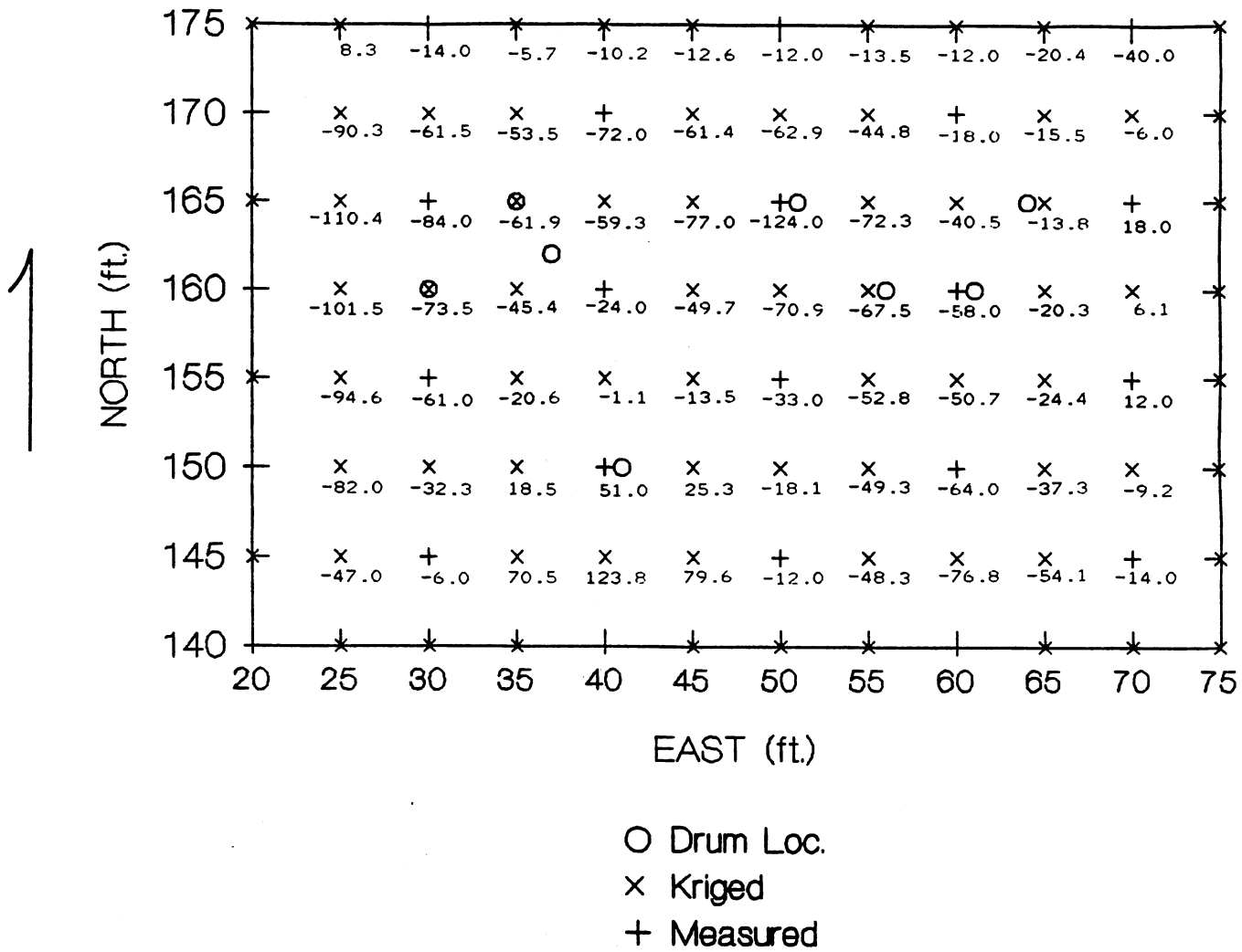

Area 2 Drum Cache

KRIGED USING NESTED LIN/EXP MODEL

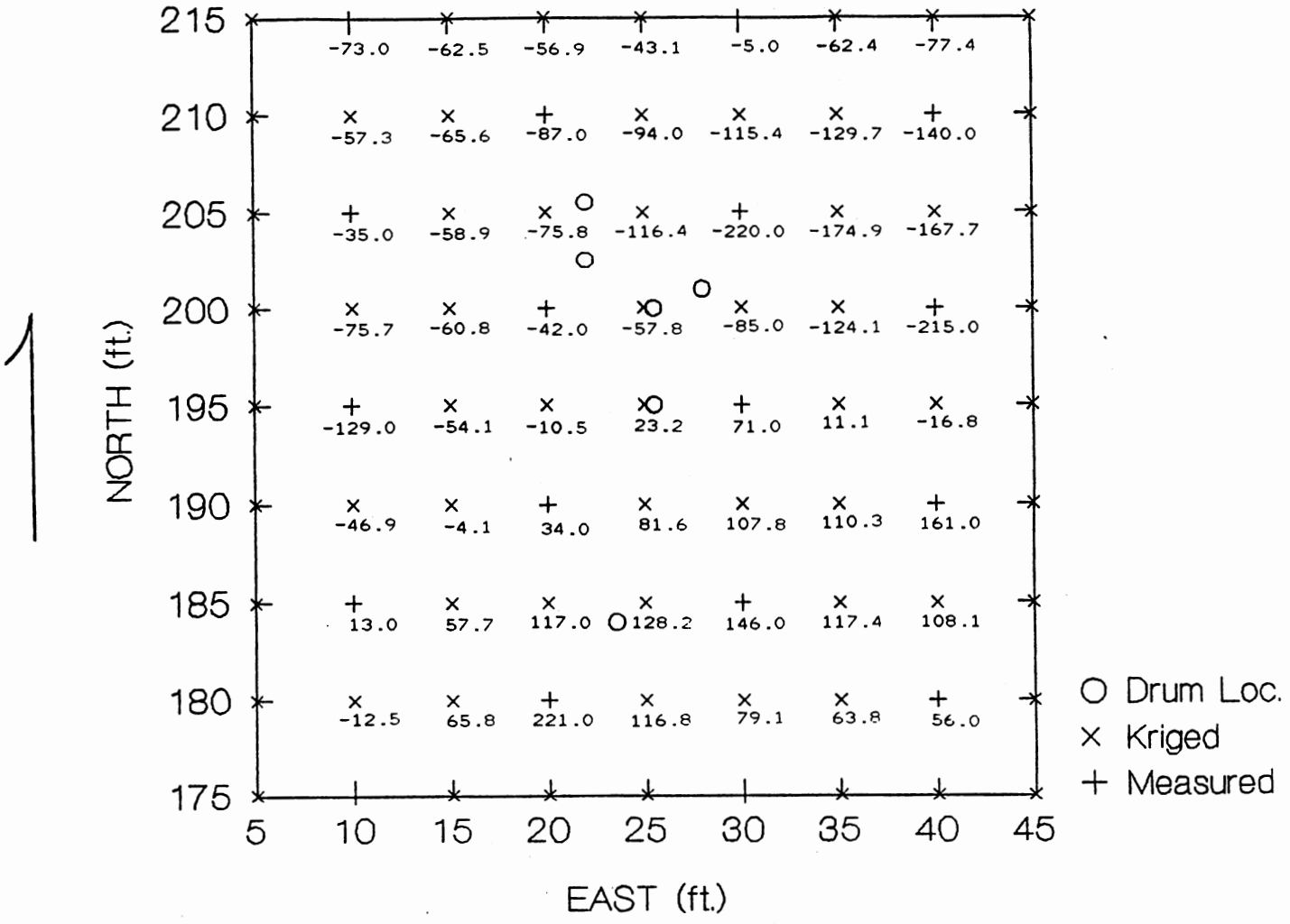

VITA

Edward Molash

Candidate for the Degree of

Master of Science

Thesis: GEOSTATISTICAL ANALYSIS OF MAGNETOMETRY TECHNIQUES TO DELINEATE LOCATIONS OF BURIED FERROMETALLIC DRUMS IN HAZARDOUS WASTE SITES

Major Field: Environmental Engineering

Biographical:

Personal Data: Born in Wilmington, Delaware, December 26, 1958, the son of Edward F. and Jean K.

Education: Graduated from Thomas McKean High School, Hockessin, Delaware, in May 1976; received Bachelor of Science Degree in Geophysics from the University of Delaware in May 1981; completed requirements for the Master of Science Degree at Oklahoma State University in December, 1991.

Professional Experience: Staff Geophysicist, Cities Service Oil and Gas Corporation, August, 1981 to October, 1985; Senior Geophysicist Occidental Oil and Gas Corporation, October, 1985 to November, 1989.